

NUCLEAR SPINODAL INSTABILITIES IN STOCHASTIC MEAN-FIELD
APPROACHES

A THESIS SUBMITTED TO
THE GRADUATE SCHOOL OF NATURAL AND APPLIED SCIENCES
OF
MIDDLE EAST TECHNICAL UNIVERSITY

BY

NURAY ER

IN PARTIAL FULFILLMENT OF THE REQUIREMENTS
FOR
THE DEGREE OF DOCTOR OF PHILOSOPHY
IN
PHYSICS

AUGUST 2009

Approval of the thesis:

**NUCLEAR SPINODAL INSTABILITIES IN STOCHASTIC MEAN-FIELD
APPROACHES**

submitted by **NURAY ER** in partial fulfillment of the requirements for the degree of
Doctor of Philosophy in Physics Department, Middle East Technical University by,

Prof. Dr. Canan Özgen _____
Dean, Graduate School of **Natural and Applied Sciences**

Prof. Dr. Sinan Bilikmen _____
Head of Department, **Physics**

Prof. Dr. Osman Yılmaz _____
Supervisor, **Physics Department, METU**

Prof. Dr. Şakir Ayık _____
Co-supervisor, **Physics Department, Tennessee Technological Uni-
versity**

Examining Committee Members:

Prof. Dr. Ali Ulvi Yılmaz _____
Physics Eng. Dept., Ankara University

Prof. Dr. Osman Yılmaz _____
Physics Dept., METU

Prof. Dr. Ahmet Gökçalp _____
Physics Dept., METU

Prof. Dr. Ersan Akyıldız _____
Mathematics Dept., METU

Prof. Dr. Gürsevil Turan _____
Physics Dept., METU

Date: _____

I hereby declare that all information in this document has been obtained and presented in accordance with academic rules and ethical conduct. I also declare that, as required by these rules and conduct, I have fully cited and referenced all material and results that are not original to this work.

Name, Last Name: NURAY ER

Signature :

ABSTRACT

NUCLEAR SPINODAL INSTABILITIES IN STOCHASTIC MEAN-FIELD APPROACHES

Er, Nuray

Ph.D., Department of Physics

Supervisor : Prof. Dr. Osman Yılmaz

Co-Supervisor : Prof. Dr. Şakir Ayık

August 2009, 81 pages

Nuclear spinodal instabilities are investigated in non-relativistic and relativistic stochastic mean-field approaches for charge asymmetric and charge symmetric nuclear matter. Quantum statistical effect on the growth of instabilities are calculated in non-relativistic approach. Due to quantal effects, in both symmetric and asymmetric matter, dominant unstable modes shift towards longer wavelengths and modes with wave numbers larger than the Fermi momentum are strongly suppressed. As a result of quantum statistical effects, in particular at lower temperatures, amplitude of density fluctuations grows larger than those calculated in semi-classical approximation.

Relativistic calculations in the semi-classical limit are compared with the results of non-relativistic calculations based on Skyrme-type effective interactions under similar conditions. A qualitative difference appears in the unstable response of the system: the system exhibits most unstable behavior at higher baryon densities around $\rho_B = 0.4 \rho_0$ in the relativistic approach while most unstable behavior occurs at lower baryon densities around $\rho_B = 0.2 \rho_0$ in the non-relativistic calculations.

Keywords: Spinodal instabilities, nuclear multi-fragmentation, stochastic mean-field approach, time-dependent Hartree-Fock theory, Vlasov equation.

ÖZ

STOKASTİK ORTALAMA ALAN YAKLAŞIMLARINDA NÜKLEER SPİNODAL KARARSIZLIKLAR

Er, Nuray

Doktora, Fizik Bölümü

Tez Yöneticisi : Prof. Dr. Osman Yılmaz

Ortak Tez Yöneticisi : Prof. Dr. Şakir Ayık

August 2009, 81 sayfa

Relativistik ve relativistik olmayan stokastik ortalama alan yaklaşımları kullanılarak simetrik ve elektrik yükü bakımından asimetrik nükleer maddeler için nükleer spinodal kararsızlıklar incelendi. Kararsızlıkların gelişiminde kuantum istatistiksel etkiler relativistik olmayan yaklaşımda hesaplandı. Kuantal etkilerden dolayı simetrik ve asimetrik nükleer maddenin her ikisinde de baskın kararsız modlar uzun dalga boylarına doğru kayar ve dalga numarası Fermi momentumdan büyük olan modlar önemini kaybeder. Kuantum istatistiksel etkilerin sonucu olarak, özellikle düşük sıcaklıklarda, yoğunluk dalgalanmalarının genliği yarı-klasik yaklaşımla elde edilenlerden daha hızlı gelişir.

Yarı-klasik limitteki relativistik hesaplar, benzer koşullar altındaki Skyrme-tipi etkin etkileşimler baz alınarak yapılan relativistik olmayan hesapların sonuçları ile karşılaştırıldı. Sistemin kararsız tepkisinde kalitatif farklar ortaya çıkar: Relativistik yaklaşımda sistemin en kararsız davranışı $\rho_B = 0.4 \rho_0$ yoğunlukları civarında ortaya çıkar. Buna karşın relativistik olmayan davranış $\rho_B = 0.2 \rho_0$ civarındaki yoğunluklarda ken-

dini gösterir.

Anahtar Kelimeler: Spinodal kararsızlıklar, nükleer parçalanma, stokastik ortalama alan yaklaşımı, zamana bağı Hartree-Fock teorisi, Vlasov denklemi.

To My Family

ACKNOWLEDGMENTS

I would like to express my deep sincere feelings to my supervisor Prof. Dr. Osman Yılmaz and my co-supervisor, Prof. Dr. Şakir Ayık. I am grateful to them for their painstaking care in the course of this project and for their meticulous effort in teaching me numerous very precious concepts. They provided me unflinching encouragement and support in various ways. I am deeply thankful to Prof. Dr. Ahmet Gökalg for his stimulating scientific discussions and motivations during my entire Ph.D. program and also for a very thorough and critical reading of the thesis. In the initial stage of this thesis, my great thank is due to Prof. Dr. Peter Ring from Munich Technical University, Germany for his help and attitude. I am grateful to the examining committee members for their valuable hints helped and encouraged me to go ahead with my thesis. I would like to thank also TUBITAK, Turkish Scientific and Technical Research Council, for the partial support by grant No. 107T691 they granted.

TABLE OF CONTENTS

ABSTRACT	iv
ÖZ	vi
DEDICATION	viii
ACKNOWLEDGMENTS	ix
TABLE OF CONTENTS	x
LIST OF FIGURES	xii
CHAPTERS	
1 INTRODUCTION	1
2 QUANTAL EFFECTS ON SPINODAL INSTABILITIES IN CHARGE ASYMMETRIC NUCLEAR MATTER	5
2.1 Many-body Theory and Mean-field Approach	5
2.2 Stochastic Mean-field Approach	6
2.3 The Skyrme Interaction	10
2.4 Spinodal Instabilities	11
2.4.1 Dispersion Relation	11
2.4.2 Growth of Density Fluctuations	20
3 SPINODAL INSTABILITIES IN SYMMETRIC NUCLEAR MATTER IN A RELATIVISTIC MEAN-FIELD APPROACH	31
3.1 Relativistic Mean Field Model (Walecka Model)	32
3.1.1 Stochastic Relativistic Mean-Field Theory	34
3.2 Spinodal Instabilities	38
3.2.1 Dispersion Relation	38
3.2.2 Growth of Baryon Density Fluctuations	46
4 CONCLUSION	54

REFERENCES	57
APPENDICES	
A WIGNER TRANSFORMATION	60
B TIME DEPENDENCY OF DENSITY FLUCTUATIONS	62
C QUANTAL LINHARD FUNCTIONS	64
D DERIVATION OF RELATIVISTIC VLASOV EQUATION	69
E THE COUPLED ALGEBRAIC EQUATIONS OF DENSITY FLUCTUA- TIONS	71
F DERIVATIONS OF RELATIVISTIC CORRELATIONS	75
VITA	81

LIST OF FIGURES

FIGURES

Figure 2.1 Growth rates of unstable modes as a function of wave number in spinodal region corresponding initial densities and at a temperature $T = 5$ MeV. (a) for initial asymmetry $I = 0.0$, (b) for initial asymmetry $I = 0.5$	17
Figure 2.2 Same as Fig. 2.1 but for temperature $T = 1$ MeV.	18
Figure 2.3 Boundary of spinodal region in density-temperature plane corresponding to initial charge asymmetries $I = 0.0$ and $I = 0.5$ for the unstable mode: (a) with wavelength $\lambda = 9$ fm, (b) with wavelength $\lambda = 12$ fm.	19
Figure 2.4 Spectral intensity $\tilde{\sigma}_{nn}(\vec{k}, t)$ of neutron-neutron density correlation function as function of wave number k at times $t = 0$ and $t = 50$ fm/c for the initial charge asymmetry $I = 0.5$: (a) for density $n = 0.4 n_0$ at temperature $T = 1$ MeV, (b) for density $n = 0.4 n_0$ at temperature $T = 5$ MeV , (c) for density $n = 0.2 n_0$ at temperature $T = 5$ MeV.	26
Figure 2.5 Same as Fig. 2.4 but for asymmetry $I = 0.0$	27
Figure 2.6 Density correlation function $\sigma(x, t)$ as a function of distance $x = \vec{r} - \vec{r}' $ between two space points at times $t = 0$ and $t = 50$ fm/c and the initial charge asymmetry $I = 0.5$: (a) for density $n = 0.4 n_0$ at temperature $T = 1$ MeV, (b) for density $n = 0.4 n_0$ at temperature $T = 5$ MeV, (c) for density $n = 0.2 n_0$ at temperature $T = 5$ MeV.	28
Figure 2.7 Same as Fig. 2.6 but for asymmetry $I = 0.0$	29
Figure 2.8 Perturbation asymmetry as function of initial asymmetry at temperature $T = 5$ MeV for densities $n = 0.2 n_0$ and $n = 0.4 n_0$	30

Figure 3.1	Growth rates of unstable modes as a function of wave numbers in the spinodal region at baryon densities $\rho_B = 0.2 \rho_0$ and $\rho_B = 0.4 \rho_0$ at a temperature (a) $T = 2 \text{ MeV}$, (b) $T = 5 \text{ MeV}$	45
Figure 3.2	Growth rates of the most unstable modes as function of baryon density in the spinodal region at temperature $T = 5 \text{ MeV}$ in relativistic calculations (solid line) and in non-relativistic calculations (dashed line).	46
Figure 3.3	Boundary of spinodal region in baryon density-temperature plane in relativistic calculations (solid line) and in non-relativistic (dashed line) for the unstable mode with wavelengths: (a) $\lambda = 9 \text{ fm}$ and (b) $\lambda = 12 \text{ fm}$	47
Figure 3.4	Spectral intensity $\tilde{\sigma}_{BB}(\vec{k}, t)$ of baryon density correlation function as a function of wave number at times $t = 0$, $t = 20 \text{ fm}/c$, $t = 30 \text{ fm}/c$ and $t = 40 \text{ fm}/c$ at temperature $T = 2 \text{ MeV}$ in relativistic calculations at density (a) $\rho_B = 0.2 \rho_0$ and (b) $\rho_B = 0.4 \rho_0$	50
Figure 3.5	Same as Fig 3.4 but for temperature $T = 5 \text{ MeV}$	51
Figure 3.6	Baryon density correlation function $\sigma(x, t)$ as a function of distance $x = \vec{r} - \vec{r}' $ between two space points at times $t = 0$, $t = 20 \text{ fm}/c$, $t = 30 \text{ fm}/c$ and $t = 40 \text{ fm}/c$ at temperature $T = 2 \text{ MeV}$ in relativistic calculations at density (a) $\rho_B = 0.2 \rho_0$ and (b) $\rho_B = 0.4 \rho_0$	52
Figure 3.7	Same as Fig. 3.6 but at temperature $T = 5 \text{ MeV}$	53

CHAPTER 1

INTRODUCTION

Nucleons are nearly two thousand times heavier than electrons, therefore the mass of an atom more than 99.9% is found in nucleus which means that nucleus is more than 10^{14} times denser than normal matter. The normal nuclei, in equilibrium conditions its density is around 0.16 fm^{-3} , which consist of neutrons and protons and it is one of the phases of nuclear matter. The other possible phases of nuclear matter are parameterized in terms of temperature and relative baryon density, the density compared with ordinary nuclei. In heavy ion collisions, nuclear matter is excited and in these high temperature and subnormal density conditions liquid-gas phase transition from nuclei to nucleons takes place. Ordinary nuclear matter behaves like a Fermi liquid, quantum mechanical fluid of fermions, with specific quantum numbers, so it is expected that a change of phase shows the similar properties of a first order liquid-gas phase transition, because there is similarity between van der Waals and nucleon-nucleon interactions, which is attractive at long and intermediate ranges and repulsive at short range. Density fluctuations in the Fermi fluid are named as zero sound by Landau which is the longitudinal density vibrations. In the instability region the frequency of sound waves are imaginary [1].

Dynamics of density fluctuations around equilibrium density have a fundamental role in induced fission, heavy-ion fusion near barrier energies, spinodal instabilities and nuclear multi-fragmentation processes. In this thesis our main interest is spinodal instabilities and multi-fragmentation processes. The growth of small density fluctuations around an equilibrium density is known as the spinodal decompositions. The

region in which the spinodal decompositions occurs is called as the spinodal region where the system is unstable and in the spinodal boundary it changes phase and multi-fragmentation takes place. For example, at intermediate energies of forceful reactions, it can be observed that a hot and dense nuclear source expands and enters into the unstable region , i.e. the spinodal region. Then, as a result of instability the fluctuations of the local density grows and leads to a break-up of the nuclear system into many fragments.

Mean field transport models in which fluctuation and dissipation takes places together are needed for the explanation of dynamics of density fluctuation processes. But, the approaches like time-dependent Hartree-Fock (TDHF) [2, 3] and the Boltzmann-Uhling-Uhlenbeck (BUU) [4] do not have these features. Because TDHF includes, the so called, one-body dissipation mechanism, interactions of a single nucleon with the collective nuclear potential, but associated fluctuation mechanism is not incorporated into the model. Correspondingly, the extended TDHF and its semi-classical approximation BUU model involves one-body and collisional dissipation, but the associated fluctuation mechanisms are not included into the description. It is well known that no dissipation takes place without fluctuations. In order to describe dynamics of density fluctuations, we need to develop stochastic transport models by incorporating fluctuation mechanisms into the description. There are two different mechanisms for density fluctuations: (i) collisional fluctuations generated by two-body collisions and (ii) one-body mechanism or mean-field fluctuations. Much effort has been given to improve the transport description by incorporating two-body dissipation and fluctuation mechanisms. The resultant stochastic transport theory, known as Boltzmann-Langevin model [5, 6, 7], provides a suitable framework for dynamics of density fluctuations in nuclear collisions around Fermi energy. However, two-body dissipation and fluctuation mechanisms do not play an important role at low energies. At low bombarding energies, mean-field fluctuations provide the dominant mechanism for fluctuations of collective nuclear motion. In a recent work, this question is addressed [8]. Restricting the treatment at low energies, a stochastic mean-field approach for nuclear dynamics is proposed, which incorporates one-body dissipation and fluctuation mechanisms in accordance with quantal dissipation-fluctuation theo-

rem. Therefore, the stochastic mean-field approach provides a powerful microscopic tool for describing low energy nuclear processes including induced fission, heavy-ion fusion near barrier energies and spinodal decomposition of nuclear matter.

Much work has been done to understand the spinodal instabilities and their connection with liquid gas phase transformation in symmetric and more recently charge asymmetric nuclear matter. Most of these investigations have been carried out in the basis of semi-classical Boltzmann- Langevin (BL) type stochastic transport models [1]. There are two major problems with these investigations. First of all, numerical simulations of BL model are not very easy, even with approximate methods, simulations require large amount of numerical effort. The second problem is related with the semi-classical description of spinodal decomposition of nuclear matter. According to previous works, quantal statistical effects play an important role in spinodal dynamics [9, 10, 11, 12]. There are qualitatively two different regimes during evolution of nuclear collisions in Fermi energy domain. During the initial regime of heavy ion-collisions, namely, from touching until formation of hot and compressed piece of nuclear matter, collisional dissipation and fluctuations are substantially important. On the other hand, during expansion of the system into mechanically unstable spinodal region, collisional effects may be neglected. In the spinodal region, local density fluctuations, which are accumulated during the initial regime, are mainly driven by the mean-field until system breaks up into clusters. Recently proposed stochastic mean-field approach provides a useful tool for describing spinodal decomposition of expanding hot piece of nuclear matter. The approach includes quantum statistical effects and at the same time, numerical simulations of the approach can be carried out without much difficulty.

And also it has been shown in recent years that the nuclear many-body system is in principal a relativistic system driven by dynamics of large relativistic attractive scalar and repulsive vector fields. Both fields are not much smaller than the nucleon mass and therefore the average nuclear field should be described by Dirac equation. For large components of Dirac spinors, two fields nearly cancel each other leading to relatively small attractive mean field. The small components add up leading to

a very large spin orbit term, which is known since early days of nuclear physics. Relativistic models have been used with great success to describe nuclear structure. In recent years, the approach has also been applied for description of nuclear dynamics extended in the framework of time-dependent covariant density functional theory [13, 14]. A number of investigations have been carried out on spinodal instabilities in nuclear matter employing relativistic mean-field approaches [15, 16, 17].

In chapter 2, we present a brief description of the time-dependent Hartree Fock theory and the stochastic mean-field approach, and then we study early growth of density fluctuations in charge asymmetric nuclear matter and investigate quantum statistical effects on spinodal instabilities and on growth rates of dominant unstable modes on the basis of stochastic mean-field approach, we calculate early growth of density fluctuations, growth rates and phase diagram of dominant modes in charge asymmetric systems, and study quantal effects on these quantities. In chapter 3, Walecka model is introduced and the field equations of nucleons, the scalar meson and the vector meson is derived and then we consider the stochastic extension of the relativistic mean-field theory in the semi-classical approximation. Employing the stochastic extension of the relativistic mean-field approach, we investigate spinodal instabilities and early development of density fluctuations in symmetric nuclear matter. And the conclusions of these investigations are given in chapter 4.

The main body of this thesis depends on two published papers;

1. S. Ayik, N. Er, O. Yilmaz and A. Gokalp, Nucl. Phys. **A 812** (2008) 44.
2. S. Ayik, O. Yilmaz, N. Er, A. Gokalp and P. Ring, submitted to Phys. Rev. C.

CHAPTER 2

QUANTAL EFFECTS ON SPINODAL INSTABILITIES IN CHARGE ASYMMETRIC NUCLEAR MATTER

2.1 Many-body Theory and Mean-field Approach

Many-body theory provides the framework for understanding the collective behavior of big assemblies of interacting particles. Nuclear matter is also a many-body system of interacting fermions, and it is generally very difficult to solve its equation for the states of the system exactly. The many-body time-dependent Schrödinger equation of nuclear matter is

$$\left[i\hbar \frac{\partial}{\partial t} - H \right] \Phi(r_i, t) = \left[i\hbar \frac{\partial}{\partial t} - \left\{ \sum_i -\frac{\hbar^2}{2m} \nabla_i^2 + \sum_{i<j} u(i, j) \right\} \right] \Phi(r_i, t) = 0 \quad (2.1)$$

where r_i collectively symbolizes the coordinates of i^{th} nucleon which includes position \vec{r}_i , z-component of spin $s_i = \mp 1/2$ and third component isospin $t_i = 1/2$ for neutrons, $t_i = -1/2$ for protons (coordinates of i^{th} nucleon), and $u(i, j)$ represents interaction potential of two nucleons [2]. The great difficulty generated by the interaction terms in the Hamiltonian manifests itself when summing over all states. To solve this difficulty mean field theory (MFT), i.e. self-consistent field theory, is used. There is self-consistency because mean-field potential depends on local densities of neutrons and protons in nuclear matter. The goal of MFT is to replace all interactions with an average or effective one body interaction. This enables one to reduce many-body problem into an effective many one-body problem. This reduction is very worthwhile because the system at any time is defined by its one-body distribution instead of the full many-body information.

In the mean-field characterization of a many-body system, the time-dependent wave function $\Phi(t)$ is an anti-symmetric wave function assumed to be a single Slater determinant constructed with time-dependent single-particle wave functions $\phi(r_i, t)$,

$$\Phi_{k_1 \dots k_n \dots}(r_i, t) = \begin{vmatrix} \phi_{k_1}(r_1, t) & \dots & \phi_{k_1}(r_n, t) & \dots \\ \vdots & & \vdots & \\ \phi_{k_n}(r_1, t) & \dots & \phi_{k_n}(r_n, t) & \dots \\ \vdots & & \vdots & \end{vmatrix} \quad (2.2)$$

with eigenvalues $E_{k_1 \dots k_n \dots} = \epsilon_{k_1} + \dots + \epsilon_{k_n} + \dots$, and for all times it stays as a Slater determinant. Then, the motion of the system is described by the single particle density matrix defined as follows,

$$\rho(\vec{r}, \vec{r}', t) = \sum_j \phi_j(\vec{r}, t) n_j \phi_j^*(\vec{r}', t) \quad (2.3)$$

here n_j represents the occupation number of the single-particle states. Using Variational principle it is possible to derive the equation of motion of $\rho(r, r', t)$ as

$$\left\langle \delta\Phi(t) \left| H - i\hbar \frac{\partial}{\partial t} \right| \Phi(t) \right\rangle = 0 \quad (2.4)$$

which gives the well-known time-dependent Hartree-Fock (TDHF) equation in dynamics

$$i\hbar \frac{\partial \rho}{\partial t} - [h(\rho), \rho] = 0 \quad (2.5)$$

where $h(\rho)$ is the single particle Hamiltonian (TDHF Hamiltonian). In the static limit it is known as Hartree-Fock equation (HF) $[h(\rho), \rho] = 0$. In the semi-classical limit TDHF equation reduces to Vlasov equation which gives the time evolution of the phase space distribution function $f(\vec{r}, \vec{p}, t)$

$$\frac{\partial}{\partial t} f(\vec{r}, \vec{p}, t) - \vec{\nabla}_r h(\vec{r}, \vec{p}) \cdot \vec{\nabla}_p f(\vec{r}, \vec{p}, t) + \vec{\nabla}_p h(\vec{r}, \vec{p}) \cdot \vec{\nabla}_r f(\vec{r}, \vec{p}, t) = 0. \quad (2.6)$$

The detail of this semi-classical correspondence is presented in Appendix A.

2.2 Stochastic Mean-field Approach

A deterministic evaluation of the single-particle density matrix can be obtained using the standard TDHF equations starting from a well defined initial state. The standard

approach provides a good description for the average evolution of collective motion, however it severely restricts fluctuations of collective motion [2, 3]. In order to describe fluctuations, we must give up single determinantal description and consider superposition of determinantal wave functions. In the stochastic mean-field description, an ensemble of single-particle density matrices associated with the ensemble of Slater determinants is generated in a stochastic framework by retaining only initial correlations [8].

Correlation is an important concept in the probability theory and statistical physics because it gives information about the strength and direction of a linear relationship between two random variables [18]. In the stochastic mean-field approximation the initial correlations are the source of stochasticity. Due to stochastic behavior of the initial correlations it is impossible to find a well-defined single determinantal form of the initial state. As a result, initial correlations can be integrated by dealing, instead of a single initial state with a distribution of initial Slater determinants, and thus initial correlations can be simulated in a stochastic description. To be able to build up a stochastic description, enough number of unoccupied and occupied single-particle states must be determined. A member of single-particle density matrix, indicated by label λ , can be expressed as,

$$\rho_a^\lambda(\vec{r}, \vec{r}', t) = \sum_{ij} \phi_i(\vec{r}, t; \lambda) \langle i | \rho_a^\lambda(0) | j \rangle \phi_j^*(\vec{r}', t; \lambda). \quad (2.7)$$

In this expression and in the rest of this thesis label $a = n, p$ represents neutron and proton species and $\langle i | \rho_a^\lambda(0) | j \rangle$ are time-independent elements of density matrix determined by the initial correlations. The main assumption of the approach is that each matrix element is a Gaussian random number specified by a mean value $\overline{\langle i | \rho_a^\lambda(0) | j \rangle} = \delta_{ij} f_0^a(i)$, i.e. the mean-field Hamiltonian h_0 at $t = 0$ assumed uniform, and a variance of $\delta \rho_a(0)$, which is measure of statistical dispersion of a random variable initial correlation, is

$$\overline{\langle i | \delta \rho_a^\lambda(0) | j \rangle \langle j' | \delta \rho_b^\lambda(0) | i' \rangle} = \frac{1}{2} \delta_{ab} \delta_{ii'} \delta_{jj'} \{ f_0^a(i) [1 - f_0^a(j)] + f_0^a(j) [1 - f_0^a(i)] \}. \quad (2.8)$$

In these expressions $\langle i | \delta \rho_a^\lambda(0) | j \rangle$ represents fluctuating elements of initial density matrix, $\rho_a(j)$ denotes the average occupation number. At zero temperature, the average

occupation numbers are zero for unoccupied states and one for occupied states, and at finite temperature, the average occupation numbers are given by the Fermi-Dirac distribution,

$$f_0^a(j) = \frac{1}{e^{(\epsilon_j - \mu_a)/T} + 1} \quad (2.9)$$

where μ_a is chemical potential of nucleons determined as $\mu_a = \epsilon_F [1 - (\pi^2/12)(T/\epsilon_F)^2]$ in terms of Fermi energy $\epsilon_F = (3\pi^2 n_0/2)^{2/3}/2m$ with the equilibrium density n_0 .

In each event, different from the standard TDHF, time-dependent single-particle wave functions of neutrons and protons are determined by their own self-consistent mean-field according to,

$$i\hbar \frac{\partial}{\partial t} \phi_j^a(\vec{r}, t; \lambda) = h_a^\lambda \phi_j^a(\vec{r}, t; \lambda) \quad (2.10)$$

where $h_a^\lambda = p^2/2m_a + U_a(n_n^\lambda, n_p^\lambda)$ denotes the mean-field Hamiltonian in the event, and in the mean-field approach $U_a(n_n^\lambda, n_p^\lambda)$ is the density dependent self-consistent mean-field potential which depends on proton and neutron local densities $n_a^\lambda(r, t)$.

We can express stochastic mean-field evolution in terms of single-particle density matrices of neutrons and protons as

$$i\hbar \frac{\partial}{\partial t} \rho_a^\lambda(t) = [h_a^\lambda[\rho_a^\lambda], \rho_a^\lambda(t)], \quad (2.11)$$

where the collision term is neglected in the frame of mean-field approximation. In the stochastic mean-field approach an ensemble of single-particle density matrices is generated associated with different events. In this approach, we can calculate, not only the mean value of observables, also probability distribution of observables. Even if the magnitude of initial fluctuations is small, in particular in the vicinity of instabilities mean-field evolution can enhance the fluctuations, and hence events can substantially deviate from one to another. By projecting on a collective path, it is demonstrated that the stochastic mean-field approach incorporates one-body dissipation and one-body fluctuation mechanisms in accordance with quantal dissipation-fluctuation relation [8].

In this part of the thesis, we investigate the early growth of density fluctuations in spinodal region in charge asymmetric nuclear matter. For this purpose it is sufficient

to consider the linear response treatment of dynamical evolution [1]. Only to the early development of spinodal instabilities linear treatment is applied, if the density fluctuations grow large the dynamics of the system becomes non-linear and more complete treatment is needed. The small amplitude fluctuations of the single-particle density matrix around an equilibrium state are determined by the linearized TDHF equations. The linearized TDHF equations for fluctuations of neutron and proton density matrices $\delta\rho_a^\lambda(t) = \rho_a^\lambda(t) - \rho_a^0$, are given by

$$i\hbar\frac{\partial}{\partial t}\delta\rho_a^\lambda(t) = [h_a^0, \delta\rho_a^\lambda(t)] + [\delta U_a^\lambda(t), \rho_a^0], \quad (2.12)$$

where the linearized effective one-body Hamiltonian is $h_a^\lambda[\rho_a^0 + \delta\rho_a^\lambda(t)] = p^2/2m_a + U_a[\rho_a^0 + \delta\rho_a^\lambda(t)] = h_a^0 + \delta U_a(t)$. Since for infinite matter, the equilibrium state and the associated mean-field Hamiltonian h_a^0 are homogenous, it is suitable to analyze these equations in the plane wave representations

$$\begin{aligned} i\hbar\frac{\partial}{\partial t}\langle\vec{p}_1|\delta\rho_a^\lambda(t)|\vec{p}_2\rangle &= \langle\vec{p}_1|[h_a^0, \delta\rho_a^\lambda(t)] + [\delta U_a^\lambda(t), \rho_a^0]|\vec{p}_2\rangle \\ &= [\epsilon_a(\vec{p}_1) - \epsilon_a(\vec{p}_2)]\langle\vec{p}_1|\delta\rho_a^\lambda(t)|\vec{p}_2\rangle + \langle\vec{p}_1|[\delta U_a^\lambda(t), \rho_a^0]|\vec{p}_2\rangle, \end{aligned} \quad (2.13)$$

where

$$\begin{aligned} \langle\vec{p}_1|[\delta U_a^\lambda(t), \rho_a^0]|\vec{p}_2\rangle &= \langle\vec{p}_1|\delta U_a^\lambda(t) \int d\vec{p}_2'|\vec{p}_2'\rangle\langle\vec{p}_2'|\rho_a^0|\vec{p}_2\rangle \\ &\quad - \langle\vec{p}_1|\rho_a^0 \int d\vec{p}_1'|\vec{p}_1'\rangle\langle\vec{p}_1'|U_a^\lambda(t)|\vec{p}_2\rangle \\ &= \int d\vec{p}_2'\langle\vec{p}_1|\delta U_a^\lambda(t)|\vec{p}_2'\rangle f_0^a(\vec{p}_2')\delta(\vec{p}_2 - \vec{p}_2') \\ &\quad - \int d\vec{p}_1'\langle\vec{p}_1'|U_a^\lambda(t)|\vec{p}_2\rangle f_0^a(\vec{p}_1')\delta(\vec{p}_1 - \vec{p}_1'), \end{aligned} \quad (2.14)$$

and thus finally

$$\begin{aligned} i\hbar\frac{\partial}{\partial t}\langle\vec{p}_1|\delta\rho_a^\lambda(t)|\vec{p}_2\rangle &= [\epsilon_a(\vec{p}_1) - \epsilon_a(\vec{p}_2)]\langle\vec{p}_1|\delta\rho_a^\lambda(t)|\vec{p}_2\rangle \\ &\quad - [f_0^a(\vec{p}_1) - f_0^a(\vec{p}_2)]\langle\vec{p}_1|\delta U_a^\lambda(t)|\vec{p}_2\rangle. \end{aligned} \quad (2.15)$$

The main assumption of stochastic mean-field approach is that, matrix elements of the initial density matrix are Gaussian random numbers. In the plane wave representation

the second moments of the initial correlations are given by,

$$\begin{aligned} \overline{\langle \vec{p}_1 | \delta \rho_a(0) | \vec{p}_2 \rangle \langle \vec{p}_2' | \delta \rho_b(0) | \vec{p}_1' \rangle} &= \delta_{ab} (2\pi\hbar)^6 \delta(\vec{p}_1 - \vec{p}_1') \delta(\vec{p}_2 - \vec{p}_2') \\ &\quad \frac{1}{2} [f_0^a(\vec{p}_1)(1 - f_0^a(\vec{p}_2)) + f_0^a(\vec{p}_2)(1 - f_0^a(\vec{p}_1))], \end{aligned} \quad (2.16)$$

where the factor $(2\pi\hbar)^6$ arises from normalization of the plane waves.

2.3 The Skyrme Interaction

The Skyrme interaction is one of the phenomenological effective interactions used in nuclear problems, like in nuclear self-consistent field or bulk properties of nuclei. For nuclear Hartree-Fock calculations in the mean-field approximation Skyrme potential, which is zero-range, density and momentum dependent, is an effective potential. The original form of it with a two-body and a three-body term is

$$V = \sum_{i<j} V_{ij} + \sum_{i<j<k} V_{ijk}. \quad (2.17)$$

The range of nuclear force is very short, so to simplify the problem for the two-body part it is useful to use short-range expansion where the radial dependence of force is shown by δ -function and a momentum dependence is used to simulate a finite range

$$\begin{aligned} V_{ij} = & t_0 (1 + x_0 P^\sigma) \delta(\vec{r}_1 - \vec{r}_2) + \frac{1}{2} t_1 [\delta(\vec{r}_1 - \vec{r}_2) \vec{k}^2 + \vec{k}^2 \delta(\vec{r}_1 - \vec{r}_2)] \\ & + t_2 \vec{k} \delta(\vec{r}_1 - \vec{r}_2) \vec{k} + i W_0 (\vec{\sigma}^{(1)} - \vec{\sigma}^{(2)}) \vec{k} \times \delta(\vec{r}_1 - \vec{r}_2) \vec{k}, \end{aligned} \quad (2.18)$$

here $\vec{k} = 1/2i(\vec{\nabla}_1 - \vec{\nabla}_2)$ is the relative momentum operator, P^σ is a spin-exchange operator and the $\vec{\sigma}$ is Pauli spin matrix. The zero range force form of the three body part is

$$V_{ijk} = t_3 \delta(\vec{r}_1 - \vec{r}_2) \delta(\vec{r}_2 - \vec{r}_3). \quad (2.19)$$

In these equations the constants $t_0, t_1, t_2, t_3, t_0, x_0, W_0$ are fitted with experimental results of binding energies and nuclear radii, in literature for these constants there are several sets [2, 19, 20].

In numerical calculations we employ the same effective Skyrme potential as in reference [21] for the local density dependent mean-field potential

$$U_a(n_n, n_p) = \frac{\delta H_{pot}(n_n, n_p)}{\delta \rho_a}, \quad (2.20)$$

where

$$H_{pot}(n_n, n_p) = \frac{A n^2}{2 n_0} + \frac{B n^{\alpha+2}}{\alpha + 2 n_0^{\alpha+1}} + \frac{C n'^2}{2 n_0} + \frac{D}{2} (\vec{\nabla} n)^2 - \frac{D'}{2} (\vec{\nabla} n')^2. \quad (2.21)$$

Thus the potential energy density is

$$U_a(n_n, n_p) = A \left(\frac{n}{n_0} \right) + B \left(\frac{n}{n_0} \right)^{\alpha+1} + C \left(\frac{n'}{n_0} \right) \tau_a + \frac{1}{2} \frac{dC}{dn} \frac{n'^2}{n_0} - D \Delta n + D' \Delta n' \tau_a, \quad (2.22)$$

here $n = n_n + n_p$ and $n' = n_n - n_p$ are total and relative densities, and the sign of isospin $\tau_a = +1$ for neutrons and $\tau_a = -1$ for protons. The parameters A, B, C, D and D' are functions of Skyrme parameters, and their numerical values $A = -356.8 \text{ MeV}$, $B = +303.9 \text{ MeV}$, $\alpha = 1/6$ and $D = +130.0 \text{ MeV fm}^5$ are adjusted to reproduce the saturation properties of symmetric nuclear matter: The binding energy $\varepsilon_0 = 15.7 \text{ MeV/nucleon}$ and zero pressure at the saturation density $n_0 = 0.16 \text{ fm}^{-3}$, compressibility modulus $K = 201 \text{ MeV}$ and the surface energy coefficient in the Weizsacker mass formula $a_{surf} = 18.6 \text{ MeV}$ [22]. Magnitude of the parameter $D' = +34 \text{ MeV fm}^5$ is close to the value given by the SkM^* interaction [23]. The potential symmetry energy coefficient is $C(n) = C_1 - C_2(n/n_0)^\alpha$ with $C_1 = +124.9 \text{ MeV}$ and $C_2 = 93.5 \text{ MeV}$. These parameters for the symmetry energy coefficient in Weizsacker mass formula, at saturation density gives $a_{sym} = \varepsilon_F(n_0)/3 + C(n_0)/2 = 36.9/3 + 31.4/2 = 28.0 \text{ MeV}$.

2.4 Spinodal Instabilities

2.4.1 Dispersion Relation

In this subsection, we apply the stochastic mean-field approach in small amplitude limit to investigate spinodal instabilities in charge asymmetric nuclear matter [21]. We can obtain the solution of Eqn (2.15) by employing the standard one sided Fourier

transformation method, so the transformation of density fluctuation is

$$\int_0^\infty dt e^{i\omega t} \frac{\partial}{\partial t} \langle \vec{p}_1 | \delta\rho_a(t) | \vec{p}_2 \rangle = -\langle \vec{p}_1 | \delta\rho_a(0) | \vec{p}_2 \rangle - i\omega \langle \vec{p}_1 | \delta\rho_a(\omega) | \vec{p}_2 \rangle, \quad (2.23)$$

where $\langle \vec{p}_1 | \delta\rho_a(0) | \vec{p}_2 \rangle$ is the source part coming from initial conditions, and the transformation of mean-field potential is

$$\int_0^\infty dt e^{i\omega t} \langle \vec{p}_1 | U_a(t) | \vec{p}_2 \rangle = \langle \vec{p}_1 | U_a(\omega) | \vec{p}_2 \rangle. \quad (2.24)$$

Therefore, the Fourier transformed form of linearized TDHF equation becomes

$$\begin{aligned} \langle \vec{p}_1 | \delta\rho_a(\omega) | \vec{p}_2 \rangle = & - \frac{[f_0^a(\vec{p}_1) - f_0^a(\vec{p}_2)]}{[\hbar\omega - \varepsilon_a(\vec{p}_1) + \varepsilon_a(\vec{p}_2)]} \langle \vec{p}_1 | \delta U_a(\omega) | \vec{p}_2 \rangle \\ & + i\hbar \frac{\langle \vec{p}_1 | \delta\rho_a(0) | \vec{p}_2 \rangle}{[\hbar\omega - \varepsilon_a(\vec{p}_1) + \varepsilon_a(\vec{p}_2)]}. \end{aligned} \quad (2.25)$$

By rewriting the momentum vectors as $\vec{p}_1 = \vec{p} + \hbar\vec{k}/2$, $\vec{p}_2 = \vec{p} - \hbar\vec{k}/2$ and using the position space and momentum space representations in which we have the relations [24]

$$\begin{aligned} \langle \vec{r}' | \vec{p} \rangle &= \frac{1}{(2\pi\hbar)^{3/2}} e^{(i/\hbar)\vec{p}\cdot\vec{r}'} \\ \langle \vec{p} + \frac{\hbar\vec{k}}{2} | \vec{r}' \rangle &= \frac{1}{(2\pi\hbar)^{3/2}} e^{-(i/\hbar)(\vec{p} + \frac{\hbar\vec{k}}{2})\cdot\vec{r}'} \\ \langle \vec{r}' | \vec{p} - \frac{\hbar\vec{k}}{2} \rangle &= \frac{1}{(2\pi\hbar)^{3/2}} e^{(i/\hbar)(\vec{p} - \frac{\hbar\vec{k}}{2})\cdot\vec{r}'}, \end{aligned} \quad (2.26)$$

we obtain

$$\begin{aligned} \langle \vec{p} + \frac{\hbar\vec{k}}{2} | \delta\rho_a(\omega) | \vec{p} - \frac{\hbar\vec{k}}{2} \rangle = & \int_0^\infty dt e^{i\omega t} \int_{-\infty}^\infty \int_{-\infty}^\infty d^3r d^3r' \langle \vec{p} + \frac{\hbar\vec{k}}{2} | \vec{r}' \rangle \langle \vec{r}' | \delta\rho_a(t) | \vec{r}' \rangle \langle \vec{r}' | \vec{p} - \frac{\hbar\vec{k}}{2} \rangle. \end{aligned} \quad (2.27)$$

We evaluate $\int d^3p$ integral of both sides and then use the orthonormality relation

$$\int_{-\infty}^\infty d^3p e^{-(i/\hbar)(\vec{r} - \vec{r}')\cdot\vec{p}} = (2\pi\hbar)^3 \delta(\vec{r} - \vec{r}'), \quad (2.28)$$

to obtain

$$\begin{aligned}
& \int d^3 p \langle \vec{p} + \frac{\hbar \vec{k}}{2} | \delta \rho_a(\omega) | \vec{p} - \frac{\hbar \vec{k}}{2} \rangle \\
&= \int_0^\infty dt e^{i\omega t} \int_{-\infty}^\infty \int_{-\infty}^\infty d^3 r d^3 r' \int \frac{d^3 p}{(2\pi\hbar)^3} e^{(-i/\hbar)(\vec{r}-\vec{r}')\cdot\vec{p}} e^{(-i/2)(\vec{r}+\vec{r}')\cdot\vec{k}} \langle \vec{r}' | \delta \rho_a(t) | \vec{r}' \rangle \\
&= \int_0^\infty dt e^{i\omega t} \int_{-\infty}^\infty d^3 r e^{-i\vec{k}\cdot\vec{r}} \delta \rho_a(\vec{r}, t) = \int_0^\infty dt e^{i\omega t} \delta \rho_a(\vec{k}, t).
\end{aligned} \tag{2.29}$$

Similarly, Fourier transform of the fluctuating part of mean-field potential

$$\begin{aligned}
& \langle \vec{p} + \frac{\hbar \vec{k}}{2} | \delta U_a(\omega) | \vec{p} - \frac{\hbar \vec{k}}{2} \rangle \\
&= \int_0^\infty dt e^{i\omega t} \int_{-\infty}^\infty \int_{-\infty}^\infty d^3 r d^3 r' \langle \vec{p} + \frac{\hbar \vec{k}}{2} | \vec{r} \rangle \langle \vec{r}' | \delta U_a(t) | \vec{r}' \rangle \langle \vec{r}' | \vec{p} - \frac{\hbar \vec{k}}{2} \rangle \\
&= \int_0^\infty dt e^{i\omega t} \int_{-\infty}^\infty \frac{d^3 r}{(2\pi\hbar)^3} e^{(-i/\hbar)(\vec{p}+(\hbar/2)\vec{k})\cdot\vec{r}} e^{(i/\hbar)(\vec{p}-(\hbar/2)\vec{k})\cdot\vec{r}} \delta U_a(t) \\
&= \int_0^\infty dt e^{i\omega t} \delta U_a(t) \int_{-\infty}^\infty \frac{d^3 r}{(2\pi\hbar)^3} e^{-i\vec{k}\cdot\vec{r}}
\end{aligned} \tag{2.30}$$

can be written as

$$\langle \vec{p} + \frac{\hbar \vec{k}}{2} | \delta U_a(\omega) | \vec{p} - \frac{\hbar \vec{k}}{2} \rangle = \delta U_a(\omega), \tag{2.31}$$

where $\langle \vec{r}' | \delta U_a(t) | \vec{r}' \rangle = \delta U_a(t) \delta(\vec{r}' - \vec{r}')$, because mean-field potential is local.

We have the following quantity

$$\delta \tilde{n}_a(\vec{k}, \omega) = 2 \int_{-\infty}^\infty \frac{d^3 p}{(2\pi\hbar)^3} \langle \vec{p} + \hbar \vec{k}/2 | \delta \rho_a(\omega) | \vec{p} - \hbar \vec{k}/2 \rangle, \tag{2.32}$$

which defines the Fourier transform of the local density fluctuations of neutrons and protons, where the coefficient 2 is spin factor. In these expressions and in other formulas in this section, we omit the event label λ for clarity of notation. After Fourier transformation and $d^3 p/(2\pi\hbar)^3$ integration of Eq. (2.15) there results

$$\begin{aligned}
\delta \tilde{n}_a(\vec{k}, \omega) &= 2 \int_{-\infty}^\infty \frac{d^3 p}{(2\pi\hbar)^3} \frac{[f_0^a(\vec{p} - \hbar \vec{k}/2) - f_0^a(\vec{p} + \hbar \vec{k}/2)]}{\hbar\omega - \epsilon_a(\vec{p} + \hbar \vec{k}/2) + \epsilon_a(\vec{p} - \hbar \vec{k}/2)} \delta U_a(\omega) \\
&+ 2i\hbar \int_{-\infty}^\infty \frac{d^3 p}{(2\pi\hbar)^3} \frac{\langle \vec{p} + \hbar \vec{k}/2 | \delta \rho_a(0) | \vec{p} - \hbar \vec{k}/2 \rangle}{\hbar\omega - \epsilon_a(\vec{p} + \hbar \vec{k}/2) + \epsilon_a(\vec{p} - \hbar \vec{k}/2)}.
\end{aligned} \tag{2.33}$$

The fluctuation of mean field potential depends on both neutron and proton local density fluctuations, for neutron

$$\delta U_n(\vec{k}, \omega) = \left(\frac{\delta U_n}{\delta \tilde{n}_n} \right)_0 \delta \tilde{n}_n(\vec{k}, \omega) + \left(\frac{\delta U_n}{\delta \tilde{n}_p} \right)_0 \delta \tilde{n}_p(\vec{k}, \omega), \tag{2.34}$$

and for proton

$$\delta U_p(\vec{k}, \omega) = \left(\frac{\delta U_p}{\delta \tilde{n}_n} \right)_0 \delta \tilde{n}_n(\vec{k}, \omega) + \left(\frac{\delta U_p}{\delta \tilde{n}_p} \right)_0 \delta \tilde{n}_p(\vec{k}, \omega), \quad (2.35)$$

where, the equilibrium densities of neutron and proton has the same value $\tilde{n}_0 = 0.16 \text{ fm}^{-3}$. In these expressions, derivative of the mean-field potential $U_a(n_n, n_p)$ evaluated at the equilibrium density $F_0^{ab} = (\partial U_b / \partial \tilde{n}_a)_0$ denotes the zero-order Landau parameters and the integral $\chi_a(\vec{k}, \omega)$ is the Lindhard function associated with neutron and proton distributions

$$\chi_a(\vec{k}, \omega) = -2 \int_{-\infty}^{\infty} \frac{d^3 p}{(2\pi\hbar)^3} \frac{f_0^a(\vec{p} - \hbar\vec{k}/2) - f_0^a(\vec{p} + \hbar\vec{k}/2)}{\hbar\omega - \vec{p} \cdot \hbar\vec{k}/m} \quad (2.36)$$

where $-\vec{p} \cdot \hbar\vec{k}/m = -\epsilon_a(\vec{p} + \hbar\vec{k}/2) - \epsilon_a(\vec{p} - \hbar\vec{k}/2)$. The source terms $A_a(\vec{k}, \omega)$ are determined by the initial conditions,

$$A_a(\vec{k}, \omega) = 2\hbar \int_{-\infty}^{\infty} \frac{d^3 p}{(2\pi\hbar)^3} \frac{\langle \vec{p} + \hbar\vec{k}/2 | \delta \rho_a(0) | \vec{p} - \hbar\vec{k}/2 \rangle}{\hbar\omega - \vec{p} \cdot \hbar\vec{k}/m}. \quad (2.37)$$

The angular integrations can be performed and the resulting expressions are presented in Appendix B. Therefore, we obtain a set of coupled algebraic equations for the Fourier transforms of fluctuating parts of local neutron and proton densities [25],

$$[1 + F_0^{nn} \chi_n(\vec{k}, \omega)] \delta \tilde{n}_n(\vec{k}, \omega) + F_0^{np} \chi_n(\vec{k}, \omega) \delta \tilde{n}_p(\vec{k}, \omega) = i A_n(\vec{k}, \omega) \quad (2.38)$$

and

$$[1 + F_0^{pp} \chi_p(\vec{k}, \omega)] \delta \tilde{n}_p(\vec{k}, \omega) + F_0^{pn} \chi_p(\vec{k}, \omega) \delta \tilde{n}_n(\vec{k}, \omega) = i A_p(\vec{k}, \omega). \quad (2.39)$$

The solution of the coupled algebraic equations for Fourier transform of density fluctuations are given by,

$$\delta \tilde{n}_n(\vec{k}, \omega) = i \frac{[1 + F_0^{pp} \chi_p(\vec{k}, \omega)] A_n(\vec{k}, \omega) - F_0^{np} \chi_n(\vec{k}, \omega) A_p(\vec{k}, \omega)}{\epsilon(\vec{k}, \omega)} \quad (2.40)$$

and

$$\delta \tilde{n}_p(\vec{k}, \omega) = i \frac{[1 + F_0^{nn} \chi_n(\vec{k}, \omega)] A_p(\vec{k}, \omega) - F_0^{pn} \chi_p(\vec{k}, \omega) A_n(\vec{k}, \omega)}{\epsilon(\vec{k}, \omega)}, \quad (2.41)$$

where the quantity

$$\epsilon(\vec{k}, \omega) = 1 + F_0^{nn} \chi_n(\vec{k}, \omega) + F_0^{pp} \chi_p(\vec{k}, \omega) + [F_0^{nn} F_0^{pp} - F_0^{np} F_0^{pn}] \chi_n(\vec{k}, \omega) \chi_p(\vec{k}, \omega) \quad (2.42)$$

denotes the susceptibility and $\varepsilon(\vec{k}, \omega) = 0$ gives the dispersion relation. The sign of the susceptibility gives information about the border of the spinodal region, in unstable region $\varepsilon(\vec{k}, \omega) < 0$ and in stable region $\varepsilon(\vec{k}, \omega) > 0$. In the infinite nuclear matter collective modes are characterized by wave number \vec{k} . The solution of dispersion relation gives characteristic frequencies $\pm\omega_k$ for every wave number, in the stable region, $\rho > \rho_{critical}$, frequencies are real and for unstable modes, $\rho < \rho_{critical}$, they are imaginary.

Time dependence of Fourier transform of density fluctuations $\delta\tilde{n}_a(\vec{k}, t)$ is determined by taking the inverse transformation of Eqs. (2.40) and (2.41) [26]. The inverse Fourier transformations in time can be calculated with the help of residue theorem,

$$\delta\tilde{n}_a(\vec{k}, t) = \int_{-\infty+i\sigma}^{\infty+i\sigma} \frac{d\omega}{2\pi} \delta\tilde{n}_a(\vec{k}, \omega) e^{-i\omega t} \quad (2.43)$$

keeping only the growing and decaying collective poles at $\omega = \mp i\Gamma$, because frequencies are imaginary in the spinodal region. The details of this transformation is given in Appendix B. Therefore we find

$$\begin{aligned} \delta\tilde{n}_n(\vec{k}, t) &= \frac{1}{2\pi}(2\pi i) i \left\{ \frac{[1 + F_0^{pp} \chi_p(\vec{k}, i\Gamma)] A_n(\vec{k}, i\Gamma) - F_0^{np} \chi_n(\vec{k}, i\Gamma) A_p(\vec{k}, i\Gamma)}{[\partial\varepsilon(\vec{k}, \omega)/\partial\omega]_{\omega=i\Gamma}} \right. \\ &+ \left. \frac{[1 + F_0^{pp} \chi_p(\vec{k}, -i\Gamma)] A_n(\vec{k}, -i\Gamma) - F_0^{np} \chi_n(\vec{k}, -i\Gamma) A_p(\vec{k}, -i\Gamma)}{[\partial\varepsilon(\vec{k}, \omega)/\partial\omega]_{\omega=-i\Gamma}} \right\}, \end{aligned} \quad (2.44)$$

and

$$\begin{aligned} \delta\tilde{n}_p(\vec{k}, t) &= \frac{1}{2\pi}(2\pi i) i \left\{ \frac{[1 + F_0^{nn} \chi_n(\vec{k}, i\Gamma)] A_p(\vec{k}, i\Gamma) - F_0^{pn} \chi_p(\vec{k}, i\Gamma) A_n(\vec{k}, i\Gamma)}{[\partial\varepsilon(\vec{k}, \omega)/\partial\omega]_{\omega=i\Gamma}} \right. \\ &+ \left. \frac{[1 + F_0^{nn} \chi_n(\vec{k}, -i\Gamma)] A_p(\vec{k}, -i\Gamma) - F_0^{pn} \chi_p(\vec{k}, -i\Gamma) A_n(\vec{k}, -i\Gamma)}{[\partial\varepsilon(\vec{k}, \omega)/\partial\omega]_{\omega=-i\Gamma}} \right\}. \end{aligned} \quad (2.45)$$

Growth and decay rates at poles $\omega = \mp i\Gamma_k$ are determined from the dispersion relation $\varepsilon(\vec{k}, \omega) = 0$, i.e. from the roots of susceptibility. Therefore in the short notation,

$$\delta\tilde{n}_a(\vec{k}, t) = \delta n_a^+(\vec{k}) e^{+\Gamma_k t} + \delta n_a^-(\vec{k}) e^{-\Gamma_k t}, \quad (2.46)$$

where the initial amplitude of density fluctuations are given by

$$\delta n_n^{\mp}(\vec{k}) = - \left\{ \frac{[1 + F_0^{pp} \chi_p(\vec{k}, \omega)] A_n(\vec{k}, \omega) - F_0^{np} \chi_n(\vec{k}, \omega) A_p(\vec{k}, \omega)}{\partial \varepsilon(\vec{k}, \omega) / \partial \omega} \right\}_{\omega = \mp i \Gamma_k}, \quad (2.47)$$

and

$$\delta n_p^{\mp}(\vec{k}) = - \left\{ \frac{[1 + F_0^{nn} \chi_n(\vec{k}, \omega)] A_p(\vec{k}, \omega) - F_0^{pn} \chi_p(\vec{k}, \omega) A_n(\vec{k}, \omega)}{\partial \varepsilon(\vec{k}, \omega) / \partial \omega} \right\}_{\omega = \mp i \Gamma_k}. \quad (2.48)$$

As an example, Fig. 2.1(a) shows the growth rates of unstable modes as a function of wave number in the spinodal region corresponding to initial density $n = 0.2 n_0$ and $n = 0.4 n_0$ for initial asymmetry $I = 0.0$ at a temperature $T = 5 \text{ MeV}$. The initial charge asymmetry is defined according to $I = (n_n^0 - n_p^0) / (n_n^0 + n_p^0)$. In this figure and also in other figures, solid-lines and dashed-lines show quantal and semi-classical results, respectively. Since, at low densities, wave numbers of most unstable modes are comparable to Fermi momentum, long-wavelength expansion of the Lindhard function is not valid, and hence there is important quantal effect in the dispersion relation. For example, for density $n = 0.2 n_0$, the temperature $T = 5 \text{ MeV}$ and initial charge asymmetry $I = 0.0$ the wave numbers of the most growing modes are around $k \approx 0.8 \text{ fm}^{-1}$ and for the same conditions the Fermi momentum is around $k \approx 0.78 \text{ fm}^{-1}$. At the initial density $n = 0.2 n_0$ and the initial asymmetry $I = 0.0$, i.e. symmetric nuclear matter, in the quantal calculations unstable modes are confined to a narrower range centered around wavelengths $\lambda \approx 8 - 10 \text{ fm}$, as compared to a broader range centered around $\lambda \approx 7 \text{ fm}$ in the semi-classical calculations. Growth rates in semi-classical framework are determined by the roots of semi-classical susceptibility, which is defined as in Eq. (2.42) by taking the Lindhard functions $\chi_a(\vec{k}, \omega)$ in the long wavelength limit given by Eq. (2.58). As a result, in the quantal calculations, the source has a tendency to break up into larger fragments as compared to the semi-classical calculations. Also, due to quantum effects, the maximum of dispersion relation is reduced by about a factor 1/4. Therefore, fluctuations take more time to develop when quantum effects are introduced. At higher initial density $n = 0.4 n_0$, in both quantal and semi-classical calculations, dispersion relation is shifted towards longer wavelengths and it exhibits a similar trend as the one at the initial density $n = 0.2 n_0$. This quantal

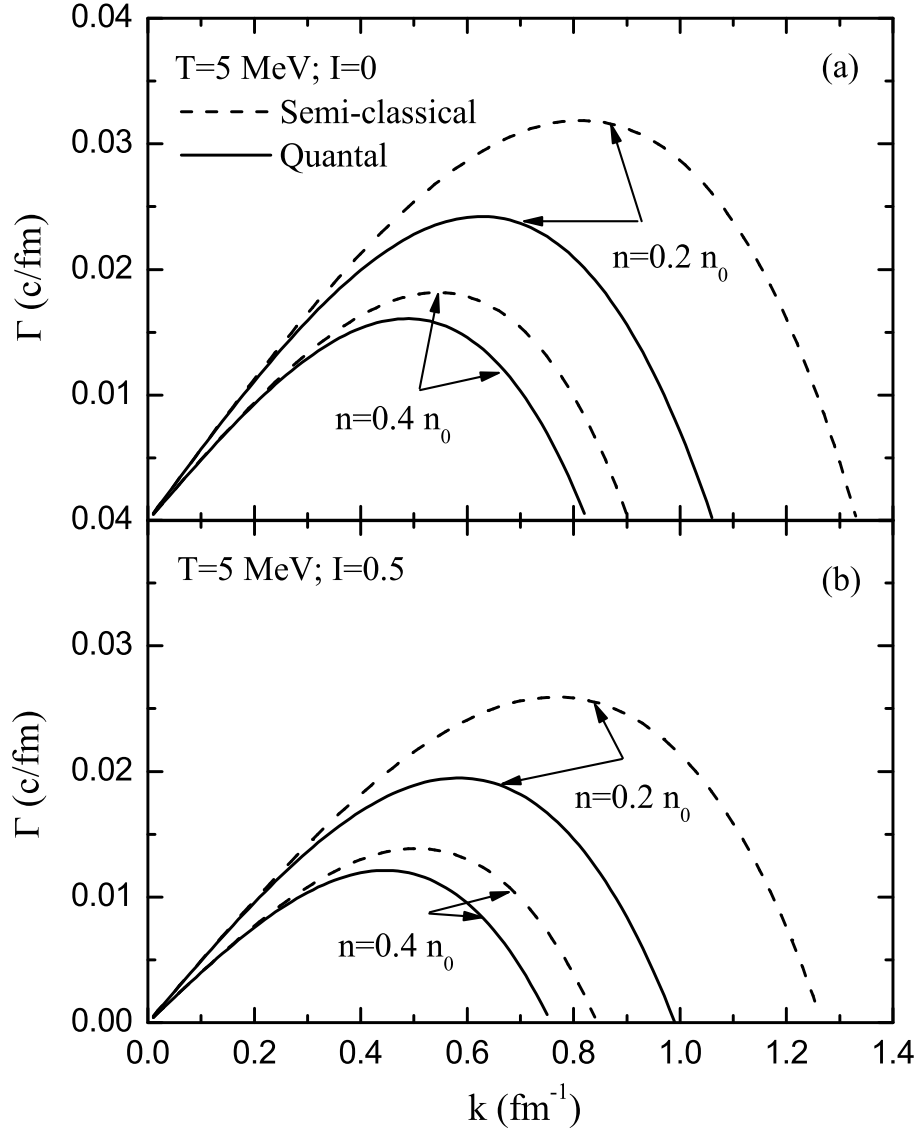


Figure 2.1: Growth rates of unstable modes as a function of wave number in spinodal region corresponding initial densities and at a temperature $T = 5$ MeV. (a) for initial asymmetry $I = 0.0$, (b) for initial asymmetry $I = 0.5$.

effect in dispersion relation of unstable modes was pointed out in the case of symmetric matter in a previous publication [27]. Charge asymmetric nuclear matter exhibits a similar behavior as seen from figure 2.1(b), which shows dispersion relation corresponding to initial densities $n = 0.2 n_0$ and $n = 0.4 n_0$ for initial charge asymmetry

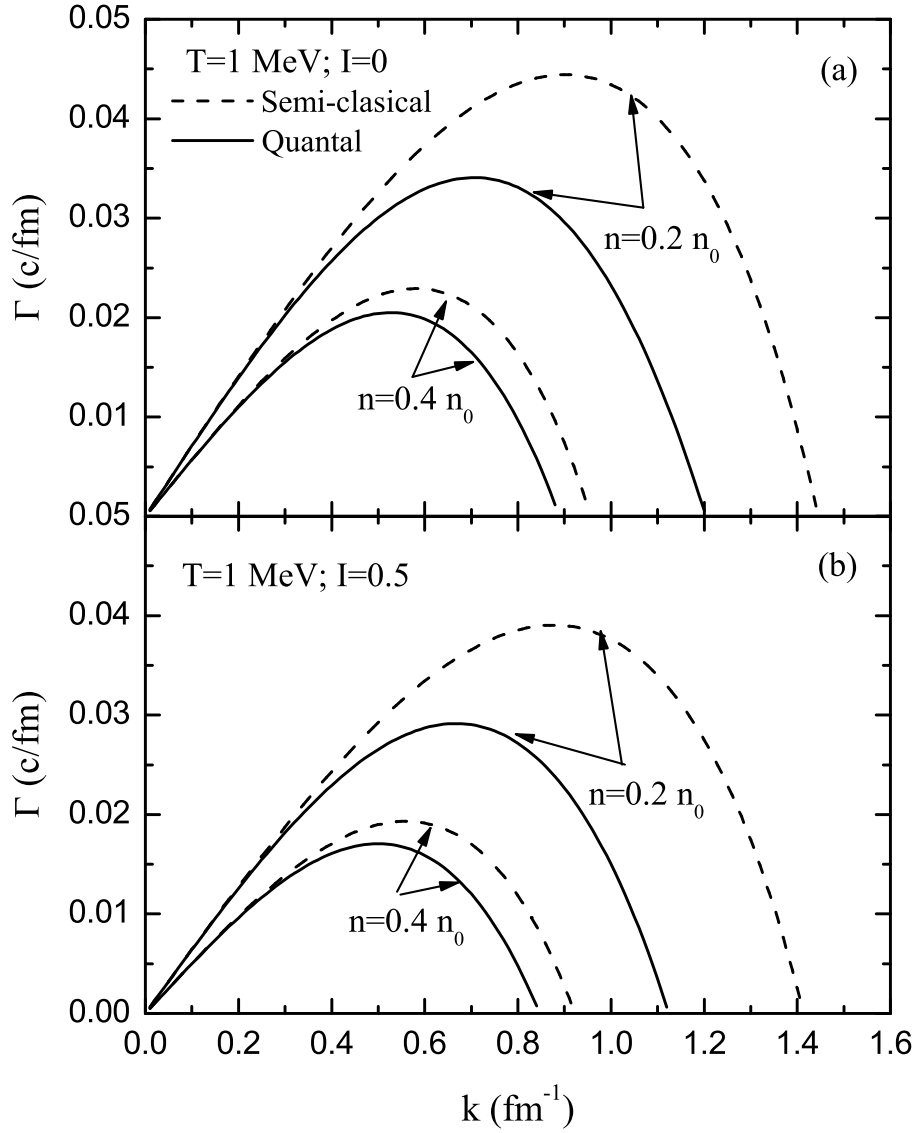


Figure 2.2: Same as Fig. 2.1 but for temperature $T = 1$ MeV.

$I = 0.5$ (i.e. neutron rich nuclear matter) at a temperature $T = 5$ MeV. Similar results can be seen for $T = 1$ MeV in Figs. 2.1(a) and 2.1(b).

Figs. 2.3(a) and 2.3(b) shows the boundary of spinodal region in density-temperature plane corresponding to initial charge asymmetries $I = 0.0$ and $I = 0.5$ for the unstable modes with wavelengths $\lambda = 9$ fm and $\lambda = 12$ fm, respectively. It is seen that with

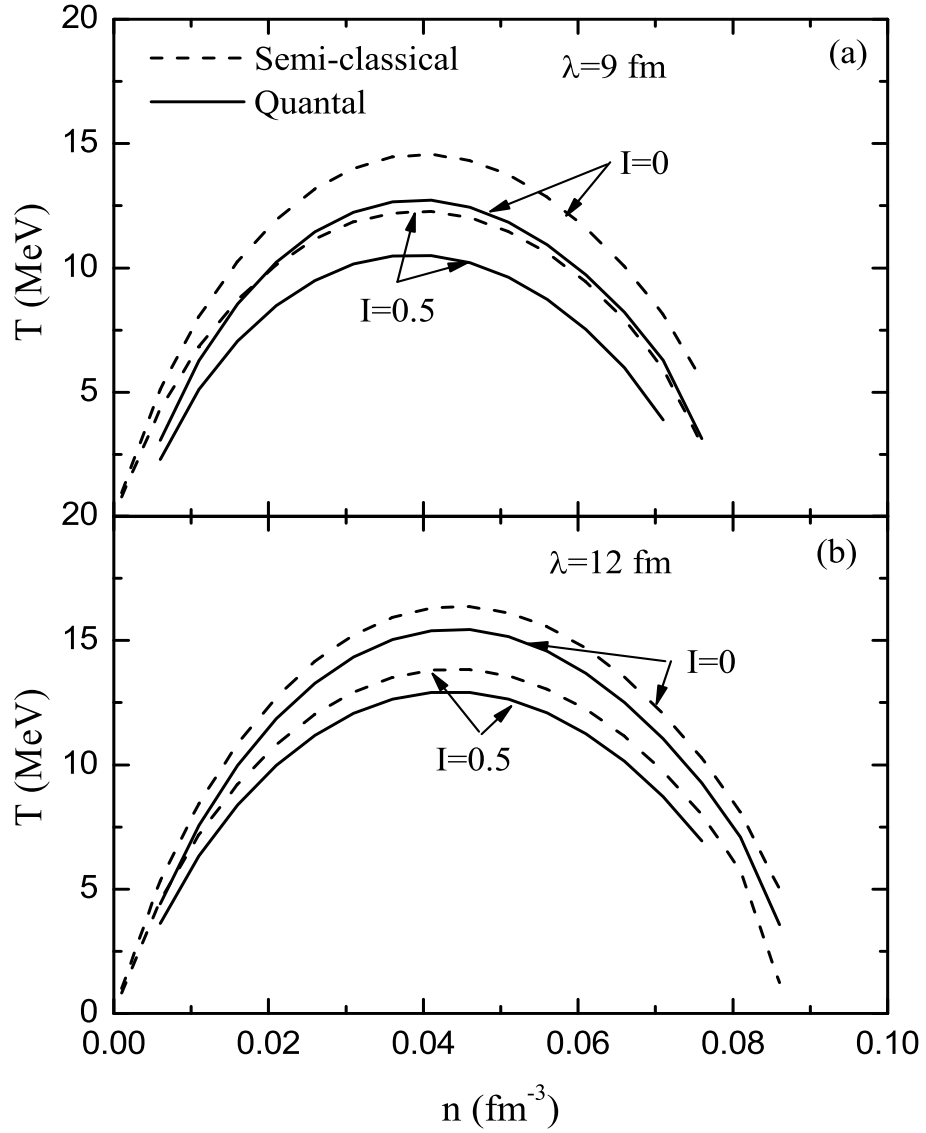


Figure 2.3: Boundary of spinodal region in density-temperature plane corresponding to initial charge asymmetries $I = 0.0$ and $I = 0.5$ for the unstable mode: (a) with wavelength $\lambda = 9 \text{ fm}$, (b) with wavelength $\lambda = 12 \text{ fm}$.

increasing charge asymmetry, spinodal region shrinks to smaller size in both quantal and semi-classical calculations. Furthermore, unstable modes are quite suppressed by quantal effects as compared to the semi-classical results in both symmetric and asymmetric matter. Results of semi-classical calculation are in agreement with the

results obtained in reference [21].

2.4.2 Growth of Density Fluctuations

In order to characterize the density fluctuations $\delta\tilde{n}_a(\vec{k}, t)$ away from the ensemble average $\tilde{n}_a(\vec{k}, 0)$ it is suitable to use the correlation function for the single particle density matrix. For this purpose in this subsection, we calculate early growth of local density fluctuations in charge asymmetric nuclear matter. Spectral intensity of density correlation function $\tilde{\sigma}_{ab}(\vec{k}, t)$ is related to the second moment of Fourier transform of density fluctuations according to,

$$\begin{aligned} \tilde{\sigma}_{ab}(\vec{k}, t)(2\pi)^3\delta(\vec{k} - \vec{k}') &= \overline{\delta\tilde{n}_a(\vec{k}, t)\delta\tilde{n}_b(-\vec{k}', t)} \\ &= \overline{\delta n_a^+(\vec{k})\delta n_b^+(-\vec{k}')e^{2\Gamma kt}} + \overline{\delta n_a^+(\vec{k})\delta n_b^-(-\vec{k}')} + \overline{\delta n_a^-(\vec{k})\delta n_b^+(-\vec{k}')} + \overline{\delta n_a^-(\vec{k})\delta n_b^-(-\vec{k}')}e^{-2\Gamma kt}. \end{aligned} \quad (2.49)$$

For neutron-neutron we obtain

$$\begin{aligned} \overline{\delta\tilde{n}_n(\vec{k}, t)\delta\tilde{n}_n(-\vec{k}', t)} &= \frac{e^{2\Gamma kt}}{\left[\frac{\partial\varepsilon(\vec{k}, \omega)}{\partial\omega}\right]_{\omega=i\Gamma}\left[\frac{\partial\varepsilon(-\vec{k}', \omega)}{\partial\omega}\right]_{\omega=i\Gamma}} \\ &\times \left\{ [1 + F_0^{pp}\chi_p]^2 \overline{A_n(\vec{k}, i\Gamma)A_n(-\vec{k}', i\Gamma)} + [F_0^{np}\chi_n]^2 \overline{A_p(\vec{k}, i\Gamma)A_p(-\vec{k}', i\Gamma)} \right\} \\ &+ \frac{e^{-2\Gamma kt}}{\left[\frac{\partial\varepsilon(\vec{k}, \omega)}{\partial\omega}\right]_{\omega=-i\Gamma}\left[\frac{\partial\varepsilon(-\vec{k}', \omega)}{\partial\omega}\right]_{\omega=-i\Gamma}} \\ &\times \left\{ [1 + F_0^{pp}\chi_p]^2 \overline{A_n(\vec{k}, -i\Gamma)A_n(-\vec{k}', -i\Gamma)} + [F_0^{np}\chi_n]^2 \overline{A_p(\vec{k}, -i\Gamma)A_p(-\vec{k}', -i\Gamma)} \right\} \\ &+ \frac{2}{\left[\frac{\partial\varepsilon(\vec{k}, \omega)}{\partial\omega}\right]_{\omega=i\Gamma}\left[\frac{\partial\varepsilon(-\vec{k}', \omega)}{\partial\omega}\right]_{\omega=-i\Gamma}} \\ &\times \left\{ [1 + F_0^{pp}\chi_p]^2 \overline{A_n(\vec{k}, i\Gamma)A_n(-\vec{k}', -i\Gamma)} + [F_0^{np}\chi_n]^2 \overline{A_p(\vec{k}, i\Gamma)A_p(-\vec{k}', -i\Gamma)} \right\}, \end{aligned} \quad (2.50)$$

for proton-proton

$$\begin{aligned}
\overline{\delta\tilde{n}_p(\vec{k}, t)\delta\tilde{n}_p(-\vec{k}', t)} &= \frac{e^{2\Gamma_k t}}{\left[\frac{\partial\varepsilon(\vec{k}, \omega)}{\partial\omega}\right]_{\omega=i\Gamma}\left[\frac{\partial\varepsilon(-\vec{k}', \omega)}{\partial\omega}\right]_{\omega=i\Gamma}} \\
&\times \left\{ [1 + F_0^{nm}\chi_n]^2 \overline{A_p(\vec{k}, i\Gamma)A_p(-\vec{k}', i\Gamma)} + [F_0^{pn}\chi_p]^2 \overline{A_n(\vec{k}, i\Gamma)A_n(-\vec{k}', i\Gamma)} \right\} \\
&+ \frac{e^{-2\Gamma_k t}}{\left[\frac{\partial\varepsilon(\vec{k}, \omega)}{\partial\omega}\right]_{\omega=-i\Gamma}\left[\frac{\partial\varepsilon(-\vec{k}', \omega)}{\partial\omega}\right]_{\omega=-i\Gamma}} \\
&\times \left\{ [1 + F_0^{nm}\chi_n]^2 \overline{A_p(\vec{k}, -i\Gamma)A_p(-\vec{k}', -i\Gamma)} + [F_0^{pn}\chi_p]^2 \overline{A_n(\vec{k}, -i\Gamma)A_n(-\vec{k}', -i\Gamma)} \right\} \\
&+ \frac{2}{\left[\frac{\partial\varepsilon(\vec{k}, \omega)}{\partial\omega}\right]_{\omega=i\Gamma}\left[\frac{\partial\varepsilon(-\vec{k}', \omega)}{\partial\omega}\right]_{\omega=-i\Gamma}} \\
&\times \left\{ [1 + F_0^{nm}\chi_n]^2 \overline{A_p(\vec{k}, i\Gamma)A_p(-\vec{k}', -i\Gamma)} + [F_0^{pn}\chi_p]^2 \overline{A_n(\vec{k}, i\Gamma)A_n(-\vec{k}', -i\Gamma)} \right\},
\end{aligned} \tag{2.51}$$

and neutron-proton

$$\begin{aligned}
\overline{\delta\tilde{n}_n(\vec{k}, t)\delta\tilde{n}_p(-\vec{k}', t)} &= \frac{e^{2\Gamma_k t}}{\left[\frac{\partial\varepsilon(\vec{k}, \omega)}{\partial\omega}\right]_{\omega=i\Gamma}\left[\frac{\partial\varepsilon(-\vec{k}', \omega)}{\partial\omega}\right]_{\omega=i\Gamma}} \\
&\times \left\{ [1 + F_0^{pp}\chi_p]F_0^{pn}\chi_p \overline{A_n(\vec{k}, i\Gamma)A_n(-\vec{k}', i\Gamma)} \right. \\
&\quad \left. + [1 + F_0^{nm}\chi_n]F_0^{np}\chi_n \overline{A_p(\vec{k}, i\Gamma)A_p(-\vec{k}', i\Gamma)} \right\} \\
&+ \frac{e^{-2\Gamma_k t}}{\left[\frac{\partial\varepsilon(\vec{k}, \omega)}{\partial\omega}\right]_{\omega=-i\Gamma}\left[\frac{\partial\varepsilon(-\vec{k}', \omega)}{\partial\omega}\right]_{\omega=-i\Gamma}} \\
&\times \left\{ [1 + F_0^{pp}\chi_p]F_0^{pn}\chi_p \overline{A_n(\vec{k}, -i\Gamma)A_n(-\vec{k}', -i\Gamma)} \right. \\
&\quad \left. + [1 + F_0^{nm}\chi_n]F_0^{np}\chi_n \overline{A_p(\vec{k}, -i\Gamma)A_p(-\vec{k}', -i\Gamma)} \right\} \\
&+ \frac{2}{\left[\frac{\partial\varepsilon(\vec{k}, \omega)}{\partial\omega}\right]_{\omega=i\Gamma}\left[\frac{\partial\varepsilon(-\vec{k}', \omega)}{\partial\omega}\right]_{\omega=-i\Gamma}} \\
&\times \left\{ [1 + F_0^{pp}\chi_p]F_0^{pn}\chi_p \overline{A_n(\vec{k}, i\Gamma)A_n(-\vec{k}', -i\Gamma)} \right. \\
&\quad \left. + [1 + F_0^{nm}\chi_n]F_0^{np}\chi_n \overline{A_p(\vec{k}, i\Gamma)A_p(-\vec{k}', -i\Gamma)} \right\}
\end{aligned}$$

where the cross terms of source correlations are zero, i.e. $\overline{A_n(\vec{k}, i\Gamma)A_p(-\vec{k}', i\Gamma)} = \overline{A_p(\vec{k}, i\Gamma)A_n(-\vec{k}', i\Gamma)} = 0$, because of the statistical independence of the different parts of the source, the mean values of their products vanish. The details of these derivations can be seen in Appendix C.

We calculate the spectral functions using the solution (2.46) and employing expression (2.24) for the initial correlations to find

$$\tilde{\sigma}_{ab}(\vec{k}, t) = \frac{E_{ab}^+(\vec{k}, i\Gamma_k)}{[|\partial\varepsilon(\vec{k}, \omega)/\partial\omega|_{\omega=i\Gamma_k}]^2} (e^{2\Gamma_k t} + e^{-2\Gamma_k t}) + \frac{2E_{ab}^-(\vec{k}, i\Gamma_k)}{[|\partial\varepsilon(\vec{k}, \omega)/\partial\omega|_{\omega=i\Gamma_k}]^2}, \quad (2.52)$$

where quantities $E_{ab}^\mp(\vec{k}, i\Gamma_k)$, $a, b = n, p$, are given by

$$E_{nn}^\mp(\vec{k}, i\Gamma_k) = 4\hbar^2(1 + F_0^{pp}\chi_p)^2 I_n^\mp + 4\hbar^2(F_0^{np}\chi_n)^2 I_p^\mp, \quad (2.53)$$

$$E_{pp}^\mp(\vec{k}, i\Gamma_k) = 4\hbar^2(1 + F_0^{nn}\chi_n)^2 I_p^\mp + 4\hbar^2(F_0^{pn}\chi_p)^2 I_n^\mp, \quad (2.54)$$

and

$$E_{np}^\mp(\vec{k}, i\Gamma_k) = -4\hbar^2(1 + F_0^{pp}\chi_p)F_0^{pn}\chi_p I_n^\mp - 4\hbar^2(1 + F_0^{nn}\chi_n)F_0^{np}\chi_n I_p^\mp \quad (2.55)$$

with

$$I_a^\mp = \int \frac{d^3p}{(2\pi\hbar)^3} \frac{(\hbar\Gamma_k)^2 \mp (\vec{p} \cdot \hbar\vec{k}/m)^2}{[(\hbar\Gamma_k)^2 + (\vec{p} \cdot \hbar\vec{k}/m)^2]^2} f_0^a(\vec{p} + \hbar\vec{k}/2)[1 - f_0^a(\vec{p} - \hbar\vec{k}/2)]. \quad (2.56)$$

In the semi-classical calculations, instead of the TDHF equation in quantal approach, the Vlasov transport equation is used for the dynamics of the system. Semi-classical limit of quantal expressions are obtained by replacing the integrals I_a^\mp and $\chi_a(\vec{k}, \omega)$ with following expressions in the long wave-length limit,

$$I_a^\mp(sc) = \int \frac{d^3p}{(2\pi\hbar)^3} \frac{(\hbar\Gamma_k)^2 \mp (\vec{p} \cdot \hbar\vec{k}/m)^2}{[(\hbar\Gamma_k)^2 + (\vec{p} \cdot \hbar\vec{k}/m)^2]^2} f_0^a(\vec{p})[1 - f_0^a(\vec{p})], \quad (2.57)$$

and

$$\chi_a^{sc}(\vec{k}, \omega) = -2 \int_{-\infty}^{\infty} \frac{d^3p}{(2\pi\hbar)^3} \frac{(\vec{p} \cdot \hbar\vec{k}/m)^2}{(\hbar\Gamma_k)^2 + (\vec{p} \cdot \hbar\vec{k}/m)^2} \frac{\partial}{\partial\varepsilon} f_0^a. \quad (2.58)$$

Figs. 2.4(a) and 2.4(b) shows spectral intensity $\tilde{\sigma}_{nn}(\vec{k}, t)$ of neutron-neutron density correlation function as function of wave number at times $t = 0$ and $t = 50$ fm/c for density $n = 0.4 n_0$ and the initial charge asymmetry $I = 0.5$ at temperature $T = 1$ MeV and $T = 5$ MeV, respectively.

As mentioned above, in all figures solid-lines and dashed-lines indicate quantal and semi-classical results, respectively. As seen, in particular at towards the high end of the wave number spectrum, considerable quantal effects are present at initial fluctuations. Quantum statistical effects in the initial fluctuations become even larger at

smaller temperatures. In fact at zero temperature, since the quantities $I_a^\mp(sc)$ becomes zero, spectral functions vanish $\tilde{\sigma}_{ab}(\vec{k}, t) = 0$. However, in quantal calculations spectral functions remains finite even at zero temperature, reflecting quantum zero point fluctuations of the local density. Looking at the results at $t = 50$ fm/c, we observe that largest growth occurs over the range of wave numbers corresponding to the range of dominant unstable modes. At $T = 5$ MeV, magnitude of fluctuations is about the same in both quantal and semi-classical calculations. At the lower temperature $T = 1$ MeV, magnitude of fluctuations in the most unstable range is nearly doubled in quantal calculations as compared to semi-classical calculations. Fig. 2.4(c) shows spectral intensity $\tilde{\sigma}_{nn}(\vec{k}, t)$ as function of wave number at times $t = 0$ and $t = 50$ fm/c at a lower density $n = 0.2 n_0$ for initial charge asymmetry $I = 0.5$ and temperature $T = 5$ MeV. At the lower density, growth rates of dominant modes in the semi-classical limit are considerably larger than those of quantal calculations. Consequently, the result of semi-classical calculations at time $t = 50$ fm/c overshoots the result of quantal calculations over the range of dominant modes. Fig. 2.5 illustrates that the spectral intensity for symmetric matter has similar properties as for asymmetric matter with $I = 0.0$.

We note that quantal effects enter into the spectral density in two different ways: (i) quantal effects in growth rates of modes and (ii) quantum statistical effects on the initial density fluctuations, which becomes increasingly more important at lower temperatures. We also note that in determining time evolution of $\delta\tilde{n}(\vec{k}, t)$ with the help of residue theorem, there are other contributions arising from non-collective poles of susceptibility $\epsilon(\vec{k}, \omega)$ and from poles of $A_a(\vec{k}, \omega)$. These contributions, in particular towards short wavelengths, are important at the initial state, however they damp out in a short time interval [28]. Therefore the approximate expression (2.52) for the spectral intensity $\tilde{\sigma}(\vec{k}, t)$ of density fluctuations becomes more accurate for increasing time.

Local density fluctuations $\delta n_a(\vec{r}, t)$ are determined by the Fourier transform of $\delta\tilde{n}_a(\vec{k}, t)$. In terms of spectral intensity $\tilde{\sigma}_{ab}(\vec{k}, t)$, which is defined in Eq. (2.49), equal time density correlation function as a function of distance between two space locations is

expressed as,

$$\sigma_{ab}(|\vec{r} - \vec{r}'|, t) = \overline{\delta n_a(\vec{r}, t) \delta n_b(\vec{r}', t)} = \int \frac{d^3 k}{(2\pi)^3} e^{i\vec{k} \cdot (\vec{r} - \vec{r}')} \tilde{\sigma}_{ab}(\vec{k}, t). \quad (2.59)$$

In a homogenous isotropic medium, the correlation function depends only on the magnitude $r = |\vec{r} - \vec{r}'|$ of the distance between two space points. In the limit $r \rightarrow \infty$, the fluctuations at the points \vec{r}_1, \vec{r}_2 are statistically independent, therefore correlation function becomes zero [29]. Total density correlation function is given by sum over neutrons and protons and cross-term, $\sigma(|\vec{r} - \vec{r}'|, t) = \sigma_{nn}(|\vec{r} - \vec{r}'|, t) + \sigma_{pp}(|\vec{r} - \vec{r}'|, t) + 2\sigma_{np}(|\vec{r} - \vec{r}'|, t)$. The behavior of density correlation function as a function of initial density and temperature carries valuable information about the unstable dynamics of the matter in the spinodal region. As an example, Figs. 2.6(a) and 2.6(b) illustrate total density correlation function as a function of distance between two space points at times $t = 0$ and $t = 50 \text{ fm}/c$ at density $n = 0.4 n_0$ and the initial charge asymmetry $I = 0.5$ for temperatures $T = 1 \text{ MeV}$ and $T = 5 \text{ MeV}$, respectively. At temperature $T = 5 \text{ MeV}$, quantal effects are not important, and hence semi-classical calculations provide good approximation for density correlation function. However, at lower temperature $T = 1 \text{ MeV}$, semi-classical calculations severely underestimates peak value of density correlation function. Fig. 2.6(c) shows density correlation function at times $t = 0$ and $t = 50 \text{ fm}/c$ at a lower density $n = 0.2 n_0$ for initial charge asymmetry $I = 0.5$ and a temperature $T = 5 \text{ MeV}$. On the other hand, at lower density, semi-classical approximation overestimates the peak value of the correlation function. As indicated above, this is due to the fact that growth rates of dominant modes in semi-classical limit are considerable larger than those obtained in quantal calculations. For asymmetry $I = 0.0$, as seen from Fig. 2.7, behavior of density correlation function is similar to the charge asymmetric case. Complementary to the dispersion relation, correlation length of density fluctuations provides an additional measure for the average size of primary fragmentation pattern. We can estimate the correlation length of density fluctuations as the width of correlation function at half maximum. Correlation length depends on density, and to some extent, depends on temperature as well. From these figures, we can estimate that the correlation length of density fluctuations is about 3.5 fm at density $n = 0.4 n_0$, and about 3.0 fm at density $n = 0.2 n_0$.

During spinodal decomposition, initial charge asymmetry shifts towards symmetry in liquid phase while gas phase moves toward further asymmetry. As a result, produced fragments are more symmetric than the charge asymmetry of the source. This interesting fact is experimentally observed and it may provide a useful guidance to gain information about symmetry energy in low density nuclear matter. For each event, we can define perturbation charge asymmetry during early evolution of density fluctuations as,

$$I_{pt} = \frac{\delta n_n(\vec{r}, t) - \delta n_p(\vec{r}, t)}{\delta n_n(\vec{r}, t) + \delta n_p(\vec{r}, t)} = \frac{[\delta n_n(\vec{r}, t)]^2 - [\delta n_p(\vec{r}, t)]^2}{[\delta n_n(\vec{r}, t) + \delta n_p(\vec{r}, t)]^2}. \quad (2.60)$$

We are interested in the ensemble average value of this quantity, which can approximately be evaluated according to

$$\bar{I}_{pt} \approx \frac{\sigma_{nn}(t) - \sigma_{pp}(t)}{\sigma_{nn}(t) + 2\sigma_{np}(t) + \sigma_{pp}(t)}. \quad (2.61)$$

where $\sigma_{ab}(t) = \sigma_{ab}(x = 0, t)$. The average value of the perturbation asymmetry is nearly independent of time. As an example, Fig. 2.8 shows this quantity as function of initial asymmetry at temperature $T = 5 \text{ MeV}$ for densities $n = 0.2 n_0$ and $n = 0.4 n_0$. As a result of the driving force of symmetry energy, perturbation asymmetry drifts towards symmetry. At this temperature quantal effects do not play an important role and these calculations are consistent with results of ref. [21].

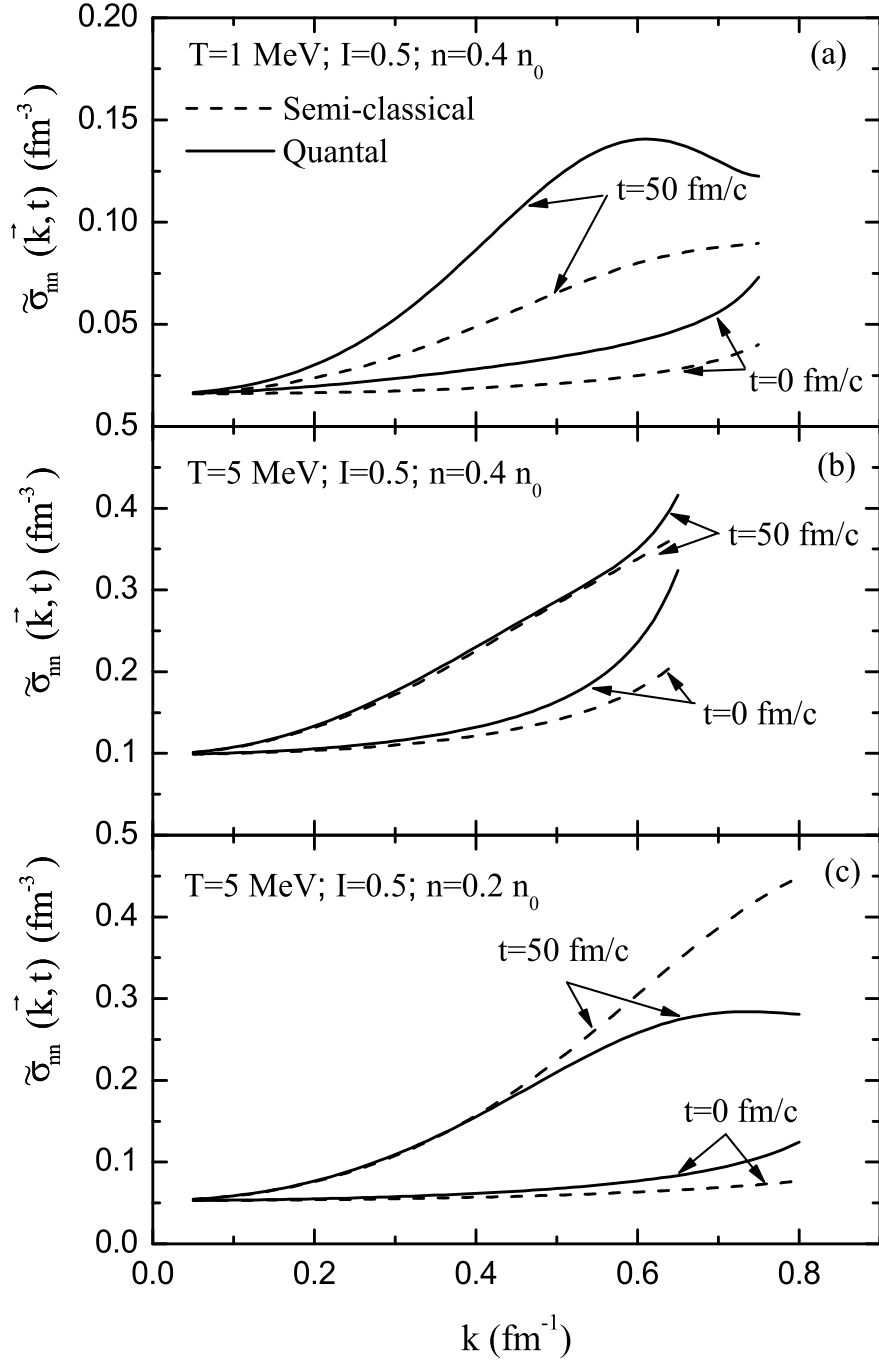


Figure 2.4: Spectral intensity $\tilde{\sigma}_{nn}(\vec{k}, t)$ of neutron-neutron density correlation function as function of wave number k at times $t = 0$ and $t = 50 \text{ fm}/c$ for the initial charge asymmetry $I = 0.5$: (a) for density $n = 0.4 n_0$ at temperature $T = 1 \text{ MeV}$, (b) for density $n = 0.4 n_0$ at temperature $T = 5 \text{ MeV}$, (c) for density $n = 0.2 n_0$ at temperature $T = 5 \text{ MeV}$.

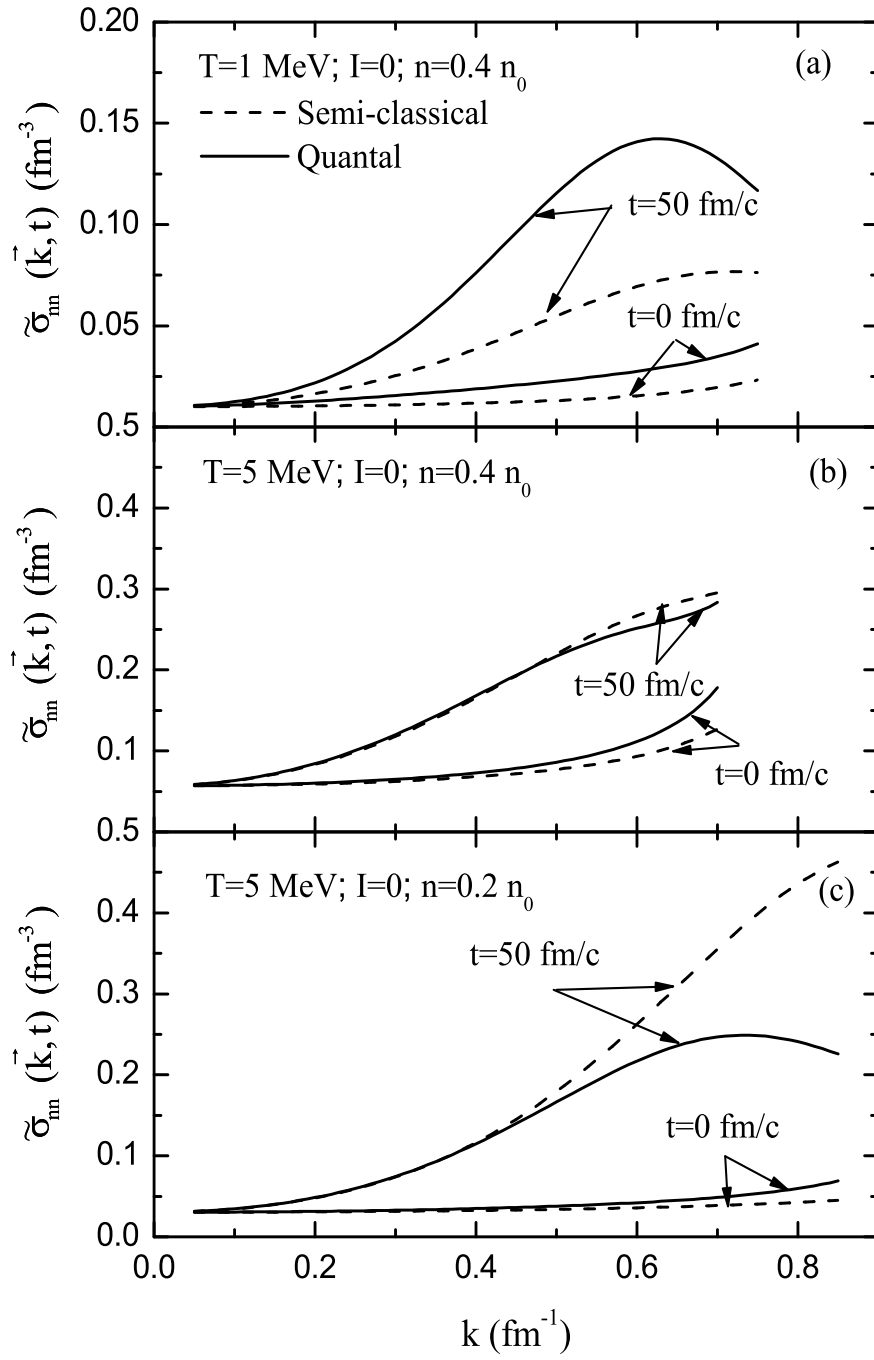


Figure 2.5: Same as Fig. 2.4 but for asymmetry $I = 0.0$.

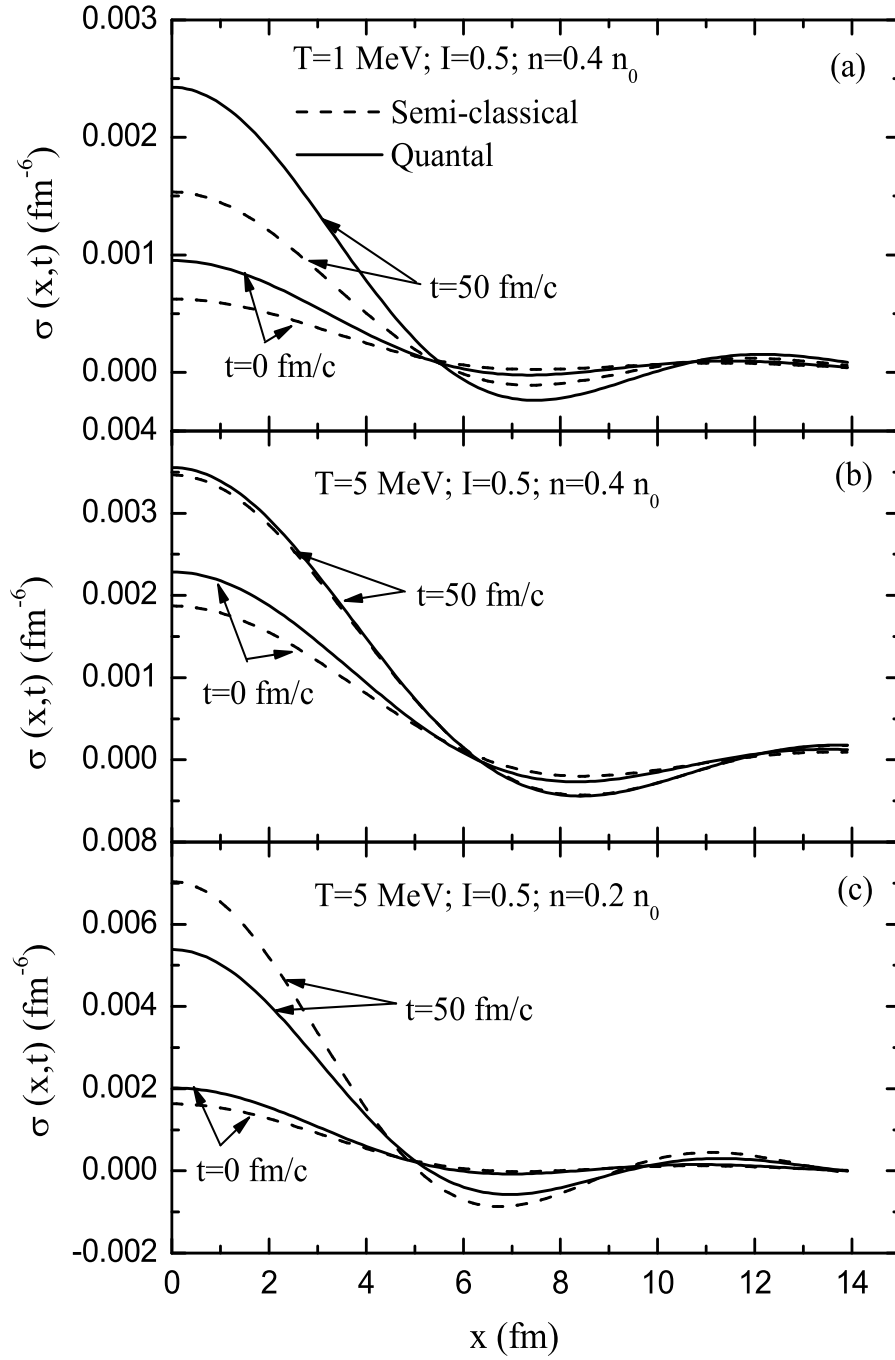


Figure 2.6: Density correlation function $\sigma(x, t)$ as a function of distance $x = |\vec{r} - \vec{r}'|$ between two space points at times $t = 0$ and $t = 50 \text{ fm}/c$ and the initial charge asymmetry $I = 0.5$: (a) for density $n = 0.4 n_0$ at temperature $T = 1 \text{ MeV}$, (b) for density $n = 0.4 n_0$ at temperature $T = 5 \text{ MeV}$, (c) for density $n = 0.2 n_0$ at temperature $T = 5 \text{ MeV}$.

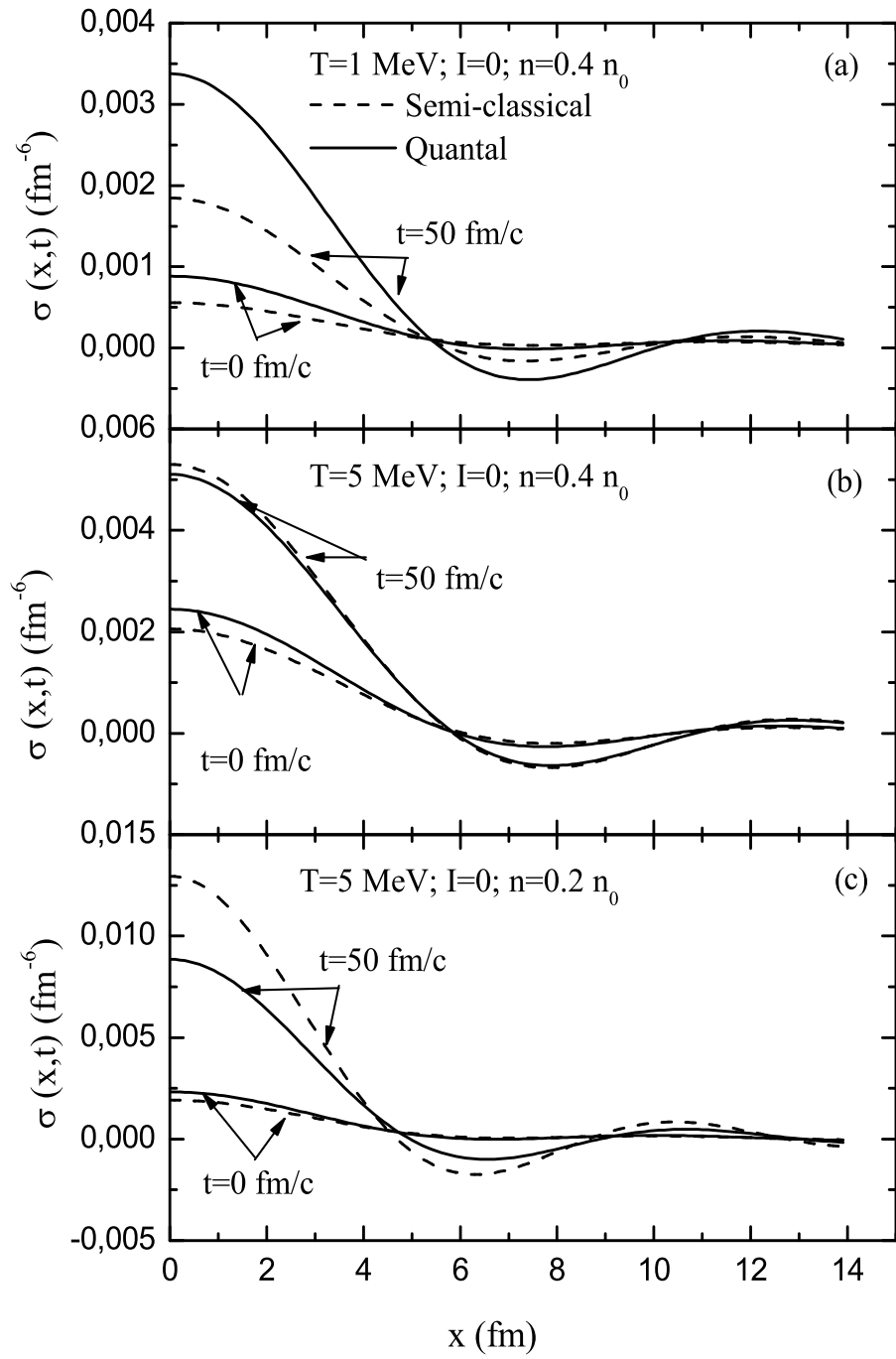


Figure 2.7: Same as Fig. 2.6 but for asymmetry $I = 0.0$.

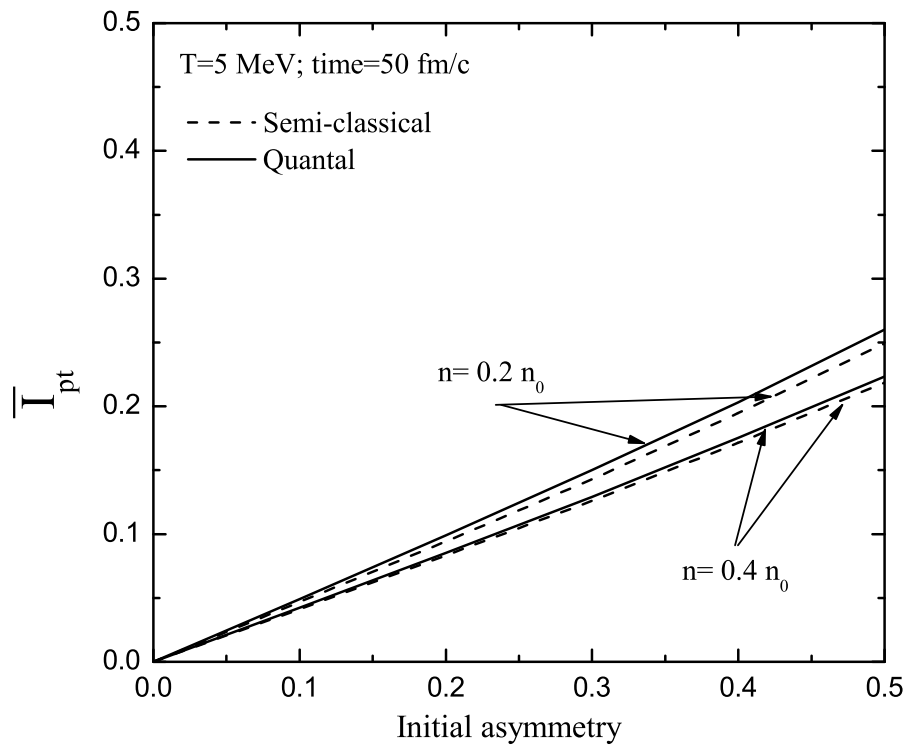


Figure 2.8: Perturbation asymmetry as function of initial asymmetry at temperature $T = 5 \text{ MeV}$ for densities $n = 0.2 n_0$ and $n = 0.4 n_0$.

CHAPTER 3

SPINODAL INSTABILITIES IN SYMMETRIC NUCLEAR MATTER IN A RELATIVISTIC MEAN-FIELD APPROACH

In the first part of this thesis, we use non-relativistic kinematics to investigate the spinodal instabilities in nuclear matter, because the relevant Fermi momenta and Fermi energy are small compared to the rest mass of the nucleons at those energies and densities. However, it has been shown in the recent years that the nuclear many-body system is in principle a relativistic system driven by the dynamics of large relativistic scalar and vector fields [30, 31]. In the nuclear interior we have an attractive scalar field ϕ of roughly -350 MeV and a repulsive vector field V_μ of roughly $+300 \text{ MeV}$. Both fields are by no means small against the nucleon mass of 939 MeV and therefore the dynamics has to be described by the Dirac equation. For the large components of the Dirac spinors the two fields nearly cancel each other and this leads to a relatively small attractive field of roughly -50 MeV and to a relatively small Fermi energy. However, for the small components both fields add up. This leads to a very large spin-orbit term known since the early days of nuclear physics [32, 33]. In the second part of the thesis, we use Quantum Hadrodynamics (QHD) as the framework to investigate the spinodal instabilities in symmetric nuclear matter. We employ the relativistic model introduced by Walecka [34, 35] known as QHD-I in the mean field approximation.

3.1 Relativistic Mean Field Model (Walecka Model)

The nuclear many-body as a relativistic system of baryons and mesons is described in a framework of quantum hydrodynamics (QHD) [30]. In the Walecka model the interaction between the nucleons are mediated by a scalar σ and a vector meson ω . A simple relativistic quantum field theory model for the nuclear many-body system is the Walecka model, known as QHD-I, consisting of baryon field ψ , neutral scalar meson field ϕ and neutral vector meson field V_μ .

The Lorentz invariant Lagrangian density of QHD-I is given by

$$\begin{aligned} \mathcal{L} = & \bar{\psi} \left[\gamma^\mu (i\partial_\mu - g_v V_\mu) - (M - g_s \phi) \right] \psi + \frac{1}{2} \partial_\mu \phi \partial^\mu \phi \\ & - \frac{1}{2} m_s^2 \phi^2 - \frac{1}{4} F_{\mu\nu} F^{\mu\nu} + \frac{1}{2} m_v^2 V_\mu V^\mu, \end{aligned} \quad (3.1)$$

where M is nucleon mass, m_s scalar meson mass and m_v vector meson mass, and the coupling constants of the mesons and the nucleon are denoted by g_s and g_v respectively, and $F_{\mu\nu} = \partial_\mu V_\nu - \partial_\nu V_\mu$. Using this Lagrangian density, one-meson exchange graphs evaluated in the limit of heavy, static baryons, result in an effective nucleon-nucleon potential of the form

$$V(r) = \frac{g_v^2}{4\pi} \frac{e^{-m_v r}}{r} - \frac{g_s^2}{4\pi} \frac{e^{-m_s r}}{r}, \quad (3.2)$$

which for the appropriate choices of the coupling constants and meson masses, is attractive at large distances and repulsive at short distances, as the observed nucleon-nucleon potential. The parameters in the Lagrangian density are obtained by the fitting of experimental data of nuclear matter in the mean field approximation. The equilibrium properties of nuclear matter, $k_F^0 = 1.3 fm^{-1}$ corresponding to $\rho_0 = 0.15 fm^{-3}$ and binding energy per nucleon $(E/A)_0 = -15.75 MeV$ are obtained with the choice of the coupling constants [32, 33]

$$C_s^2 \equiv g_s^2 \left(\frac{M^2}{m_s^2} \right) = 357.4, \quad C_v^2 \equiv g_v^2 \left(\frac{M^2}{m_v^2} \right) = 273.8. \quad (3.3)$$

In this approximation, the nuclear compression modulus is obtained as $K = 545 MeV$ which is larger than the experimental value, and the effective nucleon mass is $M^*/M = 0.541$.

The resulting field equations in QHD-I are

$$(\partial_\mu \partial^\mu + m_s^2)\phi = g_s \bar{\psi} \psi \quad (3.4)$$

$$\partial_\mu F^{\mu\nu} + m_v^2 V^\nu = g_v \bar{\psi} \gamma^\nu \psi \quad (3.5)$$

$$\left[\gamma^\mu (i\partial_\mu - g_v V_\mu) - (M - g_s \phi) \right] \psi = 0 \quad (3.6)$$

These are non-linear coupled quantum field theory equations and their exact solutions are extremely complicated. However, there is an approximate nonperturbative solution that can be used as starting point in analyzing the physical content of the above Lagrangian. For a uniform system of N nucleons in a volume V , as the nucleon density increases, the source terms in the above equations also increase, and when the source terms are large the meson fields in the mean-field approximation are considered as classical fields with the nucleons as their sources. Furthermore, if the nucleon density does not change appreciably in a time and space interval determined by the Compton wavelength of the mesons, the retardation effects for the meson fields can be neglected, and the time and space dependence of the meson fields will closely follow the time and space dependence of nucleon fields. In this local density approximation we can neglect the time and space derivatives in the meson field equations and obtain meson field as

$$m_v^2 V_0 = g_v \langle \psi^\dagger \psi \rangle \equiv g_v \rho_B, \quad (3.7)$$

$$m_v^2 \vec{V} = g_v \langle \psi^\dagger \vec{\gamma} \psi \rangle \equiv g_v \vec{\rho}_v, \quad (3.8)$$

and

$$m_s^2 \phi = g_s \langle \bar{\psi} \psi \rangle \equiv g_s \rho_s, \quad (3.9)$$

in terms of nucleon (baryon) density ρ_B , the scalar density ρ_s and the current density $\vec{\rho}_v$. For a static uniform system at equilibrium the classical fields ϕ and V_0 are constants and \vec{V} vanishes.

In mean-field theory, therefore, the nucleons are described by the Dirac equation

$$\left[\gamma_\mu (i\partial^\mu - g_v V^\mu) - (M - g_s \phi) \right] \psi = 0 \quad (3.10)$$

which is linear in the classical meson fields. Dirac equation for the nucleons may be solved directly [30]. In our investigation of spinodal instabilities in nuclear matter,

we use a semi-classical approximation based on a relativistic Vlasov equation, thus we neglect anti-baryon degrees of freedom. Therefore, the baryon density and energy density are given by [36]

$$\rho_B = \frac{g}{(2\pi)^3} \int d^3p f_0(\vec{p}) \quad (3.11)$$

$$\epsilon(\rho_B, T) = \frac{g_s^2}{2m_s^2} \rho_B^2 + \frac{2m_s^2}{g_s^2} (M - M^*)^2, \quad (3.12)$$

where the spin-isospin degeneracy factor is $g = 2$ for neutron matter and $g = 4$ for nuclear matter and the effective mass M^* is defined as,

$$M^* = M - g_s \phi, \quad (3.13)$$

therefore at thermodynamic equilibrium, the self-consistency relation

$$\phi = \frac{g_s}{m_s^2} \rho_s = \frac{g_s}{m_s^2} \frac{g}{(2\pi)^3} \int d^3p \frac{M^*}{\sqrt{\vec{p}^2 + M^{*2}}} f_0(\vec{p}) \quad (3.14)$$

must be satisfied. In these expressions, the thermal distribution function is defined by

$$f_0(\vec{p}) = \frac{1}{e^{\beta(E_p^* - \mu^*)} + 1}, \quad (3.15)$$

where $E_p^* = \sqrt{\vec{p}^2 + M^{*2}}$ and $\mu^* = \mu - g_v V_0$.

3.1.1 Stochastic Relativistic Mean-Field Theory

The stochastic mean-field approach is based on a very appealing stochastic mode proposed for describing deep-inelastic heavy-ion collisions and sub-barrier fusion [37, 38, 39]. In that model, dynamics of relative motion is coupled to collective surface modes of colliding ions and treated in a classical framework. The initial quantum zero point and thermal fluctuations are incorporated into the calculations in a stochastic manner by generating an ensemble of events according to the initial distribution of collective modes. In the mean-field evolution, coupling of relative motion with all other collective and non-collective modes are automatically taken into account. In the stochastic extension of the mean-field approach, the zero point and thermal fluctuations of the initial state are taken into account in a stochastic manner, in a similar manner presented in Refs. [37, 38, 39]. The initial fluctuations, which are specified

by a specific Gaussian random ensemble, are simulated by considering evolution of an ensemble of single-particle density matrices. It is possible to incorporate quantal and thermal fluctuations of the initial state into the relativistic mean-field description in a similar manner.

In Refs. [26, 36], the authors derived a relativistic Vlasov equation from the Walecka model in the local density and the semi-classical approximation. The details of this derivation can be seen in Appendix D. Introducing phase space distribution function $f(\vec{r}, \vec{p}, t)$ for the nucleons, the following relativistic Vlasov equation has been obtained,

$$\partial_t f(\vec{r}, \vec{p}, t) + \vec{\nabla}_p h(\vec{r}, \vec{p}) \cdot \vec{\nabla}_r f(\vec{r}, \vec{p}, t) - \vec{\nabla}_r h(\vec{r}, \vec{p}) \cdot \vec{\nabla}_p f(\vec{r}, \vec{p}, t) = 0 \quad (3.16)$$

where $\vec{\nabla}_p h(\vec{r}, \vec{p}) = \vec{v} = \vec{p}^* / \epsilon^*$ and $h = \epsilon^* + g_v V_0$. In these expressions $\vec{p}^* = \vec{p} - g_v \vec{V}$ and $\epsilon^* = (\vec{p}^{*2} + M^{*2})^{1/2}$ with $M^* = M - g_s \phi$. In the mean-field approximation, the meson fields are treated as classical fields and their evolutions are determined by the field equations,

$$[\partial_t^2 - \vec{\nabla}^2 + m_s^2] \phi(\vec{r}, t) = g_s \rho_s(\vec{r}, t) \quad (3.17)$$

and

$$[\partial_t^2 - \vec{\nabla}^2 + m_v^2] V^\mu(\vec{r}, t) = g_v \rho_v^\mu(\vec{r}, t). \quad (3.18)$$

In these expressions, the baryon density $\rho_0(\vec{r}, t) = \rho_B(\vec{r}, t)$, the scalar density $\rho_s(\vec{r}, t)$, and the current density $\vec{\rho}_v(\vec{r}, t)$ can be expressed in terms of phase-space distribution function as follows,

$$\rho_B(\vec{r}, t) = g \int \frac{d^3 p}{(2\pi)^3} f(\vec{r}, \vec{p}, t), \quad (3.19)$$

$$\rho_s(\vec{r}, t) = g \int \frac{d^3 p}{(2\pi)^3} \frac{M^*}{\epsilon^*} f(\vec{r}, \vec{p}, t), \quad (3.20)$$

and

$$\vec{\rho}_v(\vec{r}, t) = g \int \frac{d^3 p}{(2\pi)^3} \frac{\vec{p}^*}{\epsilon^*} f(\vec{r}, \vec{p}, t). \quad (3.21)$$

The original Walecka model gives a nuclear compressibility that is much larger than the one extracted from the giant monopole resonances in nuclei. It also leads to an

effective nucleon mass which is smaller than the value determined from the analysis of nucleon-nucleon scattering. In order to have a model which allows different values of nuclear compressibility and the nucleon effective mass, it is possible to improve the Walecka model by including the self-interaction of the scalar mesons or by considering density dependent coupling constants. However, in the present thesis, we employ the original Walecka model without including the self interaction of the scalar meson.

In the stochastic mean-field approach an ensemble $\{f^\lambda(\vec{r}, \vec{p}, t)\}$ of the phase-space distributions is generated in accordance with the initial fluctuations, where λ indicates the event label. In the following for simplicity of notation, since equations of motions do not change in the stochastic evolution, we do not use the event label for the phase-space distributions and also on the other quantities. However it is understood that the phase-space distribution, scalar meson and vector meson fields are fluctuating quantities. Each member of the ensemble of phase-space distributions evolves by the same Vlasov equation [1] according to its own self-consistent mean-field, but with different initial conditions. The main assumption of the approach in the semi-classical representation is the following: In each phase-space cell, the initial phase-space distribution $f(\vec{r}, \vec{p}, 0)$ is a Gaussian random number with its mean value determined by $\overline{f(\vec{r}, \vec{p}, 0)} = f_0(\vec{r}, \vec{p})$, and its second moment is determined by [8, 40]

$$\overline{f(\vec{r}, \vec{p}, 0)f(\vec{r}', \vec{p}', 0)} = (2\pi\hbar^3)\delta(\vec{r} - \vec{r}')\delta(\vec{p} - \vec{p}')f_0(\vec{r}, \vec{p})[1 - f_0(\vec{r}, \vec{p})] \quad (3.22)$$

where the overline represents the ensemble averaging and $f_0(\vec{r}, \vec{p})$ denotes the average phase-space distribution describing the initial state. In the special case of a homogenous initial state, it is given by the Fermi-Dirac distribution $f_0(\vec{p}) = 1/[e^{(\epsilon_0^* - \mu_0^*)/T} + 1]$. In this expression $\mu_0^* = \mu_0 - (g_v/m_v)^2\rho_B^0$ where μ_0 is the chemical potential and ρ_B^0 is the baryon density in the homogenous initial state.

In this part of the thesis our aim is using the linearized relativistic Vlasov equation around the equilibrium to investigate instabilities and early development of density fluctuations in symmetric nuclear matter. For this purpose, it is sufficient to consider the linear response treatment of dynamical evolution. The small amplitude fluctua-

tions of the phase-space distribution around an equilibrium state $f_0(\vec{p})$ is,

$$\delta f(\vec{r}, \vec{p}, t) = f(\vec{r}, \vec{p}, t) - f_0(\vec{p}) \quad (3.23)$$

and with the density fluctuations

$$\delta \rho_B(\vec{r}, t) = \rho_B(\vec{r}, t) - \rho_B^0 \quad (3.24)$$

$$\delta \rho_s(\vec{r}, t) = \rho_s(\vec{r}, t) - \rho_s^0 \quad (3.25)$$

$$\delta \vec{\rho}_v(\vec{r}, t) = \vec{\rho}_v(\vec{r}, t) \quad (3.26)$$

here ρ_s^0 is a dynamical quantity whose equilibrium quantity must be calculated self-consistently, and equilibrium current density $\vec{\rho}_v^0$ vanishes because at equilibrium we have a stationary and uniform system. Therefore, the linearized relativistic Vlasov equation can then be obtained by neglecting second order fluctuation terms,

$$\partial_t \delta f(\vec{r}, \vec{p}, t) + \vec{v}_0 \cdot \vec{\nabla}_r \delta f(\vec{r}, \vec{p}, t) - \vec{\nabla}_r \delta h(\vec{r}, \vec{p}, t) \cdot \vec{\nabla}_p f_0(\vec{p}) = 0. \quad (3.27)$$

In these expression the local velocity is defined as $\vec{v}_0 = \vec{p}/\epsilon_0^*$ with $\epsilon_0^* = \sqrt{\vec{p}^2 + M_0^{*2}}$, $M_0^* = (M - g_s \phi_0)$ and $\vec{\nabla}_p f_0 = \frac{\partial f_0}{\partial \epsilon_0^*} \vec{\nabla}_p \epsilon_0^* = \frac{\partial f_0}{\partial \epsilon_0^*} \vec{v}_0$.

The mean-field Hamiltonian can be linearized around equilibrium $h = h_0 + \delta h$

$$h = \sqrt{(\vec{p} - g_v \vec{V})^2 + (M - g_s \phi)^2} + g_v V_0 = \epsilon^* + g_v V_0 \quad (3.28)$$

and

$$h_0 = \epsilon_0^* + g_v V_0. \quad (3.29)$$

The small fluctuations of mean-field Hamiltonian is functions of baryon, scalar meson and vector meson fields

$$\delta h(\vec{r}, \vec{p}, t) = \left(\frac{\partial h}{\partial V_i} \right)_0 \delta V_i + \left(\frac{\partial h}{\partial V_0} \right)_0 \delta V_0 + \left(\frac{\partial h}{\partial \phi} \right)_0 \delta \phi \quad (3.30)$$

where

$$\left(\frac{\partial h}{\partial V_0} \right)_0 = g_v \quad (3.31)$$

$$\left(\frac{\partial h}{\partial \phi} \right)_0 = -g_s \frac{M_0^*}{\epsilon_0^*} \quad (3.32)$$

$$\left(\frac{\partial h}{\partial V_i} \right)_0 = -g_v \frac{p_i}{\epsilon_0^*} \quad (3.33)$$

and it is given by

$$\delta h(\vec{r}, \vec{p}, t) = -D_v \frac{1}{\epsilon_0^*} \vec{p} \cdot \delta \vec{\rho}_v - D_s \frac{M_0^*}{\epsilon_0^*} \delta \rho_s + D_v \delta \rho_B \quad (3.34)$$

with the coefficients

$$D_{s,v} = \frac{g_{s,v}^2}{-\omega^2 + \vec{k}^2 + \mu_{s,v}^2}. \quad (3.35)$$

The equilibrium fields are $\vec{V}_0 = 0$, $\phi_0 = \frac{g_s}{m_s^2} \rho_s^0$, $V_0^0 = \frac{g_v}{m_v^2} \rho_B^0$. The small fluctuations of the scalar and vector mesons are determined by the linearized field equations,

$$[\partial_t^2 - \vec{\nabla}^2 + m_s^2] \delta \phi(\vec{r}, t) = g_s \delta \rho_s(\vec{r}, t) \quad (3.36)$$

and

$$[\partial_t^2 - \vec{\nabla}^2 + m_v^2] \delta \vec{V}(\vec{r}, t) = g_v \delta \vec{\rho}_v(\vec{r}, t). \quad (3.37)$$

so the relations between the field fluctuations and density fluctuations are

$$\delta \phi(\vec{r}, t) = D_s \delta \rho_s(\vec{r}, t), \quad (3.38)$$

$$\delta V_0(\vec{r}, t) = D_v \delta \rho_B(\vec{r}, t), \quad (3.39)$$

and

$$\delta \vec{V}(\vec{r}, t) = D_v \delta \vec{\rho}_v(\vec{r}, t). \quad (3.40)$$

3.2 Spinodal Instabilities

3.2.1 Dispersion Relation

In this section, we employ the stochastic relativistic mean-field approach in small amplitude limit to investigate spinodal instabilities in symmetric nuclear matter. We can obtain the solution of linear response equations Eqs. (3.27)-(3.34) and Eqs. (3.36)-(3.37) by employing the standard method of one-sided Fourier transform in time [28]. It is also convenient to introduce the Fourier transform of the phase-space distribution in space,

$$\delta \tilde{f}(\vec{k}, \vec{p}, \omega) = \int_0^\infty dt e^{i\omega t} \int_{-\infty}^\infty \frac{d^3 r}{(2\pi)^3} e^{-i\vec{k} \cdot \vec{r}} f(\vec{r}, \vec{p}, t) \quad (3.41)$$

$$\delta \tilde{\rho}_i(\vec{k}, \omega) = \int_0^\infty dt e^{i\omega t} \int_{-\infty}^\infty \frac{d^3 r}{(2\pi)^3} e^{-i\vec{k} \cdot \vec{r}} \rho_i(\vec{r}, t) \quad (3.42)$$

here i denotes the current, the scalar and the baryon densities, and the one-sided Fourier transform of the small amplitude fluctuations of the phase-space distribution function is

$$\int_0^\infty \frac{\partial}{\partial t} \delta \tilde{f}(\vec{k}, \vec{p}, t) e^{i\omega t} dt = -\delta \tilde{f}(\vec{k}, \vec{p}, 0) - i\omega \delta \tilde{f}(\vec{k}, \vec{p}, \omega) \quad (3.43)$$

where $\delta \tilde{f}(\vec{k}, \vec{p}, 0)$ denotes the Fourier transform of the initial fluctuations. This leads to the relativistic Vlasov equation

$$\begin{aligned} \delta \tilde{f}(\vec{k}, \vec{p}, \omega) = & \frac{\vec{\nabla}_p \tilde{f}_0 \cdot \vec{k}}{\omega - \vec{v}_0 \cdot \vec{k}} \left[D_v \frac{1}{\epsilon_0^*} \vec{p} \cdot \delta \vec{\rho}_v(\vec{k}, \omega) \right. \\ & \left. + D_s \frac{M_0^*}{\epsilon_0^*} \delta \tilde{\rho}_s(\vec{k}, \omega) - D_v \delta \tilde{\rho}_B(\vec{k}, \omega) \right] - i \frac{\delta \tilde{f}(\vec{k}, \vec{p}, 0)}{\omega - \vec{v}_0 \cdot \vec{k}}. \end{aligned} \quad (3.44)$$

In this expression, the fluctuations of the meson fields are expressed in terms of Fourier transforms of the scalar density $\delta \tilde{\rho}_s(\vec{k}, \omega)$, the baryon density $\delta \tilde{\rho}_B(\vec{k}, \omega)$ and the current density $\delta \vec{\rho}_v(\vec{k}, \omega)$ fluctuations by employing the field equations Eq. (3.36) and Eq. (3.37). In Eq. (3.44) only the initial fluctuations of the phase-space distribution $\delta \tilde{f}(\vec{k}, \vec{p}, 0)$ is kept, but the initial fluctuations associated with the scalar and the vector fields are neglected. In the spinodal region since it is expected to have a small contribution, we neglect the frequency terms in the propagators, i.e., $-\omega^2 + k^2 + m_s^2 \approx k^2 + m_s^2$ and $-\omega^2 + k^2 + m_v^2 \approx k^2 + m_v^2$. Small fluctuations of the baryon density, the scalar density and the current density are related to the fluctuation of phase-space distribution function $\delta \tilde{f}(\vec{k}, \vec{p}, \omega)$ according to,

$$\delta \tilde{\rho}_B(\vec{k}, \omega) = g \int \frac{d^3 p}{(2\pi)^3} \delta \tilde{f}(\vec{k}, \vec{p}, \omega), \quad (3.45)$$

$$\begin{aligned} \delta \tilde{\rho}_s(\vec{k}, \omega) = & g \int \frac{d^3 p}{(2\pi)^3} \left[\delta \left(\frac{M^*}{\epsilon^*} \right) f_0(\vec{p}) + \frac{M_0^*}{\epsilon_0^*} \delta \tilde{f}(\vec{k}, \vec{p}, \omega) \right] \\ = & g \int \frac{d^3 p}{(2\pi)^3} \left[\left(D_v \frac{M_0^*}{\epsilon_0^{*3}} \vec{p} \cdot \delta \vec{\rho}_v(\vec{k}, \omega) - D_s \frac{P^2}{\epsilon_0^{*3}} \delta \tilde{\rho}_s(\vec{k}, \omega) \right) f_0(\vec{p}) + \frac{M_0^*}{\epsilon_0^*} \delta \tilde{f}(\vec{k}, \vec{p}, \omega) \right] \end{aligned} \quad (3.46)$$

and

$$\begin{aligned} \delta \vec{\rho}_v(\vec{k}, \omega) = & g \int \frac{d^3 p}{(2\pi)^3} \left[\delta \left(\frac{\vec{p}^*}{\epsilon^*} \right) f_0(\vec{p}) + \frac{\vec{p}}{\epsilon_0^*} \delta \tilde{f}(\vec{k}, \vec{p}, \omega) \right] \\ = & g \int \frac{d^3 p}{(2\pi)^3} \left[\left(D_v \frac{\vec{p}}{\epsilon_0^{*3}} \vec{p} \cdot \delta \vec{\rho}_v(\vec{k}, \omega) - D_v \frac{1}{\epsilon_0^*} \delta \vec{\rho}_v(\vec{k}, \omega) \right. \right. \\ & \left. \left. + D_s \frac{M_0^*}{\epsilon_0^{*3}} \vec{p} \delta \tilde{\rho}_s(\vec{k}, \omega) \right) f_0(\vec{p}) + \frac{\vec{p}}{\epsilon_0^*} \delta \tilde{f}(\vec{k}, \vec{p}, \omega) \right]. \end{aligned} \quad (3.47)$$

Multiplying both sides of Eq. (3.44) by \vec{p}/ϵ_0^* , M_0^*/ϵ_0^* , 1, and integrating over the momentum, we deduce a set of coupled algebraic equations for the small fluctuations of the current density, the scalar density and the baryon density which can be put in to a matrix form. We present these equations for zero and finite temperatures in Appendix E. Here we investigate spinodal dynamics of the longitudinal unstable modes. For longitudinal modes the current density oscillates along the direction of propagation, $\delta\vec{\rho}_v(\vec{k}, \omega) = \delta\tilde{\rho}_v(\vec{k}, \omega)\hat{k}$. Then, for the longitudinal modes, the set of equations become,

$$\begin{pmatrix} A_1 & A_2 & A_3 \\ B_1 & B_2 & B_3 \\ C_1 & C_2 & C_3 \end{pmatrix} \begin{pmatrix} \delta\tilde{\rho}_v(\vec{k}, \omega) \\ \delta\tilde{\rho}_s(\vec{k}, \omega) \\ \delta\tilde{\rho}_B(\vec{k}, \omega) \end{pmatrix} = i \begin{pmatrix} \tilde{S}_B(\vec{k}, \omega) \\ \tilde{S}_s(\vec{k}, \omega) \\ \tilde{S}_v(\vec{k}, \omega) \end{pmatrix} \quad (3.48)$$

where the element of the coefficient matrix are defined according to,

$$\begin{pmatrix} A_1 & A_2 & A_3 \\ B_1 & B_2 & B_3 \\ C_1 & C_2 & C_3 \end{pmatrix} = \begin{pmatrix} -D_v\chi_v(\vec{k}, \omega) & -D_s\chi_s(\vec{k}, \omega) & 1 + D_v\chi_B(\vec{k}, \omega) \\ -D_v\tilde{\chi}_v(\vec{k}, \omega) & 1 + D_s\tilde{\chi}_s(\vec{k}, \omega) & +D_v\chi_s(\vec{k}, \omega) \\ 1 + D_v\tilde{\chi}_B(\vec{k}, \omega) & -D_s\chi_v(\vec{k}, \omega) & +D_v\chi_v(\vec{k}, \omega) \end{pmatrix}. \quad (3.49)$$

The full expressions of the coefficients A_i , B_i and C_i are presented in Appendix E. In this expression, $\chi_B(\vec{k}, \omega)$, $\chi_s(\vec{k}, \omega)$ and $\chi_v(\vec{k}, \omega)$ denote the long wavelength limit of relativistic Lindhard functions associated with baryon, scalar and current density distribution functions,

$$\begin{pmatrix} \chi_v(\vec{k}, \omega) \\ \chi_s(\vec{k}, \omega) \\ \chi_B(\vec{k}, \omega) \end{pmatrix} = g \int \frac{d^3p}{(2\pi)^3} \begin{pmatrix} \vec{p} \cdot \hat{k} / \epsilon_0^* \\ M_0^* / \epsilon_0^* \\ 1 \end{pmatrix} \frac{\vec{k} \cdot \vec{\nabla}_p f_0(\vec{p})}{\omega - \vec{v}_0 \cdot \vec{k}}, \quad (3.50)$$

and the stochastic source terms are determined by

$$\begin{pmatrix} \tilde{S}_v(\vec{k}, \omega) \\ \tilde{S}_s(\vec{k}, \omega) \\ \tilde{S}_B(\vec{k}, \omega) \end{pmatrix} = g \int \frac{d^3p}{(2\pi)^3} \begin{pmatrix} \vec{p} \cdot \vec{k} / \epsilon_0^* \\ M_0^* / \epsilon_0^* \\ 1 \end{pmatrix} \frac{\delta\tilde{f}(\vec{k}, \vec{p}, 0)}{\omega - \vec{v}_0 \cdot \vec{k}} \quad (3.51)$$

Other three elements of the coefficient matrix in Eq. (3.49) are given by,

$$\tilde{\chi}_v(\vec{k}, \omega) = g \int \frac{d^3p}{(2\pi)^3} \vec{p} \cdot \hat{k} \left[\frac{M_0^*}{\epsilon_0^{*2}} \frac{\vec{k} \cdot \vec{\nabla}_p f_0(\vec{p})}{\omega - \vec{v}_0 \cdot \vec{k}} \right], \quad (3.52)$$

$$\tilde{\chi}_s(\vec{k}, \omega) = g \int \frac{d^3 p}{(2\pi)^3} \left[\frac{p^2}{\epsilon_0^{*3}} f_0(\vec{p}) - \frac{M_0^{*2}}{\epsilon_0^{*2}} \frac{\vec{k} \cdot \vec{\nabla}_p f_0(\vec{p})}{\omega - \vec{v}_0 \cdot \vec{k}} \right], \quad (3.53)$$

and

$$\tilde{\chi}_B(\vec{k}, \omega) = g \int \frac{d^3 p}{(2\pi)^3} \left[\frac{\epsilon_0^{*2} - (\vec{p} \cdot \hat{k})^2}{\epsilon_0^{*3}} f_0(\vec{p}) - \frac{(\vec{p} \cdot \hat{k})^2}{\epsilon_0^{*2}} \frac{\vec{k} \cdot \vec{\nabla}_p f_0(\vec{p})}{\omega - \vec{v}_0 \cdot \vec{k}} \right]. \quad (3.54)$$

We obtain the solutions by inverting the algebraic matrix equation, which gives for the current, scalar and baryon density fluctuations,

$$\delta\tilde{\rho}_v(\vec{k}, \omega) = i \frac{(B_2 C_3 - B_3 C_2) \tilde{S}_B(\vec{k}, \omega) + (A_3 C_2 - A_2 C_3) \tilde{S}_s(\vec{k}, \omega) + (A_2 B_3 - A_3 B_2) \tilde{S}_v(\vec{k}, \omega)}{\varepsilon(\vec{k}, \omega)}, \quad (3.55)$$

$$\delta\tilde{\rho}_s(\vec{k}, \omega) = i \frac{(B_3 C_1 - B_1 C_3) \tilde{S}_B(\vec{k}, \omega) + (A_1 C_3 - A_3 C_1) \tilde{S}_s(\vec{k}, \omega) + (A_3 B_1 - A_1 B_3) \tilde{S}_v(\vec{k}, \omega)}{\varepsilon(\vec{k}, \omega)}, \quad (3.56)$$

and

$$\delta\tilde{\rho}_B(\vec{k}, \omega) = i \frac{(B_1 C_2 - B_2 C_1) \tilde{S}_B(\vec{k}, \omega) + (A_2 C_1 - A_1 C_2) \tilde{S}_s(\vec{k}, \omega) + (A_1 B_2 - A_2 B_1) \tilde{S}_v(\vec{k}, \omega)}{\varepsilon(\vec{k}, \omega)} \quad (3.57)$$

where the susceptibility is

$$\varepsilon(\vec{k}, \omega) = A_1(B_2 C_3 - B_3 C_2) - A_2(B_1 C_3 - B_3 C_1) + A_3(B_1 C_2 - B_2 C_1). \quad (3.58)$$

Zero sound waves are longitudinal waves, therefore the propagation direction of $\delta\tilde{\rho}_v$ is parallel to the propagation direction of zero sound waves, i.e. $\delta\tilde{\rho}_v // \vec{k}$, and $\vec{\nabla}_p f_0 \cdot \vec{k} = (\nabla_p f_0) k \cos \theta$.

We investigated our relativistic problem for symmetric nuclear matter in two cases: at zero temperature and at finite temperature. At zero temperature, phase-space distribution function of equilibrium state $f_0(\vec{p})$ is represented by step function,

$$f_0(\vec{p}) = \Theta(\mu_0^* - \epsilon_0^*) = \begin{cases} 1, & \mu_0^* > \epsilon_0^* \\ 0, & \mu_0^* < \epsilon_0^* \end{cases} \quad (3.59)$$

here the reduced chemical potential is $\mu_0^* = \mu - \frac{g_v^2}{m_v^2} \rho_B^0$. At finite temperature the equilibrium phase space distribution function $f_0(\vec{p})$ is Fermi Dirac distribution function

$$f_0(\vec{p}) = \frac{1}{1 + e^{\beta(\epsilon_0^* - \mu_0^*)}}. \quad (3.60)$$

For the zero temperature case of the problem, we have

$$\begin{aligned}\vec{\nabla}_p f_0(\vec{p}) &= \vec{\nabla}_p \Theta(\mu_0^* - \epsilon_0^*) = -\frac{\vec{p}}{\epsilon_0^*} \delta(\mu_0^* - \epsilon_0^*) \\ &= -\hat{p} \delta(p - \sqrt{\mu_0^{*2} - (M_0^*)^2}) = -\hat{p} \delta(p - p_1)\end{aligned}\quad (3.61)$$

where δ represents Kronecker delta, \hat{p} is unit vector in the momentum direction and $p_1 = \sqrt{\mu_0^{*2} - M_0^{*2}}$. Using the self-consistency conditions at equilibrium, it is possible to calculate the equilibrium chemical potential both at zero and finite temperature cases from

$$\rho_B^0 = g \int \frac{d^3 p}{(2\pi)^3} f_0(p) \quad (3.62)$$

and

$$M_0^* = M - \frac{g_s^2}{m_s^2} g \int \frac{d^3 p}{(2\pi)^3} \frac{M_0^*}{(p^2 + M_0^{*2})^{1/2}} f_0(p). \quad (3.63)$$

Time-dependency of density fluctuations $\delta\tilde{\rho}_i(\vec{k}, t)$ are determined by taking the inverse transformation of $\delta\tilde{\rho}_i(\vec{k}, \omega)$ with the residue theorem [26]. Keeping only growing and decaying collective poles are as follows,

$$\delta\tilde{\rho}_i(\vec{k}, t) = (\delta\rho_i)^+(\vec{k})e^{+\Gamma_k t} + (\delta\rho_i)^-(\vec{k})e^{-\Gamma_k t} \quad (3.64)$$

where $i = v, s, B$ is used to denote vector, scalar and baryon density fluctuations respectively and the initial amplitude of density fluctuations are as follows,

$$\begin{aligned}\delta\rho_v^\mp(\vec{k}) &= \\ - \left\{ \frac{(B_2 C_3 - B_3 C_2) \tilde{S}_B(\vec{k}, \omega) + (A_3 C_2 - A_2 C_3) \tilde{S}_s(\vec{k}, \omega) + (A_2 B_3 - A_3 B_2) \tilde{S}_v(\vec{k}, \omega)}{\partial \epsilon(\vec{k}, \omega) / \partial \omega} \right\}_{\omega = \mp i\Gamma},\end{aligned}\quad (3.65)$$

$$\begin{aligned}\delta\rho_s^\mp(\vec{k}) &= \\ - \left\{ \frac{(B_3 C_1 - B_1 C_3) \tilde{S}_B(\vec{k}, \omega) + (A_1 C_3 - A_3 C_1) \tilde{S}_s(\vec{k}, \omega) + (A_3 B_1 - A_1 B_3) \tilde{S}_v(\vec{k}, \omega)}{\partial \epsilon(\vec{k}, \omega) / \partial \omega} \right\}_{\omega = \mp i\Gamma},\end{aligned}\quad (3.66)$$

and

$$\begin{aligned}\delta\rho_B^\mp(\vec{k}) &= \\ - \left\{ \frac{(B_1 C_2 - B_2 C_1) \tilde{S}_B(\vec{k}, \omega) + (A_2 C_1 - A_1 C_2) \tilde{S}_s(\vec{k}, \omega) + (A_1 B_2 - A_2 B_1) \tilde{S}_v(\vec{k}, \omega)}{\partial \epsilon(\vec{k}, \omega) / \partial \omega} \right\}_{\omega = \mp i\Gamma}.\end{aligned}\quad (3.67)$$

where

$$\begin{aligned} \frac{\partial \varepsilon}{\partial \omega} = & + \frac{\partial A_1}{\partial \omega} (B_2 C_3 - B_3 C_2) + A_1 \left(\frac{\partial B_2}{\partial \omega} C_3 + B_2 \frac{\partial C_3}{\partial \omega} - \frac{\partial B_3}{\partial \omega} C_2 - B_3 \frac{\partial C_2}{\partial \omega} \right) \\ & - \frac{\partial A_2}{\partial \omega} (B_1 C_3 - B_3 C_1) - A_2 \left(\frac{\partial B_1}{\partial \omega} C_3 + B_1 \frac{\partial C_3}{\partial \omega} - \frac{\partial B_3}{\partial \omega} C_1 - B_3 \frac{\partial C_1}{\partial \omega} \right) \\ & + \frac{\partial A_3}{\partial \omega} (B_1 C_2 - B_2 C_1) + A_3 \left(\frac{\partial B_1}{\partial \omega} C_2 + B_1 \frac{\partial C_2}{\partial \omega} - \frac{\partial B_2}{\partial \omega} C_1 - B_2 \frac{\partial C_1}{\partial \omega} \right) \end{aligned} \quad (3.68)$$

with

$$\begin{pmatrix} \frac{\partial A_1}{\partial \omega} \Big|_{\omega=\mp i\Gamma} \\ \frac{\partial A_2}{\partial \omega} \Big|_{\omega=\mp i\Gamma} \\ \frac{\partial A_3}{\partial \omega} \Big|_{\omega=\mp i\Gamma} \end{pmatrix} = \begin{pmatrix} -D_v \\ -D_s \\ +D_v \end{pmatrix} g' k \int_0^\infty dp \begin{pmatrix} p^4 \frac{1}{\epsilon_0^2} \frac{\partial K_2}{\partial \omega} \Big|_{\omega=\mp i\Gamma} \\ p^3 \frac{M_0^*}{\epsilon_0^2} \frac{\partial K_1}{\partial \omega} \Big|_{\omega=\mp i\Gamma} \\ p^3 \frac{1}{\epsilon_0} \frac{\partial K_1}{\partial \omega} \Big|_{\omega=\mp i\Gamma} \end{pmatrix} \frac{\partial f_0}{\partial \epsilon_0^*}, \quad (3.69)$$

$$\begin{pmatrix} \frac{\partial B_1}{\partial \omega} \Big|_{\omega=\mp i\Gamma} \\ \frac{\partial B_2}{\partial \omega} \Big|_{\omega=\mp i\Gamma} \\ \frac{\partial B_3}{\partial \omega} \Big|_{\omega=\mp i\Gamma} \end{pmatrix} = \begin{pmatrix} -D_v \\ -D_s \\ +D_v \end{pmatrix} g' k \int_0^\infty dp \begin{pmatrix} p^4 \frac{M_0^*}{\epsilon_0^3} \frac{\partial K_2}{\partial \omega} \Big|_{\omega=\mp i\Gamma} \\ p^3 \frac{(M_0^*)^2}{\epsilon_0^3} \frac{\partial K_1}{\partial \omega} \Big|_{\omega=\mp i\Gamma} \\ p^3 \frac{M_0^*}{\epsilon_0^2} \frac{\partial K_1}{\partial \omega} \Big|_{\omega=\mp i\Gamma} \end{pmatrix} \frac{\partial f_0}{\partial \epsilon_0^*}, \quad (3.70)$$

and

$$\begin{pmatrix} \frac{\partial C_1}{\partial \omega} \Big|_{\omega=\mp i\Gamma} \\ \frac{\partial C_2}{\partial \omega} \Big|_{\omega=\mp i\Gamma} \\ \frac{\partial C_3}{\partial \omega} \Big|_{\omega=\mp i\Gamma} \end{pmatrix} = \begin{pmatrix} -D_v \\ -D_s \\ +D_v \end{pmatrix} g' k \int_0^\infty dp \begin{pmatrix} p^4 \frac{M_0^*}{\epsilon_0^3} \frac{\partial K_3}{\partial \omega} \Big|_{\omega=\mp i\Gamma} \\ p^4 \frac{M_0^*}{\epsilon_0^3} \frac{\partial K_2}{\partial \omega} \Big|_{\omega=\mp i\Gamma} \\ p^4 \frac{1}{\epsilon_0^2} \frac{\partial K_2}{\partial \omega} \Big|_{\omega=\mp i\Gamma} \end{pmatrix} \frac{\partial f_0}{\partial \epsilon_0^*}, \quad (3.71)$$

where the integrals $\frac{\partial K_i}{\partial \omega} = \int_{-1}^1 \frac{x^i dx}{(\omega - \alpha x)^2}$ with $\alpha = \frac{pk}{\epsilon_0}$ are used.

The time-dependent baryon density fluctuations is denoted by,

$$\delta \tilde{\rho}_B(\vec{k}, t) = \delta \rho_B^+(\vec{k}) e^{+\Gamma_k t} + \delta \rho_B^-(\vec{k}) e^{-\Gamma_k t} \quad (3.72)$$

and the complex conjugate of it is

$$\delta \tilde{\rho}_B^*(\vec{k}, t) = \delta \rho_B^+(\vec{k})^* e^{+\Gamma_k t} + \delta \rho_B^-(\vec{k})^* e^{-\Gamma_k t} \quad (3.73)$$

here, the amplitudes of baryon density fluctuations associated with the growing and decaying modes at the initial instant are given by,

$$\delta \rho_B^\mp(\vec{k}) = - \left[\frac{D_1 \tilde{S}_B(\vec{k}, \omega) + D_2 \tilde{S}_s(\vec{k}, \omega) + D_3 \tilde{S}_v(\vec{k}, \omega)}{\partial \varepsilon(\vec{k}, \omega) / \partial \omega} \right]_{\omega=\mp i\Gamma_k} \quad (3.74)$$

with the short notations,

$$\begin{aligned}
D_1 &= B_1 C_2 - B_2 C_1 \\
D_2 &= A_2 C_1 - A_1 C_2 \\
D_3 &= A_1 B_2 - A_2 B_1
\end{aligned} \tag{3.75}$$

The growth and decay rates of the modes are obtained from the dispersion relations, $\varepsilon(\vec{k}, \omega) = 0$, i.e. from the roots of susceptibility. Solutions for the scalar density $\delta\tilde{\rho}_s(\vec{k}, \omega)$ and the current $\delta\tilde{\rho}_v(\vec{k}, \omega)$ fluctuations can be expressed in a similar manner. In the original Walecka model, there are four free parameters, coupling constants and meson masses. The binding energy per nucleon at saturation density determines the ratios of coupling constants to masses. The standard values of the ratios $(g_v/m_v)M = 16.55$ and $(g_s/m_s)M = 18.90$ give binding energy per nucleon 15.75 MeV at saturation density [32, 33]. In numerical calculations, we take for the vector meson mass $m_v = 783 \text{ MeV}$, and for the scalar meson mass, $m_s = 500 \text{ MeV}$. As an example, Fig. 3.1 shows the growth rates of unstable modes as a function of wave number in the spinodal region corresponding to the initial baryon density $\rho_B = 0.2 \rho_0$ and $\rho_B = 0.4 \rho_0$ at a temperature $T = 2 \text{ MeV}$ in Fig. 3.1(a) and at a temperature $T = 5 \text{ MeV}$ in Fig. 3.1(b). The results of non-relativistic approach with an effective Skyrme force for the same densities, but only at a temperature $T = 5 \text{ MeV}$ and symmetric case, i.e. the asymmetry parameter $I = 0.0$, can be seen in chapter 2 in Fig. 2.1(a). Although direct comparison of these calculations is rather difficult, we observe there are qualitative differences in both calculations. The range of most unstable modes in relativistic calculations is concentrated around $k = 0.6 \text{ fm}^{-1}$ in both densities, while most unstable modes shift towards larger wave numbers around $k = 0.8 \text{ fm}^{-1}$ at density $\rho_B = 0.2 \rho_0$ towards smaller wave numbers around $k = 0.5 \text{ fm}^{-1}$ at density $\rho_B = 0.4 \rho_0$. Growth rates of most unstable modes at density $\rho_B = 0.4 \rho_0$ in relativistic calculations are nearly factor of two larger than those results obtained in the non-relativistic calculations, while at low density $\rho_B = 0.2 \rho_0$ the growth rates are smaller in relativistic calculations. Fig. 3.2 illustrates growth rates of the most unstable modes as a function of density in both relativistic and non-relativistic approaches. We observe the qualitative difference in the unstable

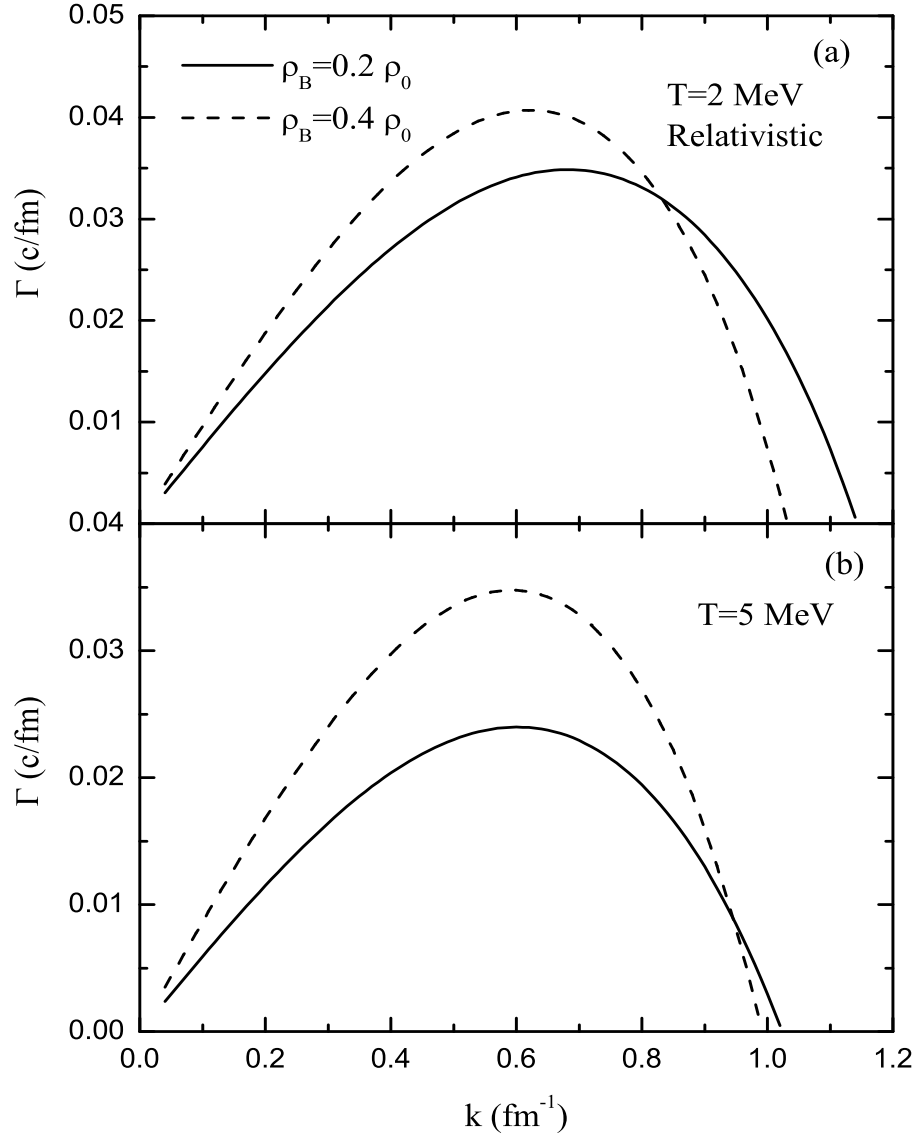


Figure 3.1: Growth rates of unstable modes as a function of wave numbers in the spinodal region at baryon densities $\rho_B = 0.2 \rho_0$ and $\rho_B = 0.4 \rho_0$ at a temperature (a) $T = 2 \text{ MeV}$, (b) $T = 5 \text{ MeV}$.

response of the system: the system exhibits most unstable behavior at higher densities around $\rho_B = 0.4 \rho_0$ in the relativistic approach while most unstable behavior occurs in the non-relativistic calculations at lower densities around $\rho_B = 0.2 \rho_0$. As an example of phase diagrams, Fig. 3.3 shows the boundary of spinodal region for the unstable

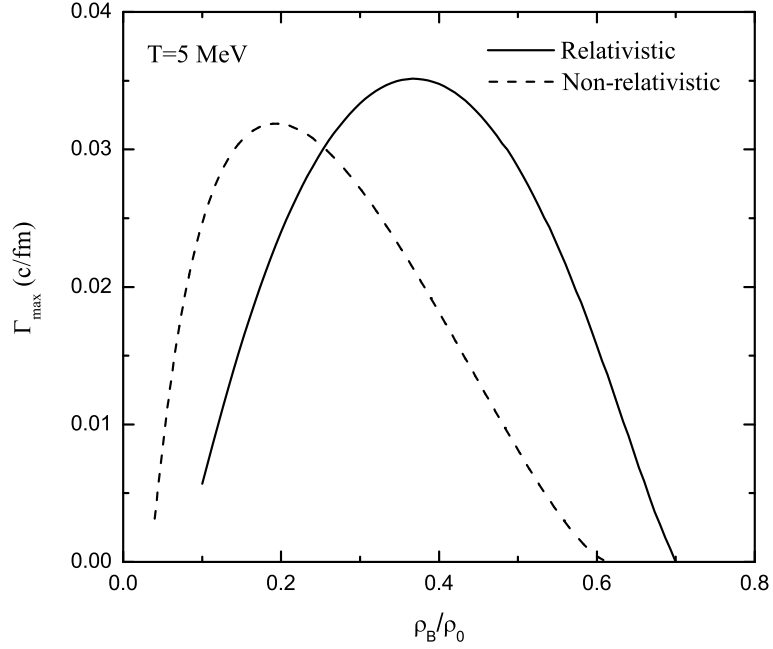


Figure 3.2: Growth rates of the most unstable modes as function of baryon density in the spinodal region at temperature $T = 5 \text{ MeV}$ in relativistic calculations (solid line) and in non-relativistic calculations (dashed line).

mode of wavelength $\lambda = 9.0 \text{ fm}$ in upper panel of figure and $\lambda = 12.0 \text{ fm}$ in lower panel of figure. Again, we observe that in both wavelengths the unstable behavior shifts towards higher densities in relativistic calculations.

3.2.2 Growth of Baryon Density Fluctuations

In this part, we calculate the early growth of baryon density fluctuations in nuclear matter. Spectral intensity of density correlation function $\tilde{\sigma}_{\text{BB}}(\vec{k}, t)$ is related to the variance of Fourier transform of baryon density fluctuation according to,

$$\begin{aligned}
 \tilde{\sigma}_{\text{BB}}(\vec{k}, t)(2\pi)^3 \delta(\vec{k} - \vec{k}') &= \overline{\delta\tilde{\rho}_{\text{B}}(\vec{k}, t)\delta\tilde{\rho}_{\text{B}}^*(\vec{k}, t)} \\
 &= \overline{\delta\rho_{\text{B}}^+(\vec{k})\delta\rho_{\text{B}}^+(\vec{k})^* e^{2\Gamma_{\text{k}}t} + \delta\rho_{\text{B}}^-(\vec{k})\delta\rho_{\text{B}}^-(\vec{k})^* e^{-2\Gamma_{\text{k}}t}} \\
 &\quad + \overline{\delta\rho_{\text{B}}^+(\vec{k})\delta\rho_{\text{B}}^-(\vec{k})^*} + \overline{\delta\rho_{\text{B}}^-(\vec{k})\delta\rho_{\text{B}}^+(\vec{k})^*} \quad (3.76)
 \end{aligned}$$

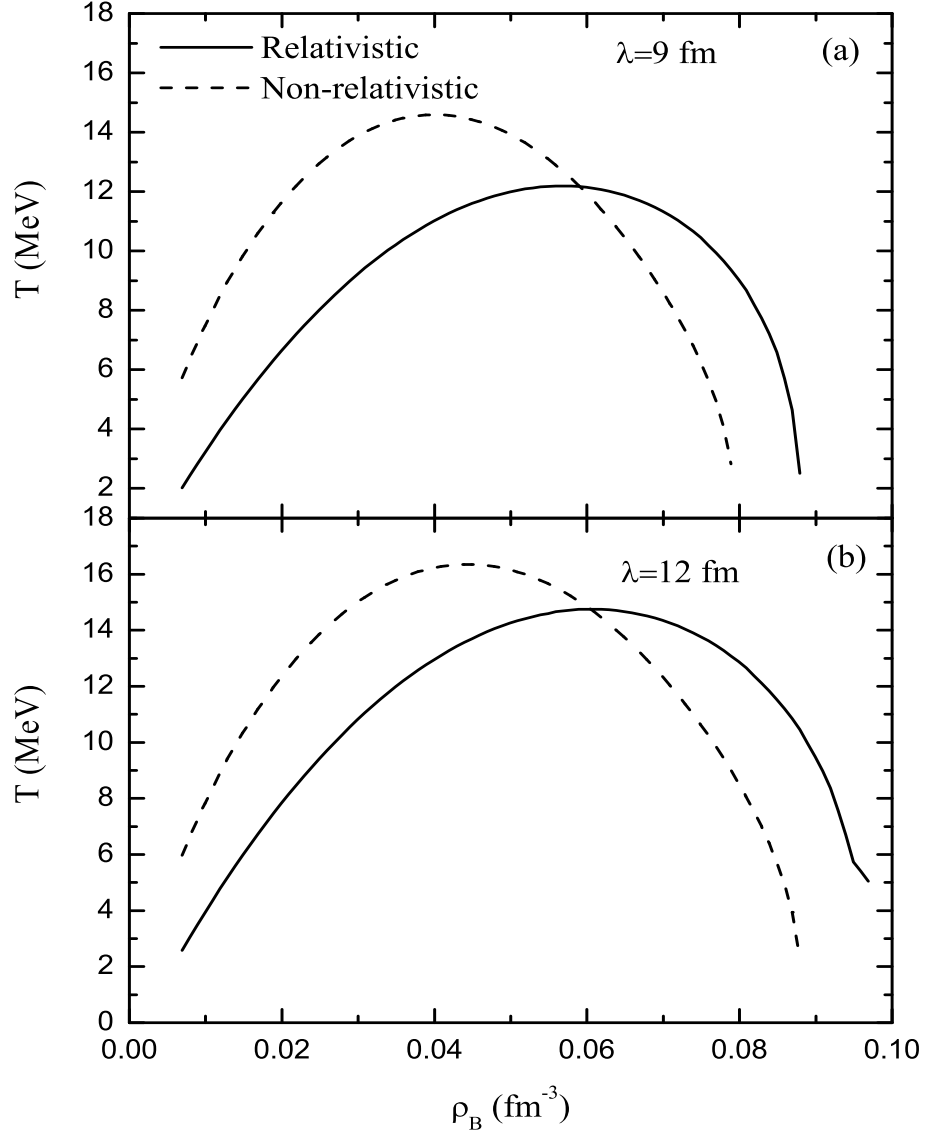


Figure 3.3: Boundary of spinodal region in baryon density-temperature plane in relativistic calculations (solid line) and in non-relativistic (dashed line) for the unstable mode with wavelengths: (a) $\lambda = 9 \text{ fm}$ and (b) $\lambda = 12 \text{ fm}$.

where

$$\overline{\delta\rho_B^+(\vec{k})\delta\rho_B^+(\vec{k})^*} = \frac{1}{\left[\left[\frac{\partial\varepsilon(\vec{k},\omega)}{\partial\omega}\right]_{\omega=i\Gamma}\right]^2} \left[D_1\tilde{S}_B(\vec{k},\omega)^+ + D_2\tilde{S}_s(\vec{k},\omega)^+ + D_3\tilde{S}_v(\vec{k},\omega)^+ \right] \times \left[D_1\tilde{S}_B(\vec{k},\omega)^+ + D_2\tilde{S}_s(\vec{k},\omega)^+ + D_3\tilde{S}_v(\vec{k},\omega)^+ \right]^* \quad (3.77)$$

Using the main assumption of the stochastic mean-field approach in the semi classical representation, the second moment of the initial phase-space distribution function $\delta\tilde{f}(\vec{k}, \vec{p}, 0)$ is determined by

$$\overline{\delta\tilde{f}(\vec{k}, \vec{p}, 0)\delta\tilde{f}^*(\vec{k}', \vec{p}', 0)} = (2\pi)^3(2\pi\hbar)^3\delta(\vec{k} - \vec{k}')\delta(\vec{p} - \vec{p}')f_0(\vec{k}, \vec{p})[1 - f_0(\vec{k}, \vec{p})] \quad (3.78)$$

for a homogenous initial state instead of $f_0(\vec{k}, \vec{p})$, the average phase-space distribution function is denoted by $f_0(\vec{p})$. The spectral intensity is defined according to Eq. (3.72) and Eq. (F.6) as follows,

$$\tilde{\sigma}_{\text{BB}}(\vec{k}, t) = \frac{E_{\text{B}}^+(\vec{k})}{|[\partial\varepsilon(\vec{k}, \omega)/\partial\omega]_{\omega=i\Gamma_{\vec{k}}}|^2}(e^{2\Gamma_{\vec{k}}t} + e^{-2\Gamma_{\vec{k}}t}) + \frac{2E_{\text{B}}^-(\vec{k})}{|[\partial\varepsilon(\vec{k}, \omega)/\partial\omega]_{\omega=i\Gamma_{\vec{k}}}|^2} \quad (3.79)$$

where

$$\begin{aligned} E_{\text{B}}^+(\vec{k}) &= |D_1|^2 K_{11}^+ + |D_2|^2 K_{22}^+ + |D_3|^2 K_{33}^+ + 2D_1 D_2 K_{12}^+ \\ E_{\text{B}}^-(\vec{k}) &= |D_1|^2 K_{11}^- + |D_2|^2 K_{22}^- - |D_3|^2 K_{33}^- + 2D_1 D_2 K_{12}^- \end{aligned} \quad (3.80)$$

with the integrals

$$\begin{pmatrix} K_{11}^\mp \\ K_{22}^\mp \\ K_{33}^\mp \\ K_{12}^\mp \end{pmatrix} = g^2 \int \frac{d^3 p}{(2\pi\hbar)^3} \begin{pmatrix} 1 \\ \left(\frac{M_0^*}{\epsilon_0^*}\right)^2 \\ \left(\frac{p_z}{\epsilon_0^*}\right)^2 \\ \frac{M_0^*}{\epsilon_0^*} \end{pmatrix} \frac{\Gamma^2 \mp (\mathbf{v}_0 \cdot \vec{k})^2}{[\Gamma^2 + (\mathbf{v}_0 \cdot \vec{k})^2]^2} f_0(\vec{p})[1 - f_0(\vec{p})] \quad (3.81)$$

the detail of these derivations can be seen in Appendix F.

Upper and lower panels of Fig. 3.4 at a temperature $T = 2 \text{ MeV}$ and Fig. 3.5 at a temperature $T = 5 \text{ MeV}$ show the spectral intensity of the baryon density correlation function as a function of wave number at times $t = 0$, $t = 20 \text{ fm}/c$, $t = 30 \text{ fm}/c$ and $t = 40 \text{ fm}/c$ in relativistic calculations at densities $\rho_{\text{B}} = 0.2 \rho_0$ and $\rho_{\text{B}} = 0.4 \rho_0$, respectively. We observe that the largest growth occurs over the range of wave numbers corresponding to the range of dominant unstable modes. Spectral intensity in the vicinity of most unstable modes of $k = 0.6 \text{ fm}^{-1}$ grows about a factor of ten at density $\rho_{\text{B}} = 0.2 \rho_0$ and about a factor of six at density $\rho_{\text{B}} = 0.4 \rho_0$ during the time interval of $t = 40 \text{ fm}/c$. In Fig. 3.5 for the same densities but at temperature $T = 5 \text{ MeV}$ similar trend can be seen. And also we can compare the results of temperature $T = 5 \text{ MeV}$

and for same densities of non-relativistic calculations in Fig. 2.5. We notice that at density $\rho_B = 0.2 \rho_0$ and at temperature $T = 5 \text{ MeV}$ the behavior of spectral intensity is rather similar in relativistic and non-relativistic approaches. However, at higher density $\rho_B = 0.4 \rho_0$ and temperature $T = 5 \text{ MeV}$, the spectral intensity grows slower in the non-relativistic calculations than those obtained in the relativistic approach. We note that in determining time evolution $\delta\rho_B(\vec{k}, t)$ with the help of the residue theorem, there are other contributions arising from the non-collective pole of the susceptibility $\varepsilon(\vec{k}, \omega)$ and from the poles of source terms $\tilde{S}_v(\vec{k}, \omega)$, $\tilde{S}_s(\vec{k}, \omega)$ and $\tilde{S}_B(\vec{k}, \omega)$. These contributions, in particular towards the short wavelengths, i.e. towards higher wave numbers, are important at the initial stage, however they damp out in a short time interval [28]. Since, we do not include effects from non-collective poles, we terminate the spectral in Fig. 2.5 at a cut-off wave number $k_c \approx 0.7 \text{ fm}^{-1} - 0.8 \text{ fm}^{-1}$. Consequently, the expression (3.79) provides a good approximation for $\tilde{\sigma}(\vec{k}, t)$ in the long wavelength regime below k_c .

Local baryon density fluctuations $\delta\rho_B(\vec{r}, t)$ are determined by the Fourier transform of $\delta\tilde{\rho}_B(\vec{r}, t)$. Equal time correlation function of baryon density fluctuations as a function of distance two space locations can be expressed in terms of the the spectral intensity as

$$\sigma_{BB}(|\vec{r} - \vec{r}'|, t) = \overline{\delta\rho_B(\vec{r}, t)\delta\rho_B(\vec{r}', t)} = \int \frac{d^3k}{(2\pi)^3} e^{i\vec{k}\cdot(\vec{r}-\vec{r}')} \tilde{\sigma}_{BB}(\vec{k}, t). \quad (3.82)$$

The baryon density correlation function carries useful information about the unstable dynamics of the matter in the spinodal region. As an example, the upper and lower panels of Fig. 3.6 illustrates the baryon density correlation function as a function distance between two space points at times $t = 0$, $t = 20 \text{ fm}/c$, $t = 30 \text{ fm}/c$ and $t = 40 \text{ fm}/c$ at temperature $T = 2 \text{ MeV}$ in relativistic calculations at densities $\rho_B = 0.2 \rho_0$ and $\rho_B = 0.4 \rho_0$, respectively. Complementary to the dispersion relation, correlation length of baryon density fluctuations provides an additional measure for the size of the primary fragmentation pattern. We can estimate the correlations length of baryon density fluctuations as the width of the correlation function at half maximum. From Fig. 3.6 at temperature $T = 2 \text{ MeV}$ and Fig. 3.7 at temperature $T = 5 \text{ MeV}$, we estimate that the correlation length is about the same at both densi-

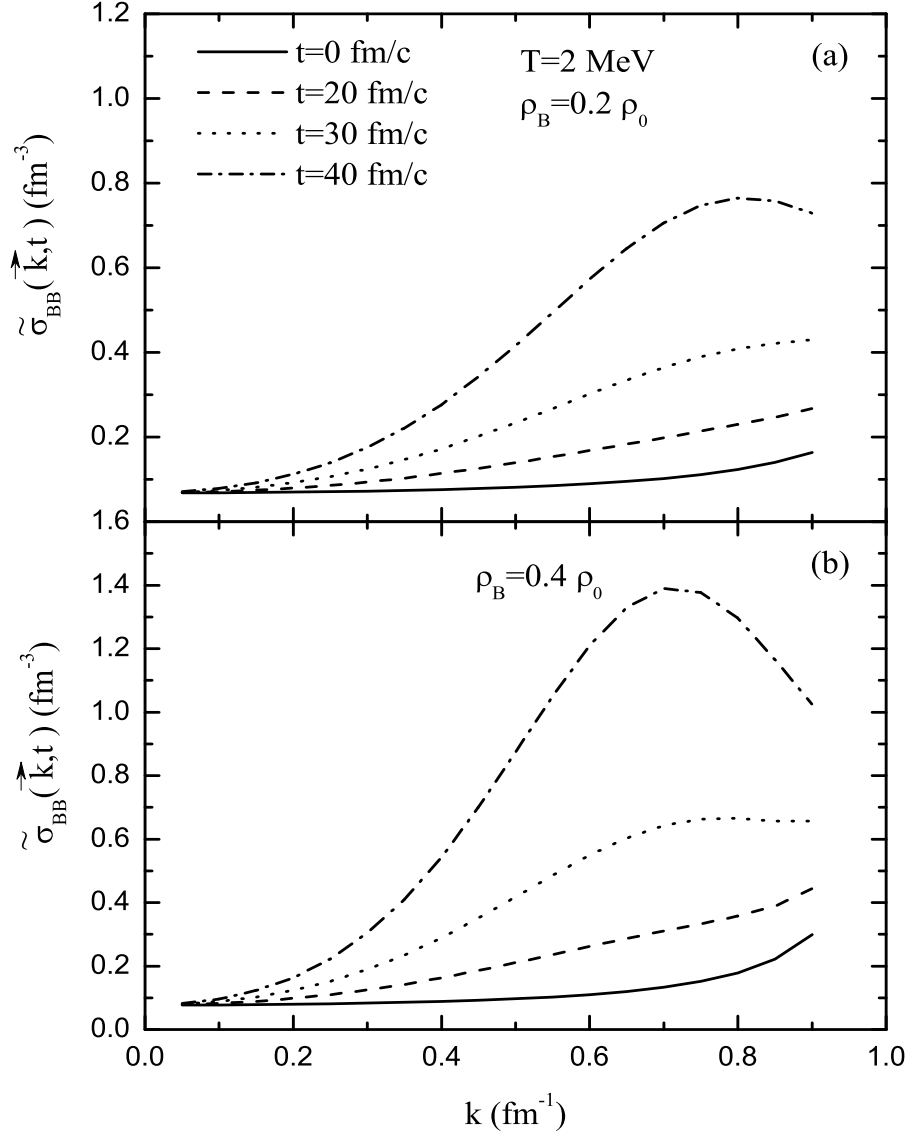


Figure 3.4: Spectral intensity $\tilde{\sigma}_{\text{BB}}(\vec{k}, t)$ of baryon density correlation function as a function of wave number at times $t = 0$, $t = 20 \text{ fm}/c$, $t = 30 \text{ fm}/c$ and $t = 40 \text{ fm}/c$ at temperature $T = 2 \text{ MeV}$ in relativistic calculations at density (a) $\rho_{\text{B}} = 0.2 \rho_0$ and (b) $\rho_{\text{B}} = 0.4 \rho_0$.

ties and temperatures around 3.0 fm , which is consistent with the dispersion relation presented in Fig. 3.1. Baryon density fluctuations grow faster at $\rho_{\text{B}} = 0.4 \rho_0$ than $\rho_{\text{B}} = 0.2 \rho_0$ at both temperatures. This is consistent with results of the non-relativistic calculations in Fig 2.7 [40]. The correlation length is around 4.0 fm at $\rho_{\text{B}} = 0.4 \rho_0$

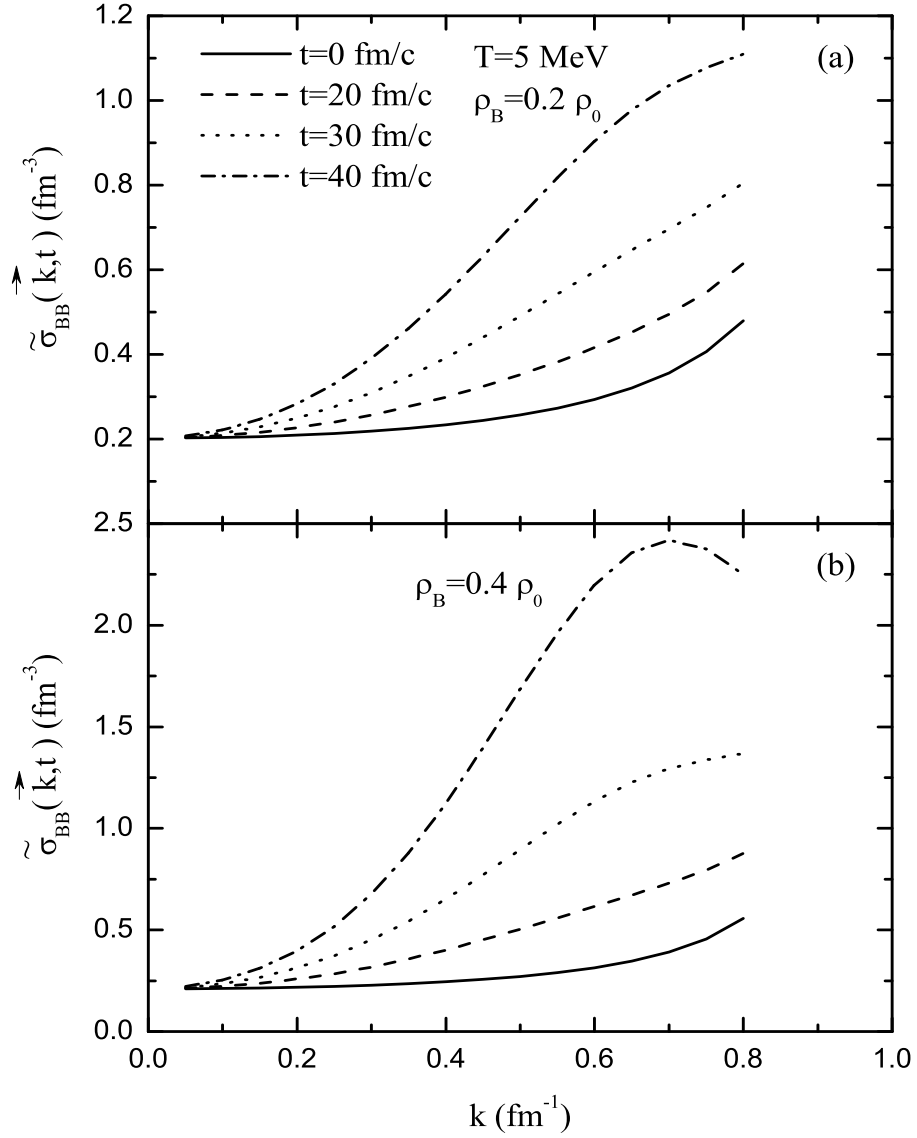


Figure 3.5: Same as Fig 3.4 but for temperature $T = 5 \text{ MeV}$.

and 3.0 fm at the lower density $\rho_B = 0.2 \rho_0$. However, unlike the relativistic calculations, the baryon density fluctuations grow faster at lower density $\rho_B = 0.2 \rho_0$ than at $\rho_B = 0.4 \rho_0$, which is consistent result presented in Fig 3.2.

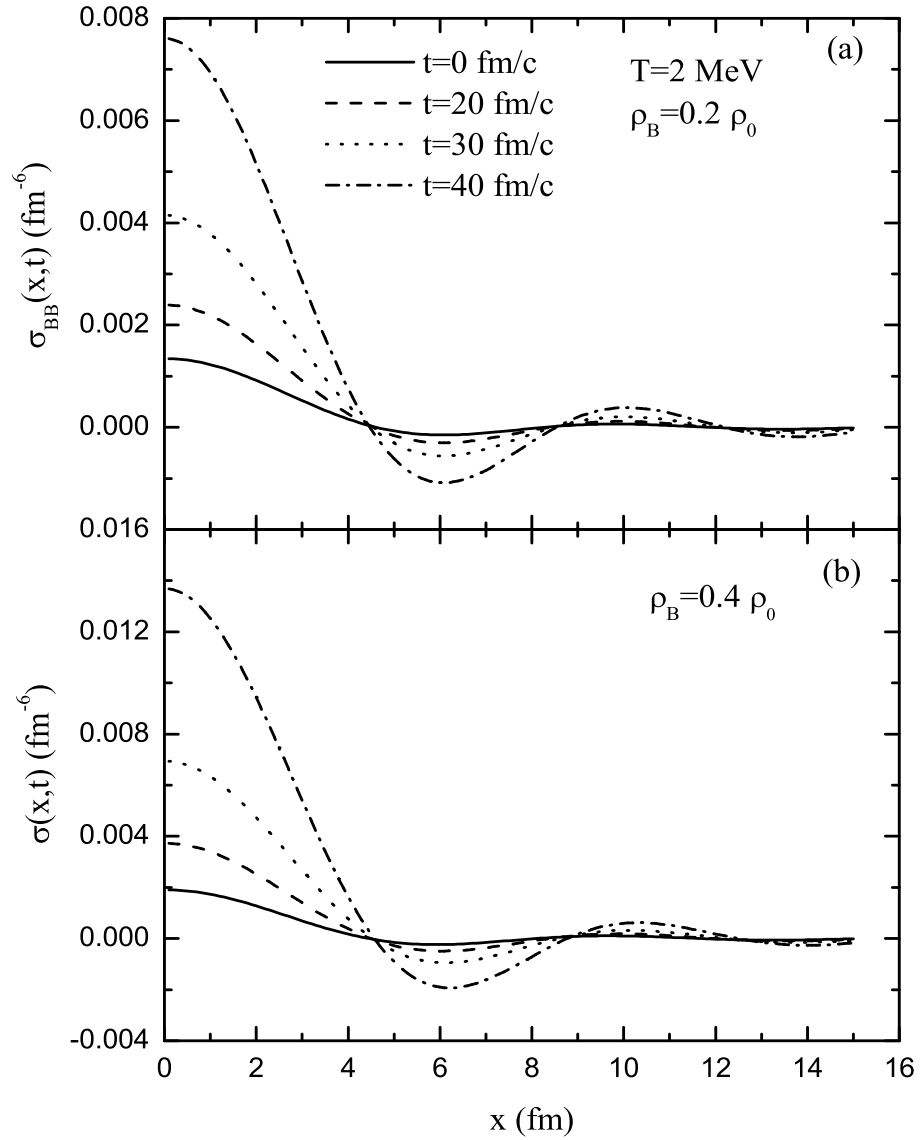


Figure 3.6: Baryon density correlation function $\sigma(x, t)$ as a function of distance $x = |\vec{r} - \vec{r}'|$ between two space points at times $t = 0$, $t = 20$ fm/c, $t = 30$ fm/c and $t = 40$ fm/c at temperature $T = 2$ MeV in relativistic calculations at density (a) $\rho_B = 0.2 \rho_0$ and (b) $\rho_B = 0.4 \rho_0$.

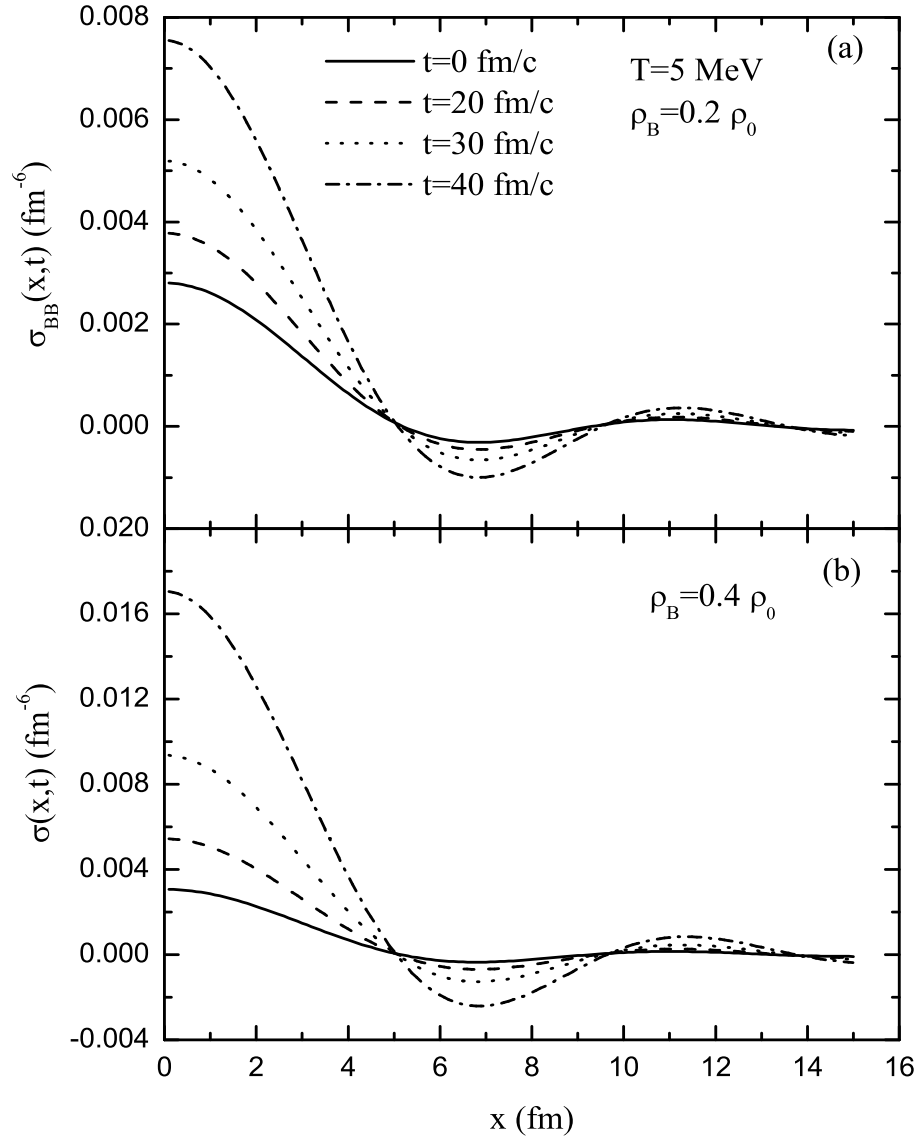


Figure 3.7: Same as Fig. 3.6 but at temperature $T = 5$ MeV.

CHAPTER 4

CONCLUSION

Recently proposed stochastic mean-field theory incorporates both one-body dissipation and fluctuation mechanisms in a manner consistent with quantal fluctuation-dissipation theorem of non-equilibrium statistical mechanics. Therefore, this approach provides a powerful tool for microscopic description of low energy nuclear processes in which two-body dissipation and fluctuation mechanisms do not play important role. The low energy processes include induced fission, heavy-ion fusion near barrier energies, spinodal decomposition of nuclear matter and nuclear multi-fragmentations.

In the first part of this thesis we investigate quantal effects on spinodal instabilities and early growth of density fluctuations in charge asymmetric nuclear matter using time-dependent Hartree Fock formalism. For this purpose it is sufficient to consider the linear response treatment of the stochastic mean-field approach. Retaining only growing and decaying collective modes, it is possible to calculate time evolution of spectral intensity of density correlation function and the density correlation function itself including quantum statistical effects. Growth rates of unstable collective modes are determined from a quantal dispersion relation, i.e. from the roots of susceptibility. Due to quantal effects, growth rates of unstable modes, in particular with wave numbers larger than the Fermi momentum, are strongly suppressed. As a result, dominant collective modes are shifted to longer wavelengths than those obtained in the semi-classical description with the same effective interaction, in both symmetric and asymmetric matter. The size of spinodal zone associated with these modes is re-

duced by the quantal effects. In calculation of density correlation function, quantal effects enter into the description through the growth rates of the modes and through the initial density fluctuations. Quantum statistical influence on density correlation functions grows larger at lower temperatures and also at lower densities. Quantal effects appear to be important for a quantitative description of spinodal instabilities and growth of density fluctuations in an expanding nuclear system. Stochastic mean-field approach incorporates both one-body dissipation and fluctuations mechanisms in a manner consistent with dissipation-fluctuation theorem. Therefore, it will be very interesting to investigate spinodal decomposition of an expanding nuclear system in this framework. We also note that numerical effort in simulation of stochastic mean-field approach is not so much greater than the effort required in solving ordinary three dimensional time dependent Hartree-Fock equations.

In the second part of this thesis, in a similar manner, it is possible to develop an extension of the relativistic mean-field theory by incorporating the initial quantal zero point fluctuations and thermal fluctuations of density in a stochastic manner. For this purpose, by employing the stochastic extension of the relativistic mean-field approach, we investigate spinodal instabilities in symmetric nuclear matter in the semi-classical framework. We determine the growth rates of unstable collective modes at different initial densities and temperatures. Stochastic approach also allows us to calculate early development of baryon density correlation functions in spinodal region, which provides valuable complementary information about the emerging fragmentation pattern of the system. We compare the results with those obtained in non-relativistic calculations under similar conditions. Our calculations indicate a qualitative different behavior in the unstable response of the system. In the relativistic approach, the system exhibits most unstable behavior at higher baryon densities around $\rho_B = 0.4 \rho_0$, while in the non-relativistic calculations most unstable behavior occurs at lower baryon densities around $\rho_B = 0.2 \rho_0$. In the present thesis, we employ the original Walecka model without self-interaction of scalar meson. The qualitative difference in the unstable behavior may be partly due to the fact that the original Walecka model leads to a relatively small value of nucleon effective mass of $M^* = 0.541 M$ and a large nuclear compressibility of 540 MeV . On the other hand, the Skyrme interaction that

we employ in non-relativistic calculations gives rise to a compressibility of 201 MeV [40]. It will be interesting to carry out further investigations of spinodal dynamics in symmetric and charge asymmetric nuclear matter by including self-interaction of the scalar meson and also including the rho meson in the calculations. Inclusion of the self-interaction of scalar meson allows us to investigate spinodal dynamics over a wide range of nuclear compressibility and nuclear effective mass. We also note by working in the semi-classical framework, we neglect the quantum statistical effects on the baryon density correlation function, which become important at lower temperatures and also at lower densities.

REFERENCES

- [1] Ph. Chomaz, M. Colonna and J. Randrup, Phys. Rep. **389** (2004) 263.
- [2] P. Ring and P. Schuck, "The Nuclear Many-Body Problem", Springer, New York, (1980).
- [3] K.T.D. Davis, K. R. S. Devi, S. E. Koonin and M. Strayer, "Treatise in Heavy-Ion Science", ed. D. A. Bromley, Nuclear Science V-4, Plenum, New York, (1984).
- [4] W. Cassing, U. Mosel, Prog. Part. Nucl. Phys. **25** (1990) 1.
- [5] S. Ayik and C. Gregoire, Phys. Lett. **B 212** (1988) 269 ; Nucl. Phys. **A 513** (1990) 187.
- [6] J. Randrup and B. Remaud, Nucl. Phys. **A 514** (1990) 339.
- [7] Y. Abe, S. Ayik, P.-G. Reinhard, and E. Suraud, Phys. Rep. **275** (1996) 49.
- [8] S. Ayik, Phys. Lett. **B 658** (2008) 174.
- [9] S. Ayik, M. Colonna and Ph. Chomaz, Phys. Lett. **353** (1995) 417.
- [10] M. Colonna, Ph. Chomaz and S. Ayik, Phys. Rev. Lett. **88** (2002) 122701.
- [11] B. Jacquot, S. Ayik, Ph. Chomaz and M. Colonna, Phys. Lett. **B383** (1996) 247.
- [12] B. Jacquot, M. Colonna, S. Ayik and Ph. Chomaz, Nucl. Phys. **A617** (1997) 356.
- [13] Y. K. Gambhir, P. Ring and Thimet, Ann. Phys. (N.Y.) **198** (1990) 132.
- [14] D. Vretenar, A. V. Afanasjev, G. A. Lalazissis and P. Ring, Phys. Rep. **409** (2005) 101.
- [15] S. S. Avancini, L. Brito, D. P. Menezes and C. Providencia, Phys. Rev. **C 71** (2005) 044323.
- [16] A. M. Santos, L. Brito and C. Providencia, Phys. Rev. **C 77** (2008) 048505.
- [17] C. Ducoin, C. Providencia, A. M. Santos, L. Brito and Ph. Chomaz, , Phys. Rev. **C 78** (2005) 055801.
- [18] R. K. Pathria, "Statistical Mechanics", Butterworth-Heinemann, Oxford, 1996.
- [19] D. Vautherin, D. M. Brink, Phys. Rev. **C 5** (1972) 626.

- [20] K. Langanke, J.A. Maruhn, S.E. Koonin "Computational Nuclear Physics I", Springer, Germany, 1991.
- [21] V. Baran, M. Colonna, M. Di Toro and A. B. Larionov, Nucl. Phys. A **632** (1998) 287.
- [22] G. Baym, H. A. Bethe and C. J. Pethick, Nucl. Phys. A **175** (1971) 225.
- [23] H. Krivine, J. Treiner and O. Bohigas, Nucl. Phys. A **336** (1990) 155.
- [24] J. J. Sakurai, "Modern Quantum Mechanics", Addison-Wesley Publishing Company (1994).
- [25] H. Heiselberg, C. J. Pethick and D. G. Ravenhall, Phys. Rev. Lett. **61** (1988) 818.
- [26] E. M. Lifshitz and L. P. Pitaevskii, "Physical Kinetics", Pergamon, (1981).
- [27] S. Ayik, M. Colonna and Ph. Chomaz, Phys. Lett. B **353** (1995) 417.
- [28] P. Bozek, Phys. Lett. B **383** (1996) 121.
- [29] L. D. Landau & Lifshitz, "Course of Theoretical Physics V.5 Statistical Physics", Pergamon Press, Oxford, 1980.
- [30] B. D. Serot, J. D. Walecka, "Advances in Nuclear Physics Vol.16", Plenum Press, New York-London, 1968.
- [31] J. D. Walecka, "Theoretical Nuclear and Subnuclear Physics", Oxford University Press, New York, (1997).
- [32] B. D. Serot, J. D. Walecka, Int. J. Mod. Phys. E **6** (1997) 515-631.
- [33] P. Ring, Prog. Part. Nucl. Phys. **37** (1996) 193
- [34] C. M. Ko, Qi Li, Phys. Rev. C **37** (1988) 2270.
- [35] J. D. Walecka, Ann. Phys. (N. Y.) **83** (1974) 491 515-631.
- [36] C. M. Ko, Qi Li, R. Wang, Phys. Rev. Lett. **59** (1987) 1084.
- [37] C. H. Dasso, T. Dossing, and H. C. Pauli, Z. Phys. A **289** (1979) 395.
- [38] H. Esbensen, A. Winther, R. A. Broglia, and C. H. Dasso, Phys. Rev. Lett. **41** (1978) 296.
- [39] C. H. Dasso, Proc. Second La Rapida Summer School on Nuclear Physics, eds. M. Lozano and G. Madurga, World Scientific, Singapore, 1985.
- [40] S. Ayik, N. Er, O. Yilmaz and A. Gokalp, Nucl. Phys. A **812** (2008) 44.

- [41] R. L. Liboff, "Kinetic Theory: Classical, Quantum, and Relativistic Descriptions", Springer, New York, 2003.
- [42] M. L. Boas, "Mathematical Methods in the Physical Science", John Wiley & Sons, (2006).
- [43] R. Machleidt, "In Relativistic Dynamics and Quark Nuclear Physics", edited by M. B. Johnson and A. Picklesimer, John Wiley & Sons, (1986).
- [44] H. Feldmeier, Rep. Prog. Phys. **50** (1987) 915.
- [45] R. Balian and M. Veneroni, Phys. Lett. **B 104** (1982) 121.
- [46] K. Washiyama, S. Ayik and D. Lacroix, submitted to Phys. Rev. Lett. (2009)

APPENDIX A

WIGNER TRANSFORMATION

In quantal description of nuclear dynamics the TDHF equation is a good starting point.

$$i\hbar \frac{\partial \rho}{\partial t} - [h(\rho), \rho] = 0 \quad (\text{A.1})$$

In classical physics phase-space distribution function $f(\vec{r}, \vec{p}, t)$ defines the position and momentum simultaneously at time t . But in quantum mechanics this kind of simultaneity is impossible because of uncertainty relation [2]. By using Wigner [41] transformation which provides a conventional connection between the quantal density matrix $\rho(\vec{r}, \vec{r}', t)$ and classical distribution function $f(\vec{r}, \vec{p}, t)$ it is possible to overcome this difficulty by the Wigner transformation as

$$f(\vec{r}, \vec{p}, t) = \int d^3 q e^{(-i/\hbar)\vec{p}\cdot\vec{q}} \langle \vec{r} + \frac{\vec{q}}{2} | \rho(t) | \vec{r} - \frac{\vec{q}}{2} \rangle \quad (\text{A.2})$$

and Wigner transform of the Hartree-Fock Hamiltonian $h[\rho]$ is named as the quasi-particle energy $\epsilon(\vec{r}, \vec{p}, t)$

$$h(\vec{r}, \vec{p}) = \int d^3 q e^{(-i/\hbar)\vec{p}\cdot\vec{q}} \langle \vec{r} + \frac{\vec{q}}{2} | h[\rho] | \vec{r} - \frac{\vec{q}}{2} \rangle. \quad (\text{A.3})$$

Since single particle density operator and related hamiltonian are Hermitian, applying Wigner transformation to both sides of the TDHF equations, we have

$$\begin{aligned} i\hbar \frac{\partial}{\partial t} f(\vec{r}, \vec{p}, t) &= (h[\rho]\rho(t))_w - (\rho(t)h[\rho])_w \\ &= h(\vec{r}, \vec{p})e^{(i\hbar/2)\vec{\lambda}} f(\vec{r}, \vec{p}, t) - f(\vec{r}, \vec{p}, t)e^{(i\hbar/2)\vec{\lambda}} h(\vec{r}, \vec{p}, t) \end{aligned} \quad (\text{A.4})$$

here in the operator $\vec{\lambda} = \overleftarrow{\nabla}_r \overrightarrow{\nabla}_p - \overleftarrow{\nabla}_p \overrightarrow{\nabla}_r$ the direction of arrows indicates the acting direction of the gradient operators from left or right. In the semi-classical limit for

small \hbar using the expansion

$$e^{(i\hbar/2)\vec{\lambda}} = 1 + (i\hbar/2)\vec{\lambda} - [(i\hbar/2)\vec{\lambda}]^3/3! + \dots \quad (\text{A.5})$$

we obtain

$$\begin{aligned} i\hbar \frac{\partial}{\partial t} f(\vec{r}, \vec{p}, t) &= h(\vec{r}, \vec{p})f(\vec{r}, \vec{p}, t) + i\frac{\hbar}{2}h(\vec{r}, \vec{p})\vec{\lambda}f(\vec{r}, \vec{p}, t) \\ &\quad - f(\vec{r}, \vec{p}, t)h(\vec{r}, \vec{p}) - i\frac{\hbar}{2}f(\vec{r}, \vec{p}, t)\vec{\lambda}h(\vec{r}, \vec{p}, t) \\ &= \frac{1}{2} \left[h(\vec{r}, \vec{p})\vec{\lambda}f(\vec{r}, \vec{p}, t) - f(\vec{r}, \vec{p}, t)\vec{\lambda}h(\vec{r}, \vec{p}, t) \right] \\ &= \frac{1}{2} \left[\vec{\nabla}_r h(\vec{r}, \vec{p}) \cdot \vec{\nabla}_p \vec{\lambda} f(\vec{r}, \vec{p}, t) - \vec{\nabla}_p h(\vec{r}, \vec{p}) \cdot \vec{\nabla}_r \vec{\lambda} f(\vec{r}, \vec{p}, t) \right. \\ &\quad \left. - \vec{\nabla}_r f(\vec{r}, \vec{p}, t) \cdot \vec{\nabla}_p \vec{\lambda} h(\vec{r}, \vec{p}, t) + \vec{\nabla}_p f(\vec{r}, \vec{p}, t) \cdot \vec{\nabla}_r \vec{\lambda} h(\vec{r}, \vec{p}, t) \right] \end{aligned} \quad (\text{A.6})$$

where terms involving higher orders of \hbar gives zero in the semi-classical limit. As a result, after Wigner transformation and $\hbar \rightarrow 0$ limit the quantal TDHF equation reduces to the semi-classical Vlasov equation without collision term as

$$\frac{\partial}{\partial t} f(\vec{r}, \vec{p}, t) - \vec{\nabla}_r h(\vec{r}, \vec{p}) \cdot \vec{\nabla}_p f(\vec{r}, \vec{p}, t) + \vec{\nabla}_p h(\vec{r}, \vec{p}) \cdot \vec{\nabla}_r f(\vec{r}, \vec{p}, t) = 0. \quad (\text{A.7})$$

APPENDIX B

TIME DEPENDENCY OF DENSITY FLUCTUATIONS

The time dependent density fluctuation including growing and decaying collective poles is,

$$\delta\tilde{n}_a(\vec{k}, t) = \delta n_a^+(\vec{k})e^{+\Gamma kt} + \delta n_a^-(\vec{k})e^{-\Gamma kt}. \quad (\text{B.1})$$

Time dependence of density fluctuation $\delta\tilde{n}_a(\vec{k}, t)$ is determined by calculating the inverse transformation of $\delta\tilde{n}_a(\vec{k}, \omega)$ and for example by keeping only growing and decaying collective poles for neutron density fluctuation, we have

$$\begin{aligned} \delta\tilde{n}_n(\vec{k}, t) &= \int \frac{d\omega}{2\pi} \delta\tilde{n}_n(\vec{k}, \omega) e^{-i\omega t} \\ &= \int_C \frac{d\omega}{2\pi} i \frac{[1 + F_0^{pp} \chi_p(\vec{k}, \omega)] A_n(\vec{k}, \omega) - F_0^{np} \chi_n(\vec{k}, \omega) A_p(\vec{k}, \omega)}{\varepsilon(\vec{k}, \omega)} e^{-i\omega t}. \end{aligned} \quad (\text{B.2})$$

We will interested in only the singularities of $\varepsilon(\vec{k}, \omega)$. For a contour integral, which includes all the singularities, has the form of

$$\int_C f(z) dz \equiv \int_C \frac{g(z)}{h(z)} dz \quad (\text{B.3})$$

and if there is a singularity at z_0 , which means $g(z) = \text{finite const.} \neq 0$, $h(z_0) = 0$ and $h'(z) = \left. \frac{\partial h}{\partial z} \right| \neq 0$, Cauchy-residue theorem gives [42]

$$\int_C f(z) dz \equiv 2\pi i \text{Res}[f(z), z_0] = 2\pi i \sum_k R_k \quad (\text{B.4})$$

where the residue of the function is defined by $R_k = \lim_{z \rightarrow z_0} \frac{g(z)}{h'(z)}$. Our problem has a this kind of singularity at poles $\omega = \mp i\Gamma$ and these singular points are inside of the

contour, so we can use this theorem in our problem and obtain

$$\delta\tilde{n}_a(\vec{k}, t) = \frac{1}{2\pi} 2\pi i \left\{ i \frac{[1 + F_0^{pp} \chi_p(\vec{k}, \omega)] A_n(\vec{k}, \omega) - F_0^{np} \chi_n(\vec{k}, \omega) A_p(\vec{k}, \omega)}{\varepsilon(\vec{k}, \omega)} e^{-i\omega t} \Big|_{\omega=i\Gamma} + i \frac{[1 + F_0^{pp} \chi_p(\vec{k}, \omega)] A_n(\vec{k}, \omega) - F_0^{np} \chi_n(\vec{k}, \omega) A_p(\vec{k}, \omega)}{\varepsilon(\vec{k}, \omega)} e^{-i\omega t} \Big|_{\omega=-i\Gamma} \right\}. \quad (\text{B.5})$$

Therefore, the initial amplitudes of density fluctuations for growing and decaying poles are

$$\delta n_a^+(\vec{k}) = - \frac{[1 + F_0^{pp} \chi_p(\vec{k}, \omega)] A_n(\vec{k}, \omega) - F_0^{np} \chi_n(\vec{k}, \omega) A_p(\vec{k}, \omega)}{\partial \varepsilon(\vec{k}, \omega) / \partial \omega} \Big|_{\omega=i\Gamma} \quad (\text{B.6})$$

$$\delta n_a^-(\vec{k}) = - \frac{[1 + F_0^{pp} \chi_p(\vec{k}, \omega)] A_n(\vec{k}, \omega) - F_0^{np} \chi_n(\vec{k}, \omega) A_p(\vec{k}, \omega)}{\partial \varepsilon(\vec{k}, \omega) / \partial \omega} \Big|_{\omega=-i\Gamma}. \quad (\text{B.7})$$

APPENDIX C

QUANTAL LINHARD FUNCTIONS

The properties of quantal Linhard functions

$$\chi_a(\vec{k}, i\Gamma) = \chi_a(\vec{k}, -i\Gamma) = \chi_a(-\vec{k}, i\Gamma) = \chi_a(-\vec{k}, -i\Gamma)$$

and their derivatives

$$\left. \frac{\partial \chi_a(\vec{k}, \omega)}{\partial \omega} \right|_{\omega=i\Gamma} = - \left. \frac{\partial \chi_a(\vec{k}, \omega)}{\partial \omega} \right|_{\omega=-i\Gamma},$$

$$\left. \frac{\partial \chi_a(\vec{k}, \omega)}{\partial \omega} \right|_{\omega=i\Gamma} = - \left. \frac{\partial \chi_a(-\vec{k}, \omega)}{\partial \omega} \right|_{\omega=i\Gamma},$$

with the resultant property of susceptibility

$$\left. \frac{\partial \varepsilon(\vec{k}, \omega)}{\partial \omega} \right|_{\omega=i\Gamma} = - \left. \frac{\partial \varepsilon(-\vec{k}, \omega)}{\partial \omega} \right|_{\omega=i\Gamma}.$$

$$\left. \frac{\partial \varepsilon(\vec{k}, \omega)}{\partial \omega} \right|_{\omega=i\Gamma} = - \left. \frac{\partial \varepsilon(\vec{k}, \omega)}{\partial \omega} \right|_{\omega=-i\Gamma}.$$

The spectral intensity of neutron-neutron density correlation function is

$$\begin{aligned} \tilde{\sigma}_{nn}(\vec{k}, t)(2\pi)^3 \delta(\vec{k} - \vec{k}') &= \overline{\delta \tilde{n}_n(\vec{k}, t) \delta \tilde{n}_n(-\vec{k}', t)} \\ &= \overline{\delta n_n^+(\vec{k}) \delta n_n^+(-\vec{k}') e^{2\Gamma kt}} + \overline{\delta n_n^+(\vec{k}) \delta n_n^-(-\vec{k}')} + \overline{\delta n_n^-(\vec{k}) \delta n_n^+(-\vec{k}')} + \overline{\delta n_n^-(\vec{k}) \delta n_n^-(-\vec{k}')} e^{-2\Gamma kt}, \end{aligned} \tag{C.1}$$

where

$$\begin{aligned} \overline{\delta n_n^+(\vec{k})\delta n_n^+(-\vec{k}')} &= \frac{1}{\left[\partial\varepsilon(\vec{k}, \omega)/\partial\omega\right]_{\omega=i\Gamma} \left[\partial\varepsilon(-\vec{k}', \omega)/\partial\omega\right]_{\omega=i\Gamma}} \\ &\quad \left\{ \left[1 + F_0^{pp}\chi_p(\vec{k}, i\Gamma)\right] \left[1 + F_0^{pp}\chi_p(-\vec{k}', i\Gamma)\right] \overline{A_n(\vec{k}, i\Gamma)A_n(-\vec{k}', i\Gamma)} \right. \\ &\quad \left. \left[F_0^{np}\chi_n(\vec{k}, i\Gamma)\right] \left[F_0^{np}\chi_n(-\vec{k}', i\Gamma)\right] \overline{A_p(\vec{k}, i\Gamma)A_p(-\vec{k}', i\Gamma)} \right\}, \end{aligned} \quad (\text{C.2})$$

$$\begin{aligned} \overline{\delta n_n^+(\vec{k})\delta n_n^-(-\vec{k}')} &= \frac{1}{\left[\partial\varepsilon(\vec{k}, \omega)/\partial\omega\right]_{\omega=i\Gamma} \left[\partial\varepsilon(-\vec{k}', \omega)/\partial\omega\right]_{\omega=-i\Gamma}} \\ &\quad \left\{ \left[1 + F_0^{pp}\chi_p(\vec{k}, i\Gamma)\right] \left[1 + F_0^{pp}\chi_p(-\vec{k}', -i\Gamma)\right] \overline{A_n(\vec{k}, i\Gamma)A_n(-\vec{k}', -i\Gamma)} \right. \\ &\quad \left. \left[F_0^{np}\chi_n(\vec{k}, i\Gamma)\right] \left[F_0^{np}\chi_n(-\vec{k}', -i\Gamma)\right] \overline{A_p(\vec{k}, i\Gamma)A_p(-\vec{k}', -i\Gamma)} \right\}, \end{aligned} \quad (\text{C.3})$$

$$\begin{aligned} \overline{\delta n_n^-(\vec{k})\delta n_n^+(-\vec{k}')} &= -\frac{1}{\left[\partial\varepsilon(\vec{k}, \omega)/\partial\omega\right]_{\omega=-i\Gamma} \left[\partial\varepsilon(-\vec{k}', \omega)/\partial\omega\right]_{\omega=i\Gamma}} \\ &\quad \left\{ \left[1 + F_0^{pp}\chi_p(\vec{k}, -i\Gamma)\right] \left[1 + F_0^{pp}\chi_p(-\vec{k}', i\Gamma)\right] \overline{A_n(\vec{k}, -i\Gamma)A_n(-\vec{k}', i\Gamma)} \right. \\ &\quad \left. \left[F_0^{np}\chi_n(\vec{k}, -i\Gamma)\right] \left[F_0^{np}\chi_n(-\vec{k}', i\Gamma)\right] \overline{A_p(\vec{k}, -i\Gamma)A_p(-\vec{k}', i\Gamma)} \right\}, \end{aligned} \quad (\text{C.4})$$

and

$$\begin{aligned} \overline{\delta n_n^-(\vec{k})\delta n_n^-(-\vec{k}')} &= -\frac{1}{\left[\partial\varepsilon(\vec{k}, \omega)/\partial\omega\right]_{\omega=-i\Gamma} \left[\partial\varepsilon(-\vec{k}', \omega)/\partial\omega\right]_{\omega=-i\Gamma}} \\ &\quad \left\{ \left[1 + F_0^{pp}\chi_p(\vec{k}, -i\Gamma)\right] \left[1 + F_0^{pp}\chi_p(-\vec{k}', -i\Gamma)\right] \overline{A_n(\vec{k}, -i\Gamma)A_n(-\vec{k}', -i\Gamma)} \right. \\ &\quad \left. \left[F_0^{np}\chi_n(\vec{k}, -i\Gamma)\right] \left[F_0^{np}\chi_n(-\vec{k}', -i\Gamma)\right] \overline{A_p(\vec{k}, -i\Gamma)A_p(-\vec{k}', -i\Gamma)} \right\} \end{aligned} \quad (\text{C.5})$$

where the cross terms of source correlations are zero $\overline{A_n(\vec{k}, i\Gamma)A_p(-\vec{k}', i\Gamma)} = \overline{A_p(\vec{k}, i\Gamma)A_n(-\vec{k}', i\Gamma)} = 0$. In the source expression

$$A_a(\vec{k}, \omega) = 2\hbar \int_{-\infty}^{\infty} \frac{d^3p}{(2\pi\hbar)^3} \frac{\langle \vec{p} + \hbar\vec{k}/2 | \delta\rho_a(0) | \vec{p} - \hbar\vec{k}/2 \rangle}{\hbar\omega - \vec{p} \cdot \hbar\vec{k}/m}. \quad (\text{C.6})$$

if we use $-\vec{k}$ instead of \vec{k} , the source expression becomes

$$A_a(-\vec{k}, \omega) = 2\hbar \int_{-\infty}^{\infty} \frac{d^3 p}{(2\pi\hbar)^3} \frac{\langle \vec{p} - \hbar\vec{k}/2 | \delta\rho_a(0) | \vec{p} + \hbar\vec{k}/2 \rangle}{\hbar\omega + \vec{p} \cdot \hbar\vec{k}/m}. \quad (\text{C.7})$$

Therefore, the source correlations in equations (C.18-C.21) can be written as

$$\overline{A_n(\vec{k}, i\Gamma)A_n(-\vec{k}', i\Gamma)} = 4\hbar^2 \int_{-\infty}^{\infty} \int_{-\infty}^{\infty} \frac{d^3 p d^3 p'}{(2\pi\hbar)^6} \frac{\langle \vec{p} + \hbar\vec{k}/2 | \delta\rho_n(0) | \vec{p} - \hbar\vec{k}'/2 \rangle \langle \vec{p}' - \hbar\vec{k}/2 | \delta\rho_n(0) | \vec{p}' + \hbar\vec{k}'/2 \rangle}{(i\hbar\Gamma - \vec{p} \cdot \hbar\vec{k}/m)(i\hbar\Gamma + \vec{p}' \cdot \hbar\vec{k}'/m)}, \quad (\text{C.8})$$

$$\overline{A_n(\vec{k}, i\Gamma)A_n(-\vec{k}', -i\Gamma)} = 4\hbar^2 \int_{-\infty}^{\infty} \int_{-\infty}^{\infty} \frac{d^3 p d^3 p'}{(2\pi\hbar)^6} \frac{\langle \vec{p} + \hbar\vec{k}/2 | \delta\rho_n(0) | \vec{p} - \hbar\vec{k}'/2 \rangle \langle \vec{p}' - \hbar\vec{k}/2 | \delta\rho_n(0) | \vec{p}' + \hbar\vec{k}'/2 \rangle}{(i\hbar\Gamma - \vec{p} \cdot \hbar\vec{k}/m)(-i\hbar\Gamma + \vec{p}' \cdot \hbar\vec{k}'/m)}, \quad (\text{C.9})$$

$$\overline{A_n(\vec{k}, -i\Gamma)A_n(-\vec{k}', i\Gamma)} = 4\hbar^2 \int_{-\infty}^{\infty} \int_{-\infty}^{\infty} \frac{d^3 p d^3 p'}{(2\pi\hbar)^6} \frac{\langle \vec{p} + \hbar\vec{k}/2 | \delta\rho_n(0) | \vec{p} - \hbar\vec{k}'/2 \rangle \langle \vec{p}' - \hbar\vec{k}/2 | \delta\rho_n(0) | \vec{p}' + \hbar\vec{k}'/2 \rangle}{(-i\hbar\Gamma - \vec{p} \cdot \hbar\vec{k}/m)(i\hbar\Gamma + \vec{p}' \cdot \hbar\vec{k}'/m)}, \quad (\text{C.10})$$

and

$$\overline{A_n(\vec{k}, i\Gamma)A_n(-\vec{k}', i\Gamma)} = 4\hbar^2 \int_{-\infty}^{\infty} \int_{-\infty}^{\infty} \frac{d^3 p d^3 p'}{(2\pi\hbar)^6} \frac{\langle \vec{p} + \hbar\vec{k}/2 | \delta\rho_n(0) | \vec{p} - \hbar\vec{k}'/2 \rangle \langle \vec{p}' - \hbar\vec{k}/2 | \delta\rho_n(0) | \vec{p}' + \hbar\vec{k}'/2 \rangle}{(-i\hbar\Gamma - \vec{p} \cdot \hbar\vec{k}/m)(-i\hbar\Gamma + \vec{p}' \cdot \hbar\vec{k}'/m)}, \quad (\text{C.11})$$

using the the second moments of the initial correlations in the plane wave representation

$$\overline{\langle \vec{p} + \hbar\vec{k}/2 | \delta\rho_n(0) | \vec{p} - \hbar\vec{k}'/2 \rangle \langle \vec{p}' - \hbar\vec{k}/2 | \delta\rho_n(0) | \vec{p}' + \hbar\vec{k}'/2 \rangle} = (2\pi)^3 \delta(\vec{k} - \vec{k}') (2\pi\hbar)^3 \delta(\vec{p} - \vec{p}') \rho_n(\vec{p} + \hbar\vec{k}/2) \left[1 - \rho_n(\vec{p} - \hbar\vec{k}/2) \right] \quad (\text{C.12})$$

we can reduce the source correlations in equations (C.8-C.11) into two simple forms as follows,

$$\begin{aligned} \overline{A_n(\vec{k}, i\Gamma)A_n(-\vec{k}', i\Gamma)} &= -(2\pi)^3 \delta(\vec{k} - \vec{k}') \\ &4\hbar^2 \int_{-\infty}^{\infty} \frac{d^3 p}{(2\pi\hbar)^3} \frac{1}{(\hbar\Gamma)^2 + (\vec{p} \cdot \hbar\vec{k}/m)^2} \rho_n(\vec{p} + \hbar\vec{k}/2) \left[1 - \rho_n(\vec{p} - \hbar\vec{k}/2)\right] \end{aligned} \quad (\text{C.13})$$

and

$$\begin{aligned} \overline{A_n(\vec{k}, i\Gamma)A_n(-\vec{k}', -i\Gamma)} &= -(2\pi)^3 \delta(\vec{k} - \vec{k}') \\ &4\hbar^2 \int_{-\infty}^{\infty} \frac{d^3 p}{(2\pi\hbar)^3} \frac{(\hbar\Gamma)^2 - (\vec{p} \cdot \hbar\vec{k}/m)^2}{[(\hbar\Gamma)^2 + (\vec{p} \cdot \hbar\vec{k}/m)^2]^2} \rho_n(\vec{p} + \hbar\vec{k}/2) \left[1 - \rho_n(\vec{p} - \hbar\vec{k}/2)\right]. \end{aligned} \quad (\text{C.14})$$

There is a relation in the other elements of source correlations

$$\overline{A_n(\vec{k}, -i\Gamma)A_n(-\vec{k}', i\Gamma)} = \overline{A_n(\vec{k}, i\Gamma)A_n(-\vec{k}', -i\Gamma)} \quad (\text{C.15})$$

$$\overline{A_n(\vec{k}, -i\Gamma)A_n(-\vec{k}', -i\Gamma)} = -\overline{A_n(\vec{k}, i\Gamma)A_n(-\vec{k}', i\Gamma)}. \quad (\text{C.16})$$

The polar parts of these integrals are evaluated analytically and then in the evaluation of the resultant integrals numerical methods are used.

For the spectral intensity of proton-proton correlations replace letter n by letter p in neutron-neutron expressions. But in the spectral intensity of neutron-proton correlations function we need some more changes

$$\begin{aligned} \tilde{\sigma}_{np}(\vec{k}, t)(2\pi)^3 \delta(\vec{k} - \vec{k}') &= \overline{\delta\tilde{n}_n(\vec{k}, t)\delta\tilde{n}_p(-\vec{k}', t)} \\ &= \overline{\delta n_n^+(\vec{k})\delta n_p^+(-\vec{k}')e^{2\Gamma kt}} + \overline{\delta n_n^+(\vec{k})\delta n_p^-(-\vec{k}')} + \overline{\delta n_n^-(\vec{k})\delta n_p^+(-\vec{k}')} + \overline{\delta n_n^-(\vec{k})\delta n_p^-(-\vec{k}')e^{-2\Gamma kt}}, \end{aligned} \quad (\text{C.17})$$

here

$$\begin{aligned} \overline{\delta n_n^+(\vec{k})\delta n_p^+(-\vec{k}')} &= -\frac{1}{\left[\partial\varepsilon(\vec{k}, \omega)/\partial\omega\right]_{\omega=i\Gamma} \left[\partial\varepsilon(-\vec{k}', \omega)/\partial\omega\right]_{\omega=i\Gamma}} \\ &\left\{ \left[1 + F_0^{pp}\chi_p(\vec{k}, i\Gamma)\right] \left[F_0^{pn}\chi_p(-\vec{k}', i\Gamma)\right] \overline{A_n(\vec{k}, i\Gamma)A_n(-\vec{k}', i\Gamma)} \right. \\ &\left. \left[F_0^{np}\chi_n(\vec{k}, i\Gamma)\right] \left[1 + F_0^{nn}\chi_n(-\vec{k}', i\Gamma)\right] \overline{A_p(\vec{k}, i\Gamma)A_p(-\vec{k}', i\Gamma)} \right\}, \end{aligned} \quad (\text{C.18})$$

$$\begin{aligned}
\overline{\delta n_n^+(\vec{k})\delta n_p^-(\vec{k}')} &= -\frac{1}{\left[\partial\varepsilon(\vec{k}, \omega)/\partial\omega\right]_{\omega=i\Gamma} \left[\partial\varepsilon(-\vec{k}', \omega)/\partial\omega\right]_{\omega=-i\Gamma}} \\
&\quad \left\{ \left[1 + F_0^{pp}\chi_p(\vec{k}, i\Gamma)\right] \left[F_0^{pn}\chi_p(-\vec{k}', -i\Gamma)\right] \overline{A_n(\vec{k}, i\Gamma)A_n(-\vec{k}', -i\Gamma)} \right. \\
&\quad \left. \left[F_0^{np}\chi_n(\vec{k}, i\Gamma)\right] \left[1 + F_0^{mn}\chi_n(-\vec{k}', -i\Gamma)\right] \overline{A_p(\vec{k}, i\Gamma)A_p(-\vec{k}', -i\Gamma)} \right\},
\end{aligned} \tag{C.19}$$

$$\begin{aligned}
\overline{\delta n_n^-(\vec{k})\delta n_p^+(\vec{k}')} &= -\frac{1}{\left[\partial\varepsilon(\vec{k}, \omega)/\partial\omega\right]_{\omega=-i\Gamma} \left[\partial\varepsilon(-\vec{k}', \omega)/\partial\omega\right]_{\omega=i\Gamma}} \\
&\quad \left\{ \left[1 + F_0^{pp}\chi_p(\vec{k}, -i\Gamma)\right] \left[F_0^{pn}\chi_p(-\vec{k}', i\Gamma)\right] \overline{A_n(\vec{k}, -i\Gamma)A_n(-\vec{k}', i\Gamma)} \right. \\
&\quad \left. \left[F_0^{np}\chi_n(\vec{k}, -i\Gamma)\right] \left[1 + F_0^{mn}\chi_n(-\vec{k}', i\Gamma)\right] \overline{A_p(\vec{k}, -i\Gamma)A_p(-\vec{k}', i\Gamma)} \right\},
\end{aligned} \tag{C.20}$$

and

$$\begin{aligned}
\overline{\delta n_n^-(\vec{k})\delta n_p^-(\vec{k}')} &= -\frac{1}{\left[\partial\varepsilon(\vec{k}, \omega)/\partial\omega\right]_{\omega=-i\Gamma} \left[\partial\varepsilon(-\vec{k}', \omega)/\partial\omega\right]_{\omega=-i\Gamma}} \\
&\quad \left\{ \left[1 + F_0^{pp}\chi_p(\vec{k}, -i\Gamma)\right] \left[F_0^{pn}\chi_p(-\vec{k}', -i\Gamma)\right] \overline{A_n(\vec{k}, -i\Gamma)A_n(-\vec{k}', -i\Gamma)} \right. \\
&\quad \left. \left[F_0^{np}\chi_n(\vec{k}, -i\Gamma)\right] \left[1 + F_0^{mn}\chi_n(-\vec{k}', -i\Gamma)\right] \overline{A_p(\vec{k}, -i\Gamma)A_p(-\vec{k}', -i\Gamma)} \right\}
\end{aligned} \tag{C.21}$$

APPENDIX D

DERIVATION OF RELATIVISTIC VLASOV EQUATION

In the mean-field approximation, the nucleons are described by the Dirac equation

$$i\partial_t\psi = \left[\vec{\alpha} \cdot (\vec{p} - g_v\vec{V}) + \beta(M - g_s\phi) + g_vV^0 \right] \psi \quad (\text{D.1})$$

where in the following notations $\vec{p}^* = \vec{p} - g_v\vec{V}$ and $M^* = M - g_s\phi$ are used.

As for free particle, the stationary state solution for a uniform system is in the form of plane waves, $\psi = \psi(\vec{p}, \lambda)e^{i(\vec{p}\cdot\vec{x} - \epsilon(k)t)}$, where

$$\psi(\vec{p}, \lambda) = \begin{pmatrix} \psi_L \\ \psi_S \end{pmatrix} \quad (\text{D.2})$$

is a four-component Dirac spinor with ψ_L large component and ψ_S small component and λ indicates the spin index. In terms of large and small components the Dirac equation can be written as two coupled equations

$$\begin{aligned} i\partial_t\psi_L &= \vec{\sigma} \cdot \vec{p}^* \psi_S + [M^* + g_vV^0] \psi_L \\ i\partial_t\psi_S &= \vec{\sigma} \cdot \vec{p}^* \psi_L + [-M^*c^2 + g_vV^0] \psi_S. \end{aligned} \quad (\text{D.3})$$

In the local density approximation, the nucleons are considered to be moving locally in constant fields, therefore one can obtain the approximate solution between large and small components as,

$$\psi_L = \frac{\vec{\sigma} \cdot \vec{p}^*}{\epsilon^* - M^*} \psi_S \quad \text{and} \quad \psi_S = \frac{\vec{\sigma} \cdot \vec{p}^*}{\epsilon^* + M^*} \psi_L \quad (\text{D.4})$$

where $\epsilon^* = \sqrt{\vec{p}^{*2} + M^{*2}}$. This coupling reduces equations in Eq. (D.3) into the single equation and operator form of it is

$$i\partial_t\psi(\vec{x}, t) = [E^* + g_vV^0] \psi(\vec{x}, t) \quad (\text{D.5})$$

with the effective one-body Hamiltonian $h = E^* + g_v V^0$, here E^* is operator form of ϵ^* . From Eq. (D.5) it follows that

$$i\partial_t [\psi(\vec{r}_1, t)\psi^\dagger(\vec{r}_2, t)] = h(\vec{r}_1)\psi(\vec{r}_1, t)\psi^\dagger(\vec{r}_2, t) - \psi(\vec{r}_1)\psi^\dagger(\vec{r}_2)h(\vec{r}_2) \quad (\text{D.6})$$

where $\psi(\vec{r}, t)$ and $\psi^\dagger(\vec{r}, t)$ are the single particle wave functions not field operators and $\psi(\vec{r}_1, t)\psi^\dagger(\vec{r}_2, t) = \rho(\vec{r}_1, \vec{r}_2, t)$ is the single particle density matrix, therefore we have

$$i\partial_t \rho(\vec{r}_1, \vec{r}_2, t) = h(\vec{r}_1)\rho(\vec{r}_1, \vec{r}_2, t) - h(\vec{r}_2)\rho(\vec{r}_1, \vec{r}_2, t). \quad (\text{D.7})$$

To derive the Vlasov equation, we need to make Wigner transformation for density matrix to obtain function $f(\vec{p}, \vec{r}, t)$ and using transformation $\vec{r} = (\vec{r}_1 + \vec{r}_2)/2$, $\vec{x} = (\vec{r}_1 - \vec{r}_2)$,

$$f(\vec{p}, \vec{r}, t) = \int d^3x e^{-i\vec{p}\cdot\vec{x}} \rho(\vec{r} + \frac{\vec{x}}{2}, \vec{r} - \frac{\vec{x}}{2}, t) \quad (\text{D.8})$$

and for $h\rho$ in Eq. (D.7)

$$[h\rho]_W = h(\vec{p}, \vec{r})e^{i\frac{\hbar}{2}\bar{\wedge}} f(\vec{p}, \vec{r}) \quad (\text{D.9})$$

here W denotes Wigner transformation and $\bar{\wedge}$ denotes the operator $\bar{\wedge} = \overleftarrow{\nabla}_r \overrightarrow{\nabla}_p - \overleftarrow{\nabla}_p \overrightarrow{\nabla}_r$.

If we use the expansion

$$e^{i\frac{\hbar}{2}\bar{\wedge}} = 1 + i\frac{\hbar}{2}\bar{\wedge} + \dots \quad (\text{D.10})$$

for small \hbar in the semi-classical approximation and then taking Wigner transform of both sides of Eq. (D.10),

$$\partial_t f(\vec{r}, \vec{p}) = \frac{1}{2}[h(\vec{r}, \vec{p})\bar{\wedge} f(\vec{r}, \vec{p}) - f(\vec{r}, \vec{p})\bar{\wedge} h(\vec{r}, \vec{p})] \quad (\text{D.11})$$

we obtain the relativistic Vlasov equation

$$\partial_t f(\vec{r}, \vec{p}) = \overrightarrow{\nabla}_r h(\vec{r}, \vec{p}) \cdot \overrightarrow{\nabla}_p f(\vec{r}, \vec{p}) - \overrightarrow{\nabla}_p h(\vec{r}, \vec{p}) \cdot \overrightarrow{\nabla}_r f(\vec{r}, \vec{p}). \quad (\text{D.12})$$

APPENDIX E

THE COUPLED ALGEBRAIC EQUATIONS OF DENSITY FLUCTUATIONS

After the linearization of relativistic Vlasov equation, we have three coupled equations with source terms for the baryon density, the scalar density and the current density fluctuations. At zero temperature these equations are

$$\begin{aligned}
& \delta\tilde{\rho}_v(\vec{k}, \omega) \left[gD_v \int \frac{d^3 p}{(2\pi)^3} \frac{1}{\epsilon_0^*} \frac{k \cos \theta \delta(p - p_1)}{\omega - \frac{p}{\epsilon_0^*} k \cos \theta} p \cos \theta \right] \\
& + \delta\tilde{\rho}_s(\vec{k}, \omega) \left[gD_s \int \frac{d^3 p}{(2\pi)^3} \frac{M_0^*}{\epsilon_0^*} \frac{k \cos \theta \delta(p - p_1)}{\omega - \frac{p}{\epsilon_0^*} k \cos \theta} \right] \\
& + \delta\tilde{\rho}_B(\vec{k}, \omega) \left[1 - gD_v \int \frac{d^3 p}{(2\pi)^3} \frac{k \cos \theta \delta(p - p_1)}{\omega - \frac{p}{\epsilon_0^*} k \cos \theta} \right] \\
& = ig \int \frac{d^3 p}{(2\pi)^3} \frac{\delta f(\vec{k}, \vec{p}, 0)}{\omega - \frac{p}{\epsilon_0^*} k \cos \theta},
\end{aligned} \tag{E.1}$$

$$\begin{aligned}
& \delta\tilde{\rho}_v(\vec{k}, \omega) \left\{ -gD_v \int \frac{d^3 p}{(2\pi)^3} \left[\frac{M_0^*}{\epsilon_0^{*3}} f_0 - \frac{M_0^*}{\epsilon_0^{*2}} \frac{k \cos \theta \delta(p - p_1)}{\omega - \frac{p}{\epsilon_0^*} k \cos \theta} \right] p \cos \theta \right\} \\
& + \delta\tilde{\rho}_s(\vec{k}, \omega) \left\{ 1 + gD_s \int \frac{d^3 p}{(2\pi)^3} \left[\frac{p^2}{\epsilon_0^{*3}} f_0 + \frac{M_0^{*2}}{\epsilon_0^{*2}} \frac{k \cos \theta \delta(p - p_1)}{\omega - \frac{p}{\epsilon_0^*} k \cos \theta} \right] \right\} \\
& + \delta\tilde{\rho}_B(\vec{k}, \omega) \left[-gD_v \int \frac{d^3 p}{(2\pi)^3} \frac{M_0^*}{\epsilon_0^*} \frac{k \cos \theta \delta(p - p_1)}{\omega - \frac{p}{\epsilon_0^*} k \cos \theta} \right] \\
& = ig \int \frac{d^3 p}{(2\pi)^3} \frac{M_0^*}{\epsilon_0^*} \frac{\delta f(\vec{k}, \vec{p}, 0)}{\omega - \frac{p}{\epsilon_0^*} k \cos \theta},
\end{aligned} \tag{E.2}$$

$$\begin{aligned}
& \delta\tilde{\rho}_v(\vec{k}, \omega) \left\{ 1 + gD_v \int \frac{d^3p}{(2\pi)^3} \left[\frac{1}{\epsilon_0^*} f_0 - f_0 \frac{p \cos \theta}{\epsilon_0^{*3}} p \cos \theta \right. \right. \\
& \quad \left. \left. - \frac{p \cos \theta k \cos \theta \delta(p - p_1)}{\epsilon_0^{*2} \omega - \frac{p}{\epsilon_0^*} k \cos \theta} p \cos \theta \right] \right\} \\
& \delta\tilde{\rho}_s(\vec{k}, \omega) \left\{ -gD_s \int \frac{d^3p}{(2\pi)^3} \left[\frac{M_0^*}{\epsilon_0^{*3}} f_0 - \frac{M_0^*}{\epsilon_0^{*2}} \frac{k \cos \theta \delta(p - p_1)}{\omega - \frac{p}{\epsilon_0^*} k \cos \theta} \right] p \cos \theta \right\} \\
& \delta\tilde{\rho}_B(\vec{k}, \omega) \left[-gD_v \int \frac{d^3p}{(2\pi)^3} \frac{p \cos \theta k \cos \theta \delta(p - p_1)}{\epsilon_0^* \omega - \frac{p}{\epsilon_0^*} k \cos \theta} \right] \\
& = ig \int \frac{d^3p}{(2\pi)^3} \frac{p \cos \theta}{\epsilon_0^*} \frac{\delta f(\vec{k}, \vec{p}, 0)}{\omega - \frac{p}{\epsilon_0^*} k \cos \theta},
\end{aligned} \tag{E.3}$$

and for the finite temperature case

$$\begin{aligned}
& \delta\tilde{\rho}_v(\vec{k}, \omega) \left[-D_v g \int \frac{d^3p}{(2\pi)^3} \frac{1}{\epsilon_0^*} \frac{\partial f_0}{\partial \epsilon_0^*} \frac{p}{\epsilon_0^*} \frac{k \cos \theta}{\omega - \frac{p}{\epsilon_0^*} k \cos \theta} p \cos \theta \right] \\
& + \delta\tilde{\rho}_s(\vec{k}, \omega) \left[-D_s g \int \frac{d^3p}{(2\pi)^3} \frac{M_0^*}{\epsilon_0^*} \frac{\partial f_0}{\partial \epsilon_0^*} \frac{p}{\epsilon_0^*} \frac{k \cos \theta}{\omega - \frac{p}{\epsilon_0^*} k \cos \theta} \right] \\
& + \delta\tilde{\rho}_B(\vec{k}, \omega) \left[1 + D_v g \int \frac{d^3p}{(2\pi)^3} \frac{\partial f_0}{\partial \epsilon_0^*} \frac{p}{\epsilon_0^*} \frac{k \cos \theta}{\omega - \frac{p}{\epsilon_0^*} k \cos \theta} \right] \\
& = ig \int \frac{d^3p}{(2\pi)^3} \frac{\delta f(\vec{k}, \vec{p}, 0)}{\omega - \frac{p}{\epsilon_0^*} k \cos \theta},
\end{aligned} \tag{E.4}$$

$$\begin{aligned}
& \delta\tilde{\rho}_v(\vec{k}, \omega) \left\{ -D_v g \int \frac{d^3p}{(2\pi)^3} \left[\frac{M_0^*}{\epsilon_0^{*3}} f_0 + \frac{M_0^*}{\epsilon_0^{*2}} \frac{\partial f_0}{\partial \epsilon_0^*} \frac{p}{\epsilon_0^*} \frac{k \cos \theta}{\omega - \frac{p}{\epsilon_0^*} k \cos \theta} \right] p \cos \theta \right\} \\
& + \delta\tilde{\rho}_s(\vec{k}, \omega) \left\{ 1 + D_s g \int \frac{d^3p}{(2\pi)^3} \left[\frac{p^2}{\epsilon_0^{*3}} f_0 - \frac{M_0^{*2}}{\epsilon_0^{*2}} \frac{\partial f_0}{\partial \epsilon_0^*} \frac{p}{\epsilon_0^*} \frac{k \cos \theta}{\omega - \frac{p}{\epsilon_0^*} k \cos \theta} \right] \right\} \\
& + \delta\tilde{\rho}_B(\vec{k}, \omega) \left[D_v g \int \frac{d^3p}{(2\pi)^3} \frac{M_0^*}{\epsilon_0^*} \frac{\partial f_0}{\partial \epsilon_0^*} \frac{p}{\epsilon_0^*} \frac{k \cos \theta}{\omega - \frac{p}{\epsilon_0^*} k \cos \theta} \right] \\
& = ig \int \frac{d^3p}{(2\pi)^3} \frac{M_0^*}{\epsilon_0^*} \frac{\delta f(\vec{k}, \vec{p}, 0)}{\omega - \frac{p}{\epsilon_0^*} k \cos \theta},
\end{aligned} \tag{E.5}$$

$$\begin{aligned}
& \delta\tilde{\rho}_v(\vec{k}, \omega) \left\{ 1 + D_v g \int \frac{d^3 p}{(2\pi)^3} \left[\frac{1}{\epsilon_0^*} f_0 - f_0 \frac{p \cos \theta}{\epsilon_0^{*3}} p \cos \theta \right. \right. \\
& \quad \left. \left. - \frac{p \cos \theta}{\epsilon_0^{*2}} \frac{\partial f_0}{\partial \epsilon_0^*} \frac{p}{\epsilon_0^*} \frac{k \cos \theta}{\omega - \frac{p}{\epsilon_0^*} k \cos \theta} p \cos \theta \right] \right\} \\
& + \delta\tilde{\rho}_s(\vec{k}, \omega) \left\{ -D_s g \int \frac{d^3 p}{(2\pi)^3} \left[\frac{M_0^*}{\epsilon_0^{*3}} f_0 + \frac{M_0^*}{\epsilon_0^{*2}} \frac{\partial f_0}{\partial \epsilon_0^*} \frac{p}{\epsilon_0^*} \frac{k \cos \theta}{\omega - \frac{p}{\epsilon_0^*} k \cos \theta} \right] p \cos \theta \right\} \\
& + \delta\tilde{\rho}_B(\vec{k}, \omega) \left[D_v g \int \frac{d^3 p}{(2\pi)^3} \frac{p \cos \theta}{\epsilon_0^*} \frac{\partial f_0}{\partial \epsilon_0^*} \frac{p}{\epsilon_0^*} \frac{k \cos \theta}{\omega - \frac{p}{\epsilon_0^*} k \cos \theta} \right] \\
& = ig \int \frac{d^3 p}{(2\pi)^3} \frac{p \cos \theta}{\epsilon_0^*} \frac{\delta f(\vec{k}, \vec{p}, 0)}{\omega - \frac{p}{\epsilon_0^*} k \cos \theta}.
\end{aligned} \tag{E.6}$$

The full expressions of the coefficients A_i, B_i and C_i for finite temperature are as follows,

$$A_1 = -D_v g \int \frac{d^3 p}{(2\pi^3)} \frac{\vec{p} \cdot \hat{k} \vec{k} \cdot \vec{\nabla}_p f_0(\vec{p})}{\epsilon_0^* \omega - \vec{v}_0 \cdot \vec{k}}, \tag{E.7}$$

$$A_2 = -D_s g \int \frac{d^3 p}{(2\pi^3)} \frac{M_0^* \vec{k} \cdot \vec{\nabla}_p f_0(\vec{p})}{\epsilon_0^* \omega - \vec{v}_0 \cdot \vec{k}}, \tag{E.8}$$

$$A_3 = 1 + D_v g \int \frac{d^3 p}{(2\pi^3)} \frac{\vec{k} \cdot \vec{\nabla}_p f_0(\vec{p})}{\omega - \vec{v}_0 \cdot \vec{k}}, \tag{E.9}$$

$$B_1 = -D_v g \int \frac{d^3 p}{(2\pi)^3} \left[\frac{p^2}{\epsilon_0^{*3}} f_0(p) - \frac{M_0^{*2} \vec{k} \cdot \vec{\nabla}_p f_0(p)}{\epsilon_0^{*2} \omega - \vec{v}_0 \cdot \vec{k}} \right], \tag{E.10}$$

$$B_2 = 1 + g \int \frac{d^3 p}{(2\pi)^3} \vec{p} \cdot \vec{k} \left[\frac{M_0^* \vec{k} \cdot \vec{\nabla}_p f_0(p)}{\epsilon_0^{*2} \omega - \vec{v}_0 \cdot \vec{k}} \right], \tag{E.11}$$

$$B_3 = +D_v g \int \frac{d^3 p}{(2\pi^3)} \frac{M_0^* \vec{k} \cdot \vec{\nabla}_p f_0(\vec{p})}{\epsilon_0^* \omega - \vec{v}_0 \cdot \vec{k}}, \tag{E.12}$$

$$C_1 = 1 + D_v g \int \frac{d^3 p}{(2\pi)^3} \left[\frac{\epsilon_0^{*2} - (\vec{p} \cdot \vec{k})^2}{\epsilon_0^{*3}} f_0(p) - \frac{(\vec{p} \cdot \vec{k})^2 \vec{k} \cdot \vec{\nabla}_p f_0(p)}{\epsilon_0^{*2} \omega - \vec{v}_0 \cdot \vec{k}} \right], \tag{E.13}$$

$$C_2 = -D_{\text{vg}} \int \frac{d^3 p}{(2\pi^3)} \frac{\vec{p} \cdot \hat{k} \vec{k} \cdot \vec{\nabla}_p f_0(\vec{p})}{\epsilon_0^* \omega - \vec{v}_0 \cdot \vec{k}}, \quad (\text{E.14})$$

$$C_3 = +D_{\text{vg}} \int \frac{d^3 p}{(2\pi^3)} \frac{\vec{p} \cdot \hat{k} \vec{k} \cdot \vec{\nabla}_p f_0(\vec{p})}{\epsilon_0^* \omega - \vec{v}_0 \cdot \vec{k}}. \quad (\text{E.15})$$

APPENDIX F

DERIVATIONS OF RELATIVISTIC CORRELATIONS

The spectral intensity of baryon density fluctuations is defined by

$$\begin{aligned}
 \tilde{\sigma}_{BB}(\vec{k}, t)(2\pi)^3 \delta(\vec{k} - \vec{k}') &= \overline{\delta\tilde{\rho}_B(\vec{k}, t)\delta\tilde{\rho}_B^*(\vec{k}', t)} \\
 &= \overline{\delta\rho_B^+(\vec{k})\delta\rho_B^+(\vec{k}')^* e^{2\Gamma t} + \delta\rho_B^-(\vec{k})\delta\rho_B^-(\vec{k}')^* e^{-2\Gamma t}} \\
 &\quad + \overline{\delta\rho_B^+(\vec{k})\delta\rho_B^-(\vec{k}')^* + \delta\rho_B^-(\vec{k})\delta\rho_B^+(\vec{k}')^*}
 \end{aligned} \tag{F.1}$$

with initial amplitudes,

$$\delta\rho_B^\mp(\vec{k}) = - \left[\frac{D_1 \tilde{S}_B(\vec{k}, \omega) + D_2 \tilde{S}_s(\vec{k}, \omega) + D_3 \tilde{S}_v(\vec{k}, \omega)}{\partial\varepsilon(\vec{k}, \omega)/\partial\omega} \right]_{\omega=\mp i\Gamma_k}. \tag{F.2}$$

For growing pole the correlation of initial amplitudes baryon density

$$\begin{aligned}
 \overline{\delta\rho_B^+(\vec{k})\delta\rho_B^+(\vec{k}')^*} &= \frac{1}{\left[\partial\varepsilon(\vec{k}, \omega)/\partial\omega\right]_{\omega=i\Gamma} \left[\partial\varepsilon(\vec{k}', \omega)/\partial\omega\right]_{\omega=i\Gamma}} \\
 &\quad \times \left[D_1 \tilde{S}_B(\vec{k}, \omega)^+ + D_2 \tilde{S}_s(\vec{k}, \omega)^+ + D_3 \tilde{S}_v(\vec{k}, \omega)^+ \right] \\
 &\quad \times \left[D_1 \tilde{S}_B(\vec{k}', \omega)^+ + D_2 \tilde{S}_s(\vec{k}', \omega)^+ + D_3 \tilde{S}_v(\vec{k}', \omega)^+ \right]^*
 \end{aligned} \tag{F.3}$$

for the elements of this correlation, the first source term is

$$\tilde{S}_B(\vec{k}, \omega)^+ = g \int \frac{d^3 p}{(2\pi)^3} \frac{\delta\tilde{f}(\vec{k}, \vec{p}, 0)}{i\Gamma - v_0 \cdot \vec{k}}, \tag{F.4}$$

its complex conjugate is

$$(\tilde{S}_B(\vec{k}', \omega)^+)^* = g \int \frac{d^3 p}{(2\pi)^3} \frac{\delta\tilde{f}^*(\vec{k}', \vec{p}, 0)}{-i\Gamma - v_0 \cdot \vec{k}'} \tag{F.5}$$

and its correlation can be written using the second moment of the initial phase-space distribution function $\delta\tilde{f}(\vec{k}, \vec{p}, 0)$

$$\overline{\delta\tilde{f}(\vec{k}, \vec{p}, 0)\delta\tilde{f}^*(\vec{k}', \vec{p}', 0)} = (2\pi)^3 (2\pi\hbar)^3 \delta(\vec{k} - \vec{k}') \delta(\vec{p} - \vec{p}') f_0(\vec{p}) [1 - f_0(\vec{p})] \tag{F.6}$$

as follows

$$\overline{\tilde{S}_B(\vec{k}, \omega)^+(\tilde{S}_B(\vec{k}', \omega)^+)^*} = g^2(2\pi)^3 \delta(\vec{k} - \vec{k}') \int \frac{d^3 p}{(2\pi)^3} \frac{f_0(\vec{p})[1 - f_0(\vec{p})]}{\Gamma^2 - (v_0 \cdot \vec{k})^2}. \quad (\text{F.7})$$

Similarly, the other terms are

$$\tilde{S}_s(\vec{k}, \omega)^+ = g \int \frac{d^3 p}{(2\pi)^3} \frac{M_0^* \delta \tilde{f}(\vec{k}, \vec{p}, 0)}{\epsilon_0^* i\Gamma - v_0 \cdot \vec{k}} \quad (\text{F.8})$$

$$(\tilde{S}_s(\vec{k}', \omega)^+)^* = g \int \frac{d^3 p}{(2\pi)^3} \frac{M_0^* \delta \tilde{f}^*(\vec{k}', \vec{p}, 0)}{\epsilon_0^* -i\Gamma - v_0 \cdot \vec{k}'} \quad (\text{F.9})$$

$$\overline{\tilde{S}_s(\vec{k}, \omega)^+(\tilde{S}_s(\vec{k}', \omega)^+)^*} = g^2(2\pi)^3 \delta(\vec{k} - \vec{k}') \int \frac{d^3 p}{(2\pi)^3} \left(\frac{M_0^*}{\epsilon_0^*} \right)^2 \frac{f_0(\vec{p})[1 - f_0(\vec{p})]}{\Gamma^2 - (v_0 \cdot \vec{k})^2}, \quad (\text{F.10})$$

and

$$\tilde{S}_v(\vec{k}, \omega)^+ = g \int \frac{d^3 p}{(2\pi)^3} \frac{c p_z \delta \tilde{f}(\vec{k}, \vec{p}, 0)}{\epsilon_0^* i\Gamma - v_0 \cdot \vec{k}} \quad (\text{F.11})$$

$$(\tilde{S}_v(\vec{k}', \omega)^+)^* = g \int \frac{d^3 p}{(2\pi)^3} \frac{c p_z \delta \tilde{f}^*(\vec{k}', \vec{p}, 0)}{\epsilon_0^* -i\Gamma - v_0 \cdot \vec{k}'} \quad (\text{F.12})$$

$$\overline{\tilde{S}_v(\vec{k}, \omega)^+(\tilde{S}_v(\vec{k}', \omega)^+)^*} = g^2(2\pi)^3 \delta(\vec{k} - \vec{k}') \int \frac{d^3 p}{(2\pi)^3} \left(\frac{c p_z}{\epsilon_0^*} \right)^2 \frac{f_0(\vec{p})[1 - f_0(\vec{p})]}{\Gamma^2 - (v_0 \cdot \vec{k})^2} \quad (\text{F.13})$$

here $p_z = p \cos \theta$, and mixed terms are

$$\begin{aligned} \overline{\tilde{S}_B(\vec{k}, \omega)^+(\tilde{S}_s(\vec{k}', \omega)^+)^*} &= g^2(2\pi)^3 \delta(\vec{k} - \vec{k}') \int \frac{d^3 p}{(2\pi)^3} \frac{M_0^* f_0(\vec{p})[1 - f_0(\vec{p})]}{\epsilon_0^* \Gamma^2 - (v_0 \cdot \vec{k})^2} \\ &= \overline{\tilde{S}_s(\vec{k}, \omega)^+(\tilde{S}_B(\vec{k}, \omega)^+)^*} \end{aligned} \quad (\text{F.14})$$

and also

$$\begin{aligned} \overline{\tilde{S}_B(\vec{k}, \omega)^+(\tilde{S}_v(\vec{k}, \omega)^+)^*} &= \overline{\tilde{S}_v(\vec{k}, \omega)^+(\tilde{S}_B(\vec{k}, \omega)^+)^*} = \\ \overline{\tilde{S}_s(\vec{k}, \omega)^+(\tilde{S}_v(\vec{k}, \omega)^+)^*} &= \overline{\tilde{S}_v(\vec{k}, \omega)^+(\tilde{S}_s(\vec{k}, \omega)^+)^*} = 0 \end{aligned} \quad (\text{F.15})$$

because the integral $\int \frac{x^n dx}{x^2+a^2}$ vanishes for odd n . Therefore the correlations of baryon density fluctuation amplitudes initially for growing poles are

$$\overline{\delta\rho_B^+(\vec{k})\delta\rho_B^+(\vec{k}')^*} = (2\pi)^3 \delta(\vec{k} - \vec{k}') \frac{|D_1|^2 K_{11}^{++} + |D_2|^2 K_{22}^{++} + |D_3|^2 K_{33}^{++} + 2D_1 D_2 K_{12}^{++}}{|\partial\epsilon(\vec{k}, \omega)/\partial\omega|_{\omega=i\Gamma}^2}, \quad (\text{F.16})$$

with the integrals,

$$K_{11}^{++} = g^2 \int \frac{d^3 p}{(2\pi)^3} \frac{f_0(\vec{p})[1 - f_0(\vec{p})]}{\Gamma^2 + (v_0 \cdot \vec{k})^2} \quad (\text{F.17})$$

$$K_{22}^{++} = g^2 \int \frac{d^3 p}{(2\pi)^3} \left(\frac{M_0^*}{\epsilon_0^*}\right)^2 \frac{f_0(\vec{p})[1 - f_0(\vec{p})]}{\Gamma^2 + (v_0 \cdot \vec{k})^2} \quad (\text{F.18})$$

$$K_{33}^{++} = g^2 \int \frac{d^3 p}{(2\pi)^3} \left(\frac{p_z}{\epsilon_0^*}\right)^2 \frac{f_0(\vec{p})[1 - f_0(\vec{p})]}{\Gamma^2 + (v_0 \cdot \vec{k})^2} \quad (\text{F.19})$$

$$K_{12}^{++} = g^2 \int \frac{d^3 p}{(2\pi)^3} \frac{M_0^*}{\epsilon_0^*} \frac{f_0(\vec{p})[1 - f_0(\vec{p})]}{\Gamma^2 + (v_0 \cdot \vec{k})^2}. \quad (\text{F.20})$$

In a similar manner for decaying pole we have the following expressions

$$\overline{\delta\rho_B^-(\vec{k})\delta\rho_B^-(\vec{k}')^*} = \frac{1}{\left|\left[\partial\epsilon(\vec{k}, \omega)/\partial\omega\right]_{\omega=-i\Gamma}\right|^2} \left[D_1 \tilde{S}_B(\vec{k}, \omega)^- + D_2 \tilde{S}_s(\vec{k}, \omega)^- + D_3 \tilde{S}_v(\vec{k}, \omega)^- \right] \times \left[D_1 \tilde{S}_B(\vec{k}', \omega)^- + D_2 \tilde{S}_s(\vec{k}', \omega)^- + D_3 \tilde{S}_v(\vec{k}', \omega)^- \right]^* \quad (\text{F.21})$$

$$\tilde{S}_B(\vec{k}, \omega)^- = g \int \frac{d^3 p}{(2\pi)^3} \frac{\delta\tilde{f}(\vec{k}, \vec{p}, 0)}{-i\Gamma - v_0 \cdot \vec{k}} \quad (\text{F.22})$$

$$(\tilde{S}_B(\vec{k}', \omega)^-)^* = g \int \frac{d^3 p}{(2\pi)^3} \frac{\delta\tilde{f}^*(\vec{k}, \vec{p}, 0)}{i\Gamma - v_0 \cdot \vec{k}} \quad (\text{F.23})$$

$$\overline{\tilde{S}_B(\vec{k}, \omega)^- (\tilde{S}_B(\vec{k}', \omega)^-)^*} = g^2 (2\pi)^3 \delta(\vec{k} - \vec{k}') \int \frac{d^3 p}{(2\pi)^3} \frac{f_0(\vec{p})[1 - f_0(\vec{p})]}{\Gamma^2 + (v_0 \cdot \vec{k})^2}, \quad (\text{F.24})$$

$$\tilde{S}_s(\vec{k}, \omega)^- = g \int \frac{d^3 p}{(2\pi)^3} \frac{M_0^*}{\epsilon_0^*} \frac{\delta \tilde{f}(\vec{k}, \vec{p}, 0)}{-i\Gamma - v_0 \cdot \vec{k}} \quad (\text{F.25})$$

$$(\tilde{S}_s(\vec{k}', \omega)^-)^* = g \int \frac{d^3 p}{(2\pi)^3} \frac{M_0^*}{\epsilon_0^*} \frac{\delta \tilde{f}^*(\vec{k}, \vec{p}, 0)}{i\Gamma - v_0 \cdot \vec{k}} \quad (\text{F.26})$$

$$\overline{\tilde{S}_s(\vec{k}, \omega)^- (\tilde{S}_s(\vec{k}', \omega)^-)^*} = g^2 (2\pi)^3 \delta(\vec{k} - \vec{k}') \int \frac{d^3 p}{(2\pi)^3} \left(\frac{M_0^*}{\epsilon_0^*} \right)^2 \frac{f_0(\vec{p}) [1 - f_0(\vec{p})]}{\Gamma^2 + (v_0 \cdot \vec{k})^2}, \quad (\text{F.27})$$

and

$$\tilde{S}_v(\vec{k}, \omega)^- = g \int \frac{d^3 p}{(2\pi)^3} \frac{p_z}{\epsilon_0^*} \frac{\delta \tilde{f}(\vec{k}, \vec{p}, 0)}{-i\Gamma - v_0 \cdot \vec{k}} \quad (\text{F.28})$$

$$(\tilde{S}_v(\vec{k}', \omega)^-)^* = g \int \frac{d^3 p}{(2\pi)^3} \frac{p_z}{\epsilon_0^*} \frac{\delta \tilde{f}^*(\vec{k}, \vec{p}, 0)}{i\Gamma - v_0 \cdot \vec{k}} \quad (\text{F.29})$$

$$\overline{\tilde{S}_v(\vec{k}, \omega)^- (\tilde{S}_v(\vec{k}', \omega)^-)^*} = g^2 (2\pi)^3 \delta(\vec{k} - \vec{k}') \int \frac{d^3 p}{(2\pi)^3} \left(\frac{p_z}{\epsilon_0^*} \right)^2 \frac{f_0(\vec{p}) [1 - f_0(\vec{p})]}{\Gamma^2 + (v_0 \cdot \vec{k})^2}. \quad (\text{F.30})$$

Therefore, it is possible to write,

$$\overline{\delta \rho_B^+(\vec{k}) \delta \rho_B^+(\vec{k}')^*} = \overline{\delta \rho_B^-(\vec{k}) \delta \rho_B^-(\vec{k}')^*}. \quad (\text{F.31})$$

Finally, for the mixed growing and decaying poles, these expressions take form

$$\begin{aligned} & \overline{\tilde{S}_B(\vec{k}, \omega)^+ (\tilde{S}_B(\vec{k}', \omega)^-)^*} = \\ & g^2 (2\pi)^3 \delta(\vec{k} - \vec{k}') \int \frac{d^3 p}{(2\pi)^3} \frac{-\Gamma^2 + (v_0 \cdot \vec{k})^2}{[\Gamma^2 + (v_0 \cdot \vec{k})^2]^2} f_0(\vec{p}) [1 - f_0(\vec{p})] \end{aligned} \quad (\text{F.32})$$

$$\begin{aligned} & \overline{\tilde{S}_s(\vec{k}, \omega)^+ (\tilde{S}_s(\vec{k}', \omega)^-)^*} = \\ & g^2 (2\pi)^3 \delta(\vec{k} - \vec{k}') \int \frac{d^3 p}{(2\pi)^3} \left(\frac{M_0^*}{\epsilon_0^*} \right)^2 \frac{-\Gamma^2 + (v_0 \cdot \vec{k})^2}{[\Gamma^2 + (v_0 \cdot \vec{k})^2]^2} f_0(\vec{p}) [1 - f_0(\vec{p})] \end{aligned} \quad (\text{F.33})$$

$$\begin{aligned} & \overline{\tilde{S}_v(\vec{k}, \omega)^+ (\tilde{S}_v(\vec{k}', \omega)^-)^*} = \\ & g^2 (2\pi)^3 \delta(\vec{k} - \vec{k}') \int \frac{d^3 p}{(2\pi)^3} \left(\frac{p_z}{\epsilon_0^*} \right)^2 \frac{-\Gamma^2 + (v_0 \cdot \vec{k})^2}{[\Gamma^2 + (v_0 \cdot \vec{k})^2]^2} f_0(\vec{p}) [1 - f_0(\vec{p})] \end{aligned} \quad (\text{F.34})$$

$$\begin{aligned} & \overline{\tilde{S}_B(\vec{k}, \omega)^+ (\tilde{S}_s(\vec{k}', \omega)^-)^*} = \\ & g^2 (2\pi)^3 \delta(\vec{k} - \vec{k}') \int \frac{d^3 p}{(2\pi)^3} \frac{M_0^*}{\epsilon_0^*} \frac{-\Gamma^2 + (v_0 \cdot \vec{k})^2}{[\Gamma^2 + (v_0 \cdot \vec{k})^2]^2} f_0(\vec{p}) [1 - f_0(\vec{p})] \end{aligned} \quad (\text{F.35})$$

$$\overline{\delta\rho_B^+(\vec{k}) \delta\rho_B^-(\vec{k}')^*} = (2\pi)^3 \delta(\vec{k} - \vec{k}') \frac{|D_1^B|^2 K_{11}^{+-} + |D_2^B|^2 K_{22}^{+-} + |D_3^B|^2 K_{33}^{+-} + 2D_1^B D_2^B K_{12}^{+-}}{||\partial\varepsilon(\vec{k}, \omega)/\partial\omega|_{\omega=i\Gamma}|^2} \quad (\text{F.36})$$

where,

$$K_{11}^{+-} = g^2 \int \frac{d^3 p}{(2\pi)^3} \frac{\Gamma^2 - (v_0 \cdot \vec{k})^2}{[\Gamma^2 + (v_0 \cdot \vec{k})^2]^2} f_0(\vec{p}) [1 - f_0(\vec{p})] \quad (\text{F.37})$$

$$K_{22}^{+-} = g^2 \int \frac{d^3 p}{(2\pi)^3} \left(\frac{M_0^*}{\epsilon_0^*} \right)^2 \frac{\Gamma^2 - (v_0 \cdot \vec{k})^2}{[\Gamma^2 + (v_0 \cdot \vec{k})^2]^2} f_0(\vec{p}) [1 - f_0(\vec{p})] \quad (\text{F.38})$$

$$K_{33}^{+-} = g^2 \int \frac{d^3 p}{(2\pi)^3} \left(\frac{p_z}{\epsilon_0^*} \right)^2 \frac{\Gamma^2 - (v_0 \cdot \vec{k})^2}{[\Gamma^2 + (v_0 \cdot \vec{k})^2]^2} f_0(\vec{p}) [1 - f_0(\vec{p})] \quad (\text{F.39})$$

$$K_{12}^{+-} = g^2 \int \frac{d^3 p}{(2\pi)^3} \frac{M_0^* p_z}{\epsilon_0^* \epsilon_0^*} \frac{\Gamma^2 - (v_0 \cdot \vec{k})^2}{[\Gamma^2 + (v_0 \cdot \vec{k})^2]^2} f_0(\vec{p}) [1 - f_0(\vec{p})] \quad (\text{F.40})$$

Consequently, the spectral intensity of baryon density correlation function can be written using these expressions

$$\begin{aligned} \tilde{\sigma}_{\text{BB}}(\vec{k}, t) &= \frac{\left[K_{11}^+ |D_1|^2 + K_{22}^+ |D_2|^2 + K_{33}^+ |D_3|^2 + K_{12}^+ D_1 D_2 \right]}{||\partial\varepsilon(\vec{k}, \omega)/\partial\omega|_{\omega=i\Gamma_k}|^2} (e^{2\Gamma_k t} + e^{-2\Gamma_k t}) \\ &+ \frac{2 \left[K_{11}^- |D_1|^2 + K_{22}^- |D_2|^2 - K_{33}^- |D_3|^2 + K_{12}^- D_1 D_2 \right]}{||\partial\varepsilon(\vec{k}, \omega)/\partial\omega|_{\omega=i\Gamma_k}|^2} \\ &= \frac{E_B^+(\vec{k}, i\Gamma)}{||\partial\varepsilon(\vec{k}, \omega)/\partial\omega|_{\omega=i\Gamma_k}|^2} (e^{2\Gamma_k t} + e^{-2\Gamma_k t}) + \frac{2E_B^-(\vec{k}, i\Gamma)}{||\partial\varepsilon(\vec{k}, \omega)/\partial\omega|_{\omega=i\Gamma_k}|^2} \end{aligned} \quad (\text{F.41})$$

where the expressions $E_B^\mp(\vec{k}, i\Gamma)$ are

$$\begin{aligned} E_B^+(\vec{k}) &= |D_1|^2 K_{11}^+ + |D_2|^2 K_{22}^+ + |D_3|^2 K_{33}^+ + 2D_1 D_2 K_{12}^+ \\ E_B^-(\vec{k}) &= |D_1|^2 K_{11}^- + |D_2|^2 K_{22}^- - |D_3|^2 K_{33}^- + 2D_1 D_2 K_{12}^- \end{aligned} \quad (\text{F.42})$$

in these expressions D_1, D_2 are real but D_3 is imaginary, and the integrals have the forms

$$K_{11}^\mp = g^2 \int \frac{d^3 p}{(2\pi\hbar)^3} \frac{\Gamma^2 \mp (v_0 \cdot \vec{k})^2}{[\Gamma^2 + (v_0 \cdot \vec{k})^2]^2} f_0(\vec{p}) [1 - f_0(\vec{p})] \quad (\text{F.43})$$

$$K_{22}^\mp = g^2 \int \frac{d^3 p}{(2\pi\hbar)^3} \left(\frac{M_0^*}{\epsilon_0^*} \right)^2 \frac{\Gamma^2 \mp (v_0 \cdot \vec{k})^2}{[\Gamma^2 + (v_0 \cdot \vec{k})^2]^2} f_0(\vec{p}) [1 - f_0(\vec{p})] \quad (\text{F.44})$$

$$K_{33}^\mp = g^2 \int \frac{d^3 p}{(2\pi\hbar)^3} \left(\frac{p_z}{\epsilon_0^*} \right)^2 \frac{\Gamma^2 \mp (v_0 \cdot \vec{k})^2}{[\Gamma^2 + (v_0 \cdot \vec{k})^2]^2} f_0(\vec{p}) [1 - f_0(\vec{p})] \quad (\text{F.45})$$

$$K_{12}^\mp = g^2 \int \frac{d^3 p}{(2\pi\hbar)^3} \frac{M_0^*}{\epsilon_0^*} \frac{\Gamma^2 \mp (v_0 \cdot \vec{k})^2}{[\Gamma^2 + (v_0 \cdot \vec{k})^2]^2} f_0(\vec{p}) [1 - f_0(\vec{p})] \quad (\text{F.46})$$

VITA

Nuray Er was born in Tokat, Turkey. She received her BS degree in physics at Middle East Technical University in Ankara, Turkey, in 1996. Having completed the BS program, she started MS studies at Physics Department of Harran University , Şanlıurfa, Turkey and received her MS degree in 2003. She started her Ph.D. studies in nuclear physics at Middle East Technical University in 2005.

e-mail:e060843@metu.edu.tr